# N3LO-Renormalon-Inspired Resummations and Fully Analytic Infra-red Freezing in Perturbative QCD

## LAI HO SHIE PASCALIUS

# $N^3$LO-Renormalon-Inspired Resummations and Fully Analytic Infra-red Freezing in Perturbative QCD

Pascalius Lai Ho Shie

11 April 2013

# Abstract

We make use of the recent calculation of $d_3$ by Baikov, Chetrykin and Kuhn of $N^3LO$ QCD vacuum polarization to analyze the inclusive tau-decay ratio $R_\tau$. We perform an all-orders resummation of the QCD Adler D function for the vector correlator, in which the part of perturbative coefficients containing the leading power of $b$, the first QCD beta-function equation coefficient, is resummed to all-orders. We match the resummation to the exactly known next-to-leading order ($NLO$), next-$NLO$ ($N^2LO$) and next-$N^2LO$ ($N^3LO$) results, we employ the Complete Renormalization Group Improvement (CORGI) approach in which all RG-predictable ultra-violet logarithms are resummed to all-orders, removing all dependence on the renormalization scale. Hence the $NLO$, $N^2LO$ and $N^3LO$ CORGI result can be obtained and compared with the "leading $b$" all-orders CORGI result. Using an appropriate weight function, we can numerically integrate these results for the Adler D function in the complex energy plane to obtain so-called "contour-improved" results for the ratio $R_{e^+e^-}$ and its tau-decay analogue $R_\tau$. A table showing the differences of $\alpha_S(M_\tau^2)$ and $\alpha_S(M_Z^2)$ extracted from $NLO$, $N^2LO$ and $N^3LO$ CORGI as well as all-orders CORGI results were made, together with $\alpha_S(M_\tau^2)$ and $\alpha_S(M_Z^2)$ extracted directly from Fixed-Order Perturbation Theory at $NLO$, $N^2LO$ and $N^3LO$. We also compared the ALEPH data for $R_\tau(s)$ with the all-orders CORGI result fitted at $s = m_\tau^2$.

We then go on to study the analyticity in energy of the leading one-chain term in a skeleton expansion for QCD observables. We show that by adding suitable non-perturbative terms in the energy regions $Q^2 > \Lambda^2$ and $Q^2 < \Lambda^2$ (where $Q^2 = \Lambda^2$ is the Landau pole of the one loop coupling), one can obtain an expression for the observables which is a holomorphic function of $Q^2$, for which all derivatives are finite and continuous at $Q^2 = \Lambda^2$. This function is uniquely constrained by the requirement of asymptotic freedom, and the finiteness as $Q^2 \longrightarrow 0$, up to addition of a non-perturabtive holomorphic function. This full analyticity replaces the piecewise analyticity and continuity exhibited by the leading one-chain term itself. Using The Analytic Perturbation Theory (APT) Euclidean functions introduced by Shirkov and collaborators, we finally matched the equations $K_{PT}^{(L)} + K_{NP}^{(L)}$ and $U_{PT}^{(L)} + U_{NP}^{(L)}$ with a resummation of coefficients extracted from their Borel Transform multiplied by the APT Euclidean functions in the one loop case. For $D_{PT}^{(L)} + D_{NP}^{(L)}$, it is shown that it freezes to $2/b$. Considering the GDH Sum Rule, we construct an analytic function which fits well with data from Jefferson Laboratory (JLab) for $0 < Q < 2\text{GeV}$.

# Acknowledgements

I thank the Lord for giving me an opportunity to be a member of IPPP. This work will not have been possible without the temporary or permanent support from MOHE (Ministry of Higher Education, Malaysia) and the Department of Physics, University of Malaya for providing me and my family substantial funding during my three and a half year Ph.D program. My gratitude goes to Mrs Brenda Ryder for her active role as a supporting officer. It has also been a pleasure to be part of IPPP, Durham, for the part-time work opportunities, seminars and summer school in the UK.

I am indebted to my supervisor Dr. Christopher Maxwell for his supervisions, Prof. Peter Richardson for his detail scrutiny, Prof. Nigel Glover for his constant support, Prof. Michael Pennington in Jefferson Lab and Prof. Michael Seymour from Manchester.

I would like to thank all my colleagues in IPPP, from the great administration work by Linda Wilkinson and Trudy Foster, as well as constant computing support from Mike Johnson and Peter Grandi. I wish to say thank you very much as well to my officemates Paul Mellor, Jennifer Archibald, Katherine Morgan, Ilan Friedman Rojas, Oliver Hall, Chris Wymant, David Winn and Xuan Chen.

This thesis is dedicated to my mother Bibiana, Ling and Judah.

# Declaration

I declare that no material in this thesis has previously been submitted for a degree at this or any other university.

All the research in this thesis has been carried out in collaboration with Dr. C.J. Maxwell. It is intended to submit the material contained in Chapters 6 and 7 for future publication.

# Contents

# Chapter 1

# QUANTUM FIELD THEORY

## 1.1 QUARKS AND GLUONS IN QUANTUM FIELD THEORY

Particle physics has been a great success in modelling the interactions of elementary particles using the formalism of quantum field theory.

Quantum Chromodynamics (QCD) provides a successful explanation regarding the importance of the existence of the fundamental quarks and gluons, which in combination give rise to the formation of protons and neutrons, the basic building blocks of nuclei. These particles are also the building blocks of mesons and baryons. These hadrons interact via the strong nuclear force, one of the four fundamental forces of nature in addition to gravitational, weak and electromagnetic forces. The strong force is a residual effect of interactions between quarks and gluons of different hadrons. This residual force holds all atomic nuclei together.

A solitary quark or gluon has never been observed, this is due to confinement which arises from the nature of the QCD colour force which grows linearly with the separation of coloured objects, and it is for this reason that quarks and gluons are always confined inside hadrons.

Quarks have a fractional electric charge in units of the electron charge, which is $+\frac{2}{3}$ or $-\frac{1}{3}$. Their presence can be recognized through electromagnetic interactions with other charged particles. An electron fired at a hadron can interact with a constituent quark or parton contained in the hadron. This deep inelastic scattering can be used to infer the quark charges from the measured cross section of the scattered electron.

Gluons act as the mediator of strong interactions between quarks, and are crucial in producing quark confinement, and the resulting hadrons. Particles with an electric charge interact electromagnetically in the theory of electro-magnetism(QED); analogously in QCD, particles have a colour charge which comes in red, green and blue varieties. In electromagnetism, the photon which plays the role of a mediator which has no electric charge. In QCD, the colour charge of gluons is constructed from colour-anti-colour combinations of the colour charges of the quarks. These colour charges result in three-point and four-point self interactions for the gluon, making non-abelian QCD a much more complex theory than abelian QED.

In this thesis, results obtained from the theory of QCD will be compared with experimental results from international facilities such as Jlab and LEP in order to test the validity of QCD.

## 1.2 THE DIRAC EQUATION

Prior to introducing Quantum Field Theory, we review advanced quantum mechanics where we are in a position to write a wave equation for a particle with no spin (a scalar particle). Having no spin implies that the field has only one component, which we denote by $\phi$. The differential operators for energy, $\mathbf{E}$, and momentum, $\mathbf{p}$ are

$$\mathbf{E} \longrightarrow i\hbar\frac{\partial}{\partial t}, \quad \mathbf{p} \longrightarrow i\hbar\nabla, \tag{1.1}$$

where in the relativistic case they are related by $E^2 = p^2c^2 + m^2c^4$ and for the non-relativistic case, $E = p^2/2m$. The wave equation is then given by

$$\left(\frac{1}{c^2}\frac{\partial^2}{\partial t^2} - \nabla^2\right)\phi + \frac{m^2c^2}{\hbar^2}\phi = 0, \tag{1.2}$$

which turns into the Klein-Gordon equation by setting $\hbar = c = 1$ (in natural units)

$$(\Box + m^2)\phi = 0, \tag{1.3}$$

where $\Box = \partial_\mu\partial^\mu$ is the four-vector partial derivative with respect to time and the 3 spatial dimensions. Note that we have used the covariant derivative $\partial^\mu = (\frac{1}{c}\partial^0, -\nabla)$. Nevertheless, the Klein-Gordon equation suffers from several flaws in particular the probability density is not positive definite since

it is proportional to the energy and the possibility for the occurrence of negative energy states [1]. $E = \pm\sqrt{p^2c^2 + m^2c^4}$ implies that the Klein-Gordon equation contains both positive-energy and negative-energy solutions. The Klein-Gordon equation involves the non-linear $\frac{\partial^2}{\partial t^2}$ term which needs to be replaced with a linear $\frac{\partial}{\partial t}$. Thus, the Klein-Gordon equation was discarded and the Dirac equation was the fittest replacement.

$$(\gamma^\mu p_\mu - m)\psi = 0. \tag{1.4}$$

It is then discovered that the equations turn out to be a $4 \times 4$ matrix, which then deduced that the $\gamma^\mu$ matrices must also be $4 \times 4$ matrices.

$$\gamma^0 = \begin{pmatrix} 0 & 1 \\ 1 & 0 \end{pmatrix}, \quad \gamma^i = \begin{pmatrix} 0 & -\sigma^i \\ \sigma^i & 0 \end{pmatrix}, \tag{1.5}$$

where $\sigma^i$ are the Pauli matrices. Substituting $p_\mu$ with $i\partial_\mu$ into Eq. (1.4)

$$(i\gamma^\mu \partial_\mu - m)\psi = 0. \tag{1.6}$$

This equation is a 1st order differential equation. With $(-i\gamma^\mu \partial_\mu - m)$ acting on the LHS of the equation shows that the Dirac equation implies the Klein Gordon equation

$$(-i\gamma^\mu \partial_\mu - m)(i\gamma^\nu \partial_\nu - m)\psi = (\gamma^\mu \gamma^\nu \partial_\mu \partial_\nu + m^2)\psi = 0. \tag{1.7}$$

In order for $\psi$ to satisfy the Klein-Gordon equation, Eq.(1.3), which can be written in the form

$$(g^{\mu\nu} \partial_\mu \partial_\nu + m^2)\psi = 0, \tag{1.8}$$

where $g^{\mu\nu}$ is a four-by-four diagonal matrix $g^{\mu\nu} = diag(1, -1, -1, -1)$, the $\gamma^\mu$ matrices must satisfy,

$$\{\gamma^\mu, \gamma^\nu\} = 2g^{\mu\nu}, \tag{1.9}$$

---

[1]The interpretation of negative energy states can be explained by Feynman-Stueckelberg picture where its interpretation does not appeal to the exclusion principle but rather to a causality principle. Causality ensures that positive energy states with time dependence $e^{-iEt}$ which propagate forwards in time is equivalent by imposing a negative energy states propagating backwards in time $e^{-i(-E)(-t)} = e^{-iEt}$. This is an acceptable theory which is consistent with causality. We can simply view that the emission of a negative energy state particle with momentum $p^\mu$ can be interpreted as the absorption of a positive energy antiparticle with opposite momentum $-p^\mu$. Note that Dirac's sea picture which is also an attempt to explain negative energy states does not work for bosons as they do not obey Pauli exclusion principle.

as $\gamma^\mu\gamma^\nu + \gamma^\nu\gamma^\mu = 0$ for $\mu \neq \nu$.

We will now construct the probability current $j^\mu$ to check whether it is positive. Taking the Hermitian conjugate of Eq.(1.6), this gives

$$\psi^\dagger(-i\gamma^0\overleftarrow{\partial_0} + i\gamma^i\overleftarrow{\partial_i} - m) = 0. \tag{1.10}$$

$\psi^\dagger$ is row vector and the $\leftarrow$ shows that the operation is performed to the left. Multiplying by $\gamma^0$ and using $\gamma^i\gamma^0 = -\gamma^0\gamma^i$, gives

$$\bar{\psi}(-i\gamma^\mu\overleftarrow{\partial_\mu} + m) = 0. \tag{1.11}$$

$\bar{\psi} = \psi^+\gamma^0$ is the adjoint spinor. Using Eqs. (1.6, 1.11), the current $j^\mu = \bar{\psi}\gamma^\mu\psi$ is conserved

$$\partial_\mu j^\mu = 0. \tag{1.12}$$

The current density $j^0$ is therefore

$$j^0 = \bar{\psi}\gamma^0\psi = \psi^+\psi = |\psi_1|^2 + |\psi_2|^2 + |\psi_3|^2 + |\psi_4|^2, \tag{1.13}$$

and *always positive* as it is made up of the combination of absolute values. $j^0$ is fit to be the probability density for the particle which shows the Dirac equation is preferred to the Klein-Gordon equation in this respect.

## 1.3 Dirac Spinors

The Dirac field $\psi$ [1, 2] can be written as a combination of plane-wave solutions since it obeys the Klein-Gordon equation.

$$\psi(x) = u(p)e^{-ip.x}, \tag{1.14}$$

where $p^2 = m^2$. Here we denote $\psi$ as a function of $x$. Plugging in $\psi(x)$ into the Eq. (1.4),

$$(\gamma^\mu p_\mu - m)u(p) = 0. \tag{1.15}$$

This equation is best analyzed in the rest frame, taking the index $i = 0$. $p_\mu$ in the rest frame $p_0 = (m, \mathbf{0})$

$$(m\gamma^0 - m)u(p_0) = m \begin{pmatrix} -1 & 1 \\ 1 & -1 \end{pmatrix} u(p_0) = 0. \tag{1.16}$$

The solutions to this equation are

$$u(p_0) = \sqrt{m} \begin{pmatrix} \xi \\ \xi \end{pmatrix}. \tag{1.17}$$

$\xi$ is a 2-component spinor which is normalized such that $\xi^\dagger \xi = 1$. The factor $\sqrt{m}$ was chosen for future convenience. For further reading on the spinor $\xi$, rapidity $\eta$ and boost in detail, refer to [2].

Applying a boost to $u(p)$ and after some algebraic manipulation and simplification

$$\begin{aligned} u(p) &= exp\left[ -\frac{1}{2}\eta \begin{pmatrix} \sigma^3 & 0 \\ 0 & -\sigma^3 \end{pmatrix} \right] \sqrt{m} \begin{pmatrix} \xi \\ \xi \end{pmatrix} \\ &= \begin{pmatrix} \left( \sqrt{E + p^3}(\frac{1-\sigma^3}{2}) + \sqrt{E - p^3}(\frac{1+\sigma^3}{2}) \right) \xi \\ \left( \sqrt{E + p^3}(\frac{1+\sigma^3}{2}) + \sqrt{E - p^3}(\frac{1-\sigma^3}{2}) \right) \xi \end{pmatrix} \\ &= \begin{pmatrix} \sqrt{p.\sigma}\xi \\ \sqrt{p.\overline{\sigma}}\xi \end{pmatrix}. \end{aligned} \tag{1.18}$$

where we have used the boost generator

$$S^{0i} = \frac{i}{4}[\gamma^i, \gamma^j] = -\frac{i}{2} \begin{pmatrix} \sigma^i & 0 \\ 0 & -\sigma^i \end{pmatrix}. \tag{1.19}$$

In summary, the general solution for a positive-frequency wave can be written as a linear combination of plane waves,

$$\psi(x) = u(p)e^{-ip.x}, \qquad p^2 = m^2, \quad p^0 > 0. \tag{1.20}$$

Thus, there are two independent solution as the spinor $\xi$ can be spin up or spin down.

$$u^s(p) = \begin{pmatrix} \sqrt{p.\sigma}\xi^s \\ \sqrt{p.\overline{\sigma}}\xi^s \end{pmatrix}, \qquad s = 1, 2, \qquad \xi^1 = \begin{pmatrix} 1 \\ 0 \end{pmatrix}, \qquad \xi^1 = \begin{pmatrix} 0 \\ 1 \end{pmatrix}. \tag{1.21}$$

Applying it analogously to the negative-frequency solutions:

$$\psi(x) = v(p)e^{+ip.x}, \qquad p^2 = m^2, \quad p^0 > 0 \tag{1.22}$$

(It is impossible to set $p^0 < 0$, the logical approach is to add a $+$ sign into the exponential). The 2 independent solutions are

$$v^s(p) = \begin{pmatrix} \sqrt{p.\sigma}\xi^s \\ -\sqrt{p.\bar{\sigma}}\xi^s \end{pmatrix}, \qquad s = 1, 2. \tag{1.23}$$

These $u$ and $v$ spinors are spin eigenstates for particles and antiparticles, respectively.

## 1.4  SPIN SUMS

A crucial part of QED and QCD is the evaluation of Feynman Diagrams, which will involve a sum over the polarization states of a fermion.

$$\sum_{s=1,2} u^s(p)\bar{u}^s(p) = \sum_s \begin{pmatrix} \sqrt{p.\sigma}\xi^s \\ \sqrt{p.\bar{\sigma}}\xi^s \end{pmatrix} (\xi^{s\dagger}\sqrt{p.\bar{\sigma}}, \xi^{s\dagger}\sqrt{p.\sigma}). \tag{1.24}$$

Using the relation below

$$\sum_{s=1,2} \xi^s\xi^{s\dagger} = \mathbf{1} = \begin{pmatrix} 1 & 0 \\ 0 & 1 \end{pmatrix}. \tag{1.25}$$

Thus, we obtain the completeness relations

$$\sum_{s=1,2} u^s(p)\bar{u}^s(p) = \gamma.p + m, \tag{1.26}$$

$$\sum_{s=1,2} v^s(p)\bar{v}^s(p) = \gamma.p - m. \tag{1.27}$$

$\gamma.p$ occurs very often and is useful to introduce a new notation $\not{p} = \gamma^\mu p_\mu$.

## 1.5  GAUGE INVARIANCE AND NOETHER'S THEOREM

Quantum Field Theory (QFT) can provide a clear description of all the fundamental interactions with the exception of gravity.

We define a field theory as a three dimensional space time 4-vector field; for example is the gravitational field which takes the value of a vector everywhere. The action $\mathcal{S}$ defined by the Hamiltonian principle (a particle travels with the least action between two points) is the integral of the Lagrangian density $\mathcal{L}$

$$\mathcal{S} = \int \mathcal{L} d^4 x. \tag{1.28}$$

Let us define the Lagrangian density in field theory as, $\mathcal{L}$, a function of the auxiliary fields $(\phi_j)$, and their derivatives with respect to space and time $(\partial \phi_j / \partial x^\mu)$

$$\mathcal{L} = \mathcal{L}(\phi_j, \frac{\partial \phi_j}{\partial x^\mu}), \tag{1.29}$$

with the subscript $j$ labeling different fields, and the standard $x^\mu$ which denotes the space time coordinates with indices $\mu = 0, 1, 2, 3$. 0 denotes time while $1, 2, 3$ denotes the 3-dimensional spatial coordinates. Using Hamilton's Principle of least action, the Lagrangian density should remain unchanged with respect to the field(s) as well as to a change in the field(s); this leads to the E-L equations,

$$\partial_\mu (\frac{\partial \mathcal{L}}{\partial (\partial_\mu \phi_j)}) - \frac{\partial \mathcal{L}}{\partial \phi_j} = 0, \tag{1.30}$$

where $\partial_\mu$ denotes the partial derivative with respect to $x^\mu$.

Noether's theorem states that global gauge invariance is equivalent to the conservation of a current. Consider a complex scalar field theory given by

$$\mathcal{L} = \partial_\mu \phi^* \partial^\mu \phi - m^2 \phi^* \phi. \tag{1.31}$$

The $\mathcal{L}$ remains invariant under the global transformation $\phi \longrightarrow \phi' = \phi e^{i\alpha}$, for a constant $\alpha$. Assuming that $\alpha$ is infinitesimally small, $\phi' = \phi + i\alpha\phi$, thus, the Lagrangian density is changed by

$$\frac{\partial \mathcal{L}}{\partial \phi} i\alpha\phi + \frac{\partial \mathcal{L}}{\partial (\partial_\mu \phi)} i\alpha \partial_\mu \phi + c.c, \tag{1.32}$$

$c.c$ denotes its complex conjugate. For global gauge invariance of $\mathcal{L}$, this must be equal to zero up to an $\alpha^2$ term. Applying the E-L equation for the field, the terms with $\alpha$ to the first power are

$$\alpha \partial_\mu (\frac{\partial L}{\partial (\partial_\mu \phi)}) + c.c = 0. \tag{1.33}$$

This shows that the current density is conserved

$$\begin{aligned} j^\mu &= i(\phi \partial_\mu \phi^* - \phi^* \partial_\mu \phi) \\ \partial_\mu j^\mu &= 0 \, . \end{aligned} \tag{1.34}$$

## 1.6 LORENTZ INVARIANCE OF WAVE EQUATION

In this section, we will discuss the definition of "relativistically invariant" when addressing an equation. A field or a collection of fields denoted by $\phi$ with an operator $\mathcal{D}$ acting on $\phi$ is said to be "relativistically invariant" if $\phi$ satisfies $\mathcal{D}\phi = 0$, and when we apply a boost or rotation to the field to a different frame of reference, the transformed field will still satisfy the same equation.

Thus, by the definition above, the equation of motion is Lorentz invariant if the Lagrangian is a Lorentz scalar. Let us consider the Klein-Gordon equation, the corresponding Lorentz transformation is given by

$$x^\mu \longrightarrow x^{'\mu} = \Lambda^\mu_\nu x^\nu, \tag{1.35}$$

for some $4 \times 4$ matrix $\Lambda$. Assuming, we transform $x$ by a boost, the transformed field is then

$$\phi(x) \longrightarrow \phi'(x) = \phi(\Lambda^{-1}x'). \tag{1.36}$$

The equation shows that the transformed field (evaluated at a boosted point) is equivalent to the original field (evaluated before boosting).

Note that the Klein-Gordon Lagrangian remains unchanged after Lorentz transformation. The derivative of the field transforms such that

$$\partial_\mu \phi(x) \longrightarrow \partial'_\mu(\phi(\Lambda^{-1}x')) = (\Lambda^{-1})^\nu_\mu (\partial_\nu \phi)(\Lambda^{-1}x'). \tag{1.37}$$

Note that one of the properties of metric tensor $g^{\mu\nu}$ is that it is Lorentz invariant, the inverse matrices $\Lambda^{-1}$ must obey the identity

$$(\Lambda^{-1})^\rho_\mu (\Lambda^{-1})^\sigma_\nu g^{\mu\nu} = g^{\rho\sigma}, \tag{1.38}$$

while the transformation for the kinetic term of the Klein-Gordon Lagrangian is

$$\begin{aligned} (\partial_\mu \phi(x))^2 &\longrightarrow g^{\mu\nu}(\partial_\mu \phi'(x))(\partial_\nu \phi'(x)) \\ &= g^{\mu\nu}[(\Lambda^{-1})^\rho_\mu \partial_\rho \phi][(\Lambda^{-1})^\sigma_\nu \partial_\sigma \phi](\Lambda^{-1}x') \\ &= g^{\rho\sigma}(\partial_\rho \phi)(\partial_\sigma \phi)(\Lambda^{-1}x') \\ &= (\partial_\rho \phi)^2(\Lambda^{-1}x'). \end{aligned} \tag{1.39}$$

Thus the Lagrangian remains unchanged

$$\mathcal{L}(x) \longrightarrow \mathcal{L}(\Lambda^{-1}x'). \tag{1.40}$$

Consequently, the action $\mathcal{S}$ found by integrating $\mathcal{L}$ over space time, is Lorentz invariant. We now show that the equation of motion is also Lorentz invariant

$$
\begin{aligned}
(\partial^2 + m^2)\phi'(x) &= [g^{\mu\rho}(\Lambda^{-1})^{\nu}_{\mu}\partial_{\nu}(\Lambda^{-1})^{\sigma}_{\rho}\partial_{\sigma} + m^2]\phi(\Lambda^{-1}x') \\
&= (g^{\nu\sigma}\partial_{\nu}\partial_{\sigma} + m^2)\phi(\Lambda^{-1}x') \\
&= 0.
\end{aligned} \tag{1.41}
$$

Eq. (1.36) is the simplest transformation law for a field with just one component $\phi(x)$. Of course, we know examples of other multi-component fields which transform in a much complicated manner, in particular vector fields like the vector potential $A^{\mu}(x)$. Quantities distributed in space time are oriented by performing boost or rotation, by expressing them in the form of tensors which also obey the transformation law. Using such tensor fields, a variety of Lorentz invariant equations can be written, a simple example is the Maxwell's equation

$$\partial^{\mu}F_{\mu\nu} = 0, \quad \text{or} \quad \partial^2 A_{\nu} - \partial_{\nu}\partial^{\mu}A_{\mu} = 0. \tag{1.42}$$

## 1.7 Local Gauge Transformation

The Lagrangian density for a Dirac field is

$$\mathcal{L}_{Dirac} = \overline{\psi}(i\gamma_{\mu}\partial^{\mu} - m)\psi. \tag{1.43}$$

The Dirac equation which describes free fermions in relativistic quantum mechanics follows from the E-L equation for the field $\psi$. Under local gauge transformation $\psi \longrightarrow \psi' = \psi e^{i\alpha(x)}$, there will be an extra term $\overline{\psi}\gamma_{\mu}(\partial^{\mu}\alpha)\psi$ in the free Dirac Lagrangian. Nevertheless, the Lagrangian should remain invariant and by replacing $\partial_{\mu}$ with the term $\partial_{\mu} + ieA^{\mu}$ in Eq. (1.43), the Lagrangian density will then remain invariant under the transformation $\psi \longrightarrow \psi' = \psi e^{i\alpha(x)}$ with the condition that the new field transforms from $A_{\mu} \longrightarrow A'_{\mu} = A_{\mu} - \frac{1}{e}\partial_{\mu}\alpha$. $A_{\mu}$ is an electromagnetic field. For a free field

$$
\begin{aligned}
\mathcal{L}_{Maxwell} &= -\frac{1}{4}F^{\mu\nu}F_{\mu\nu}, \\
F_{\mu\nu} &= \partial_{\mu}A_{\nu} - \partial_{\nu}A_{\mu},
\end{aligned} \tag{1.44}
$$

which remains invariant under the transformation $A_\mu \longrightarrow A'_\mu = A_\mu - \frac{1}{e}\partial_\mu\alpha$. Using Eqs. (1.43, 1.44), the E-L equation for $A_\mu$ is

$$\partial_\mu F^{\mu\nu} = ej^\nu,$$
$$j^\mu = \overline{\psi}\gamma^\mu\psi. \tag{1.45}$$

This is Maxwell's inhomogeneous equations in the presence of a current, the current is also conserved by Noether's theorem. $e$ is a constant which is the magnitude of the charge. In the case for several Dirac fields, the fields charge Q should appear in the transformation for the Dirac field $\psi \longrightarrow \psi e^{iQ\alpha(x)}$ as well as the Lagrangian density $\partial_\mu + ieQA_\mu$. The electron has a charge of $Q = -1$ and a proton has a charge $Q = +1$.

Quantum Electrodynamics (QED), the quantum field theory of electromagnetism, results from combining separate field theories of free fields. Demanding invariance under the local gauge transformation has introduced interactions given by $j^\mu A_\mu$ which will appear in the Lagrangian density in addition to the free (non-interacting) field theory terms. In order to also have a better description of the real world, we must include non-linear terms into the Hamiltonian. Thus the Interacting Hamiltonian will be given by

$$H_{int} = \int d^3x \mathcal{H}_{int}[\phi(x)] = -\int d^3x \mathcal{L}_{int}[\phi(x)], \tag{1.46}$$

with the corresponding interaction Lagrangian (for further reading [2]) given by

$$\mathcal{L}_{int} = -eQ\overline{\psi}\gamma^\mu\psi A_\mu. \tag{1.47}$$

The E-L equation for the Dirac field with the interacting field is now given by

$$(i\slashed{D} - m)\psi = 0, \tag{1.48}$$

where we use the notation $\slashed{D} = \gamma^\mu D_\mu$, with

$$D_\mu = \partial_\mu - ieQA_\mu. \tag{1.49}$$

$D_\mu = \partial_\mu + ieA_\mu$ is the gauge covariant derivative which transforms under Lorentz Gauge Transformation such that $(D_\mu\psi) = D'_\mu\psi' = e^{i\alpha(x)}(D_\mu\psi)$, so $(D_\mu\psi)$ transforms in the same way as the field $\psi$ itself.

The QED Lagrangian is given by

$$\begin{aligned}
\mathcal{L}_{QED} &= \mathcal{L}_{Maxwell} + \mathcal{L}_{Dirac} + \mathcal{L}_{int}, \\
\mathcal{L}_{QED} &= -\frac{1}{4}F^{\mu\nu}F_{\mu\nu} + \overline{\psi}(i\slashed{D} - m)\psi,
\end{aligned} \qquad (1.50)$$

where

$$[D_\mu, D_\nu]\psi = -ieF_{\mu\nu}\psi, \qquad (1.51)$$

$$F_{\mu\nu} = \partial_\mu A_\nu - \partial_\nu A_\mu. \qquad (1.52)$$

## 1.8 QED Lagrangian and Feynman Rules

Quantum Electrodynamics (QED) is an abelian gauge theory. The electromagnetic field act as a mediator for the interaction between the charged $\psi$ spin-1/2 fields. The QED Lagrangian is given by

$$\mathcal{L}_{QED} = -\frac{1}{4}F_{\mu\nu}F^{\mu\nu} + \overline{\psi}(i\slashed{D} - m)\psi - \frac{1}{2\xi}(\partial^\mu A_\mu)^2, \qquad (1.53)$$

with their corresponding Feynman rules
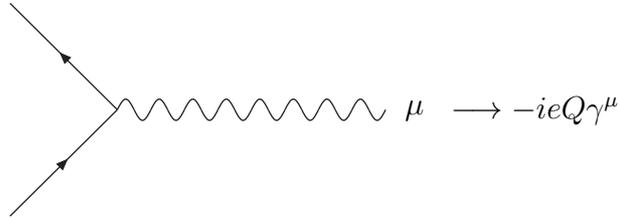


Figure 1.1: *QED vertex*
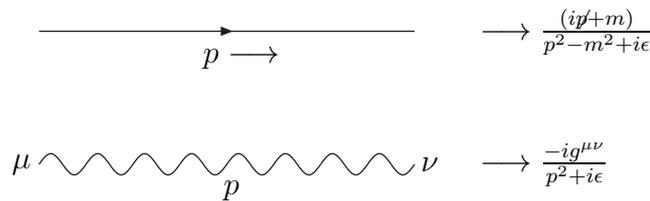


Figure 1.2: *QED Propagators*
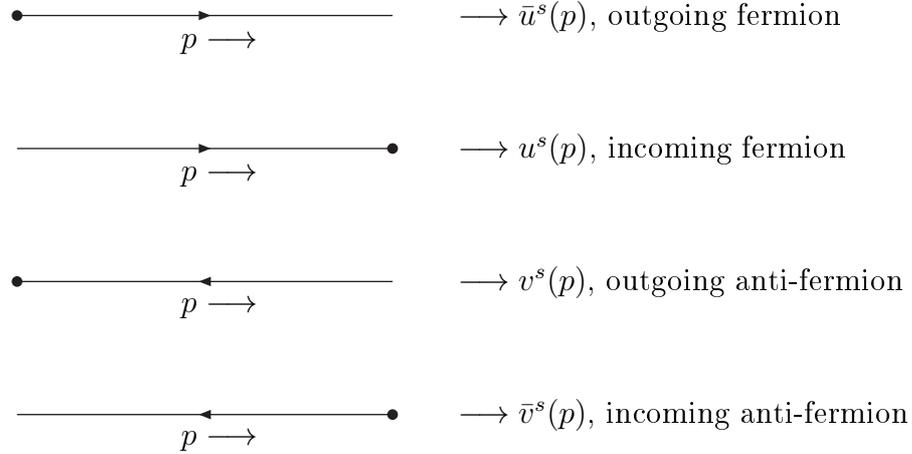
Figure 1.3: *External Fermions*
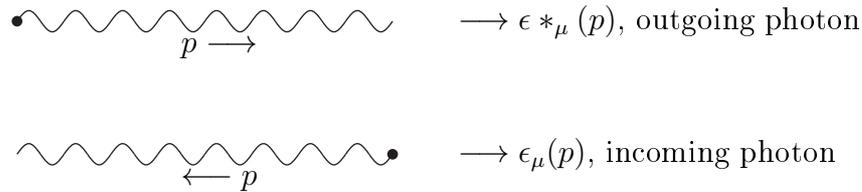


Figure 1.4: *External Photons*

$\psi$ obeys the covariant derivative expression of Eq. (1.51) and $A_\mu$ photon field is related to the electromagnetic tensor Eq. (1.52). The spinors and their conjugates obey the Dirac equation. The direction of the arrow shows whether they are fermions or anti-fermions with the vertex having an arrow coming in and the other coming out to keep the same number of fermions and antifermions.

One also has to impose momentum conservation at each vertex and to integrate for each undetermined loop momentum $\int \frac{d^4 p}{(2\pi)^4}$. Finally one needs to divide by the symmetry factor. Note also that the QED vertex, photon propagator as well as the external fermions (polarization vectors and its conjugate initial- or final-state photon) arises from the interaction Lagrangian $\mathcal{L}_{int}$.

It is impossible to obtain the photon propagator from the first two terms of the Lagrangian as the inverted matrix has zero determinant [3]. This is

due to gauge invariance but in order to have a defined photon propagator, we need to fix the gauge by adding a gauge-fixing term

$$-\frac{1}{2\xi}(\partial_\mu A^\mu)^2. \tag{1.54}$$

$\xi$ is the gauge-fixing parameter defining a class of covariant gauges satisfying the Lorentz condition $\partial_\mu A^\mu = 0$, $\xi = 1$ corresponds to Feynman gauge and $\xi = 0$ to Landau gauge. The third term does not change physics: physical results are gauge-invariant and gauge-independant. The complication that arises is not easily defined but the photon propagator should be the solution for the function $D_{\mu\rho}(x, y)$ such that

$$(\Box g^{\mu\nu} - \partial^\mu\partial^\nu)\int d^4y D_{\mu\rho}(x,y)A(y) = ig_\rho^\nu A(x). \tag{1.55}$$

$A(x)$ is an arbitrary function. Eq. (1.55) has no solution. Adding the term Eq. (1.54) into the Lagrangian alters Eq. (1.55) to

$$(\Box g^{\mu\nu} - (1 - 1/(\xi))\partial^\mu\partial^\nu)\int d^4y D_{\mu\rho}(x,y)A(y) = ig_\mu^\nu A(x). \tag{1.56}$$

Eq. (1.56) has the solution

$$D_{\mu\nu}(x,y) = \int \frac{d^4k}{(2\pi)^4} \frac{-id_{\mu\nu}(k)}{k^2 + i\epsilon} e^{-ik.(x-y)}, \tag{1.57}$$

where $d_{\mu\nu} = g_{\mu\nu} - (1 - \xi)\frac{k_\mu k_\nu}{k^2}$. A more straightforward derivation proposed in [1] is to consider

$$\begin{aligned} \mathcal{L} &= \mathcal{L}_{classical} + \mathcal{L}_{gauge-fixing}, \\ &= \frac{1}{2}A^\mu \left[ g_{\mu\nu}\Box + \left(\frac{1}{\xi} - 1\right)\partial_\mu\partial_\nu \right] A^\nu. \end{aligned} \tag{1.58}$$

Taking $\xi$ to be finite, the quadratic operator in momentum space is

$$-k^2 g_{\mu\nu} + \left(1 - \frac{1}{\xi}\right)k_\mu k_\nu, \tag{1.59}$$

and its corresponding inverse gives the propagator

$$D(k)_{\mu\nu} = -\frac{1}{k^2}\left[ g_{\mu\nu} + (\xi - 1)\frac{k_\mu k_\nu}{k^2} \right]. \tag{1.60}$$

$\xi$ is an arbitrary parameter, thus results from QED calculations for physical quantities are totally independent of $\xi$. Note that we have used Feynman gauge in defining the photon propagator in Fig. (1.2).

## 1.9 QCD Lagrangian and Feynman Rules

Just as in QED, the calculation of physical process in QCD requires Feynman rules which describe the interactions of quarks and gluons. The Lagrangian [4] which describes strong interactions is given by

$$\mathcal{L}_{QCD} = \mathcal{L}_{classical} + \mathcal{L}_{gauge-fixing} + \mathcal{L}_{ghost}. \tag{1.61}$$

This Lagrangian is based on the SU(N) group non-abelian gauge theory. The classical part of the QCD Lagrangian density is given by

$$\mathcal{L}_{classical} = \sum_f \overline{\psi}_{f,i}(i\gamma_\mu D^\mu_{i,j} - m_f \delta_{i,j})\psi_{f,j} - \frac{1}{4}F_a^{\mu\nu}F^a_{\mu\nu}. \tag{1.62}$$

$f$ is the number of quark flavours. $\psi_{f,i}$ is the quark field (fundamental representation) with colour index $i = 1, \ . \ . \ . \ ,N$ and $A^a_\mu$ is the gluon field (adjoint representation) runs over $N^2 - 1$ degrees of freedom $a = 1, \ . \ . \ . \ ,N^2$ - 1 described by $SU(N)$ group. As in QED, the $\gamma_\mu$ satisfy the Dirac anti commutation relation

$$\{\gamma^\mu, \gamma^\nu\} = \gamma^\mu\gamma^\nu + \gamma^\nu\gamma^\mu = 2g^{\mu\nu}. \tag{1.63}$$

The covariant derivative in the non-abelian gauge theory is defined as

$$D^\mu_{ij} = \partial^\mu \delta_{ij} - igA^\mu_a T^a_{ij}. \tag{1.64}$$

$g$ is the strong coupling constant which determines the strength of interaction between quanta. $T^a$ are matrices which can be expressed in the form of Hermitian traceless Gell-Mann matrices. They are generators of the SU(N) group which satisfy the commutation relation

$$[T^a, T^b] = if_{abc}T^c, \tag{1.65}$$

where $f_{abc}$ are the structure constant. As in QED, the commutator of two covariant derivatives is related to the field strength tensor $F^a_{\mu\nu}$ of the gluon fields, from which we can build the kinetic energy part in the classical Lagrangian of QCD,

$$[D_\mu, D_\nu] = iT^a F^a_{\mu\nu}, \tag{1.66}$$

$$tr(T^a T^b) = \frac{1}{2}\delta^{ab}, \tag{1.67}$$

$$\sum T^a_{ij}T^a_{jk} = C_F \delta_{ik}, \ \ C_F = \frac{N^2 - 1}{2N}, \tag{1.68}$$

where

$$F^a_{\mu\nu} = \partial_\mu A^a_\nu - \partial_\nu A^a_\mu + g f_{abc} A^b_\mu A^c_\nu. \tag{1.69}$$

Unlike photons in QED, the non-abelian property of the last term in Eq. (1.69) gives rise to triplet and quartic gluon self interactions and also asymptotic freedom. Note that the Lagrangian has mass dimension of 4, thus it should follow that $\psi$ and $A^a_\mu$ have mass dimensions of 3/2 and 1 separately. As required, $\mathcal{L}$ should be locally gauge invariant and all of their components transform under these local gauge transformations,

$$\psi_f \longrightarrow \Lambda(x)\psi_f, \tag{1.70}$$

$$T^a A^a_\mu \longrightarrow \Lambda(x)\left(T^a A^a_\mu - \tfrac{i}{g}\Lambda^{-1}(x)\partial_\mu\Lambda(x)\right)\Lambda^{-1}(x), \tag{1.71}$$

$$\Lambda(x) = exp(-iT^a\theta^a(x)), \tag{1.72}$$

where $\theta^a(x)$ is a space time dependent function. Like QED, a gauge fixing term which satisfies the *Lorentz gauge* condition $\partial_\mu A^{a\mu} = 0$ has to be added. The physical reason for such a choice is to put a constraint on $A^a_\mu$ (which has 2 polarization states) to avoid any unphysical states

$$\mathcal{L}_{gauge-fixing} = -\frac{1}{2\xi}(\partial^\mu A^a_\mu)^2. \tag{1.73}$$

In QCD, the longitudinal part of the gluon field can interact with the transverse (physical) component of $A^a_\mu$, this results in gluon loops and a subtraction is of these contributions is necessary. Therefore, we will now introduce a ghost field called the Faddeev-Popov ghost which acts like a scalar field.

$$\mathcal{L}_{ghost} = (\partial_\mu \eta^{a*})(\partial^\mu \delta_{ab} + g f_{abc} A^\mu_c)\eta^b. \tag{1.74}$$

The origin of the Faddeev-Popov ghosts is to ensure consistency with the path integral formulation which demands an unambiguous and non-singular solutions. The presence of gauge symmetry makes this impossible to construct. This is because there is no particular procedure for selecting a solution from a choice of equivalently physical solutions (all derived by gauge transformation). Such problem occurs from the path integrals overcounting field configurations due to gauge symmetries. This will correspond to the same physical state as the measurement of the path integrals contain factors prohibiting to extract various results from the action obtained from the Feynman diagrams. One possible choice is to modify the action by applying

additional fields, breaking the gauge symmetry as a consequence. Such technique is called the Faddeev-Popov procedure with the additional fields being called the ghost fields. Ghosts field do not interpret into any physical real particle in the external states. Their appearance only in the form of virtual particles in Feynman diagrams. Nevertheless, their presence are a necessity to preserve unitarity of the S-matriix. The approach in the formulation of ghosts varies and is dependent on the choice of gauge, however, the same results must be obtained for all choices. The simplest choice for this purpose is the Feynman-'t Hooft gauge.

Thus, we have the final form of the Lagrangian

$$\mathcal{L}_{QCD} = \sum_f \overline{\psi}_{f,i}(i\gamma_\mu D^\mu - m_f \delta_{i,j})\psi_{f,j} - \frac{1}{4}F_a^{\mu\nu}F_{\mu\nu}^a - \frac{1}{2\xi}(\partial^\mu A_\mu^a)^2 + (\partial_\mu \eta^{a*})D_{ab}^\mu \eta_b.$$

$$(1.75)$$

where $\eta^a$ is a complex scalar field obeying Fermi statistics. The Feynman rules corresponding to this QCD Lagrangian are



$$\longrightarrow \frac{(i\not{p}+m)}{p^2+m^2+i\epsilon}$$

Figure 1.5: *Quark propagator*



$$\longrightarrow \frac{-i\delta^{ab}}{p^2+i\epsilon}\left(g^{\mu\nu} - (1-\xi)\frac{p^\mu p^\nu}{p^2}\right)$$
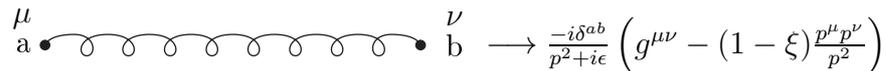
Figure 1.6: *Gluon propagator*



$$\longrightarrow \frac{-i\delta^{ab}}{p^2+i\epsilon}$$
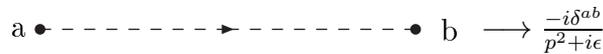
Figure 1.7: *Ghost propagator*

$$\longrightarrow ig\gamma^{\mu}T^a$$
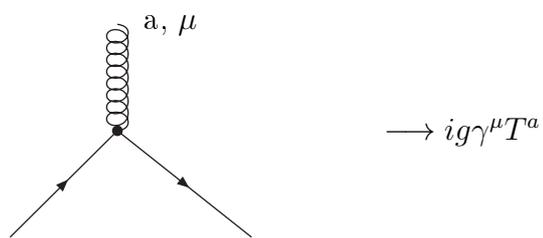
Figure 1.8: *Quark-Gluon Vertex*



$$\longrightarrow gf^{abc}[g^{\mu\nu}(k-p)^{\rho}$$
$$-g^{\nu\rho}(p-q)^{\mu}+g^{\rho\mu}(q-k)^{\nu}]$$
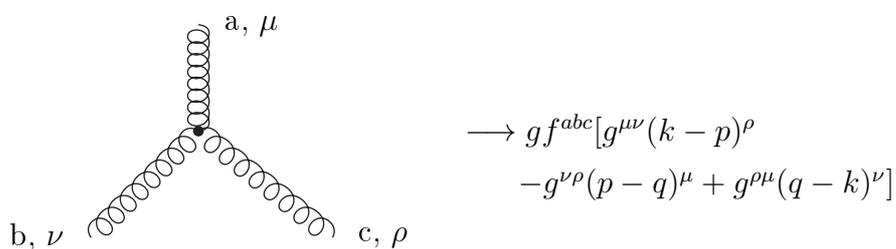
Figure 1.9: *3-Gluon Vertex*



$$\longrightarrow -gf^{abc}p^{\mu}$$

Figure 1.10: *Gluon-Ghost Vertex*



$$\longrightarrow g^2[f^{abc}f_{cde}g^{\mu\rho}g^{\nu\sigma}-g^{\mu\sigma}g^{\nu\rho}$$
$$+f^{ace}f_{bde}(g^{\mu\nu}g^{\rho\sigma}-g^{\mu\sigma}g^{\nu\rho})$$
$$+f^{ade}f_{bce}(g^{\mu\nu}g^{\rho\sigma}-g^{\mu\rho}g^{\nu\sigma})]$$

Figure 1.11: *4-Gluon Vertex*

## 1.10 SUMMARY

Quantum field theory (QFT) is an essential guide in constructing quantum mechanical models of systems parametrized by an infinite number of dynamical degrees of freedom and variables, that is, fields and spinors in QED and QCD. It is found that the forces between particles are mediated by the presence of other particles. In QED, the electromagnetic force is mediated by the exchange of photons, in QCD gluons mediate the strong force. In this Chapter, we briefly summarized the important points selected from various textbooks of QFT which are relevant to the topic of this research.

We reviewed the fundamentals of relativistic quantum mechanics where we can write a wave equation for scalar particles. The energy and momentum operator is analogous to the ones in Classical Mechanics and the wave equation is the Klein-Gordon equation. Nevertheless, the equation has a probability which is not positive definite and there is the possibility of the occurrence of negative energy states. The interpretation on negative energy states was discussed using the Feynman-Stueckelberg picture base on the principle of causality. The Dirac equation was introduced as an extra equation to be satisfied in addition to the Klein-Gordon equation. The Dirac current density is a combination of absolute values implying that it will always be positive, although there are still negative energy states which correspond to antiparticles. It was through Dirac's equation that the prediction of antiparticles was made and they were subsequently found. This seems a good indicator that particle physics is on the right track experimentally.

The Dirac field obeys the Klein-Gordon equation and can be expressed as a combination of plane-wave solutions. Plugging this solutions into the Dirac equation provides us a four component spinor which obeys the rotation and boost generators. Considering the positive and negative frequency and the spinor $\xi$ which might be spin up or down. There will be four spinors 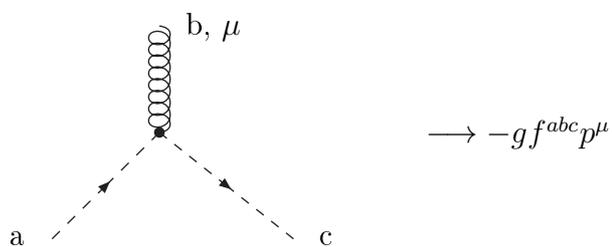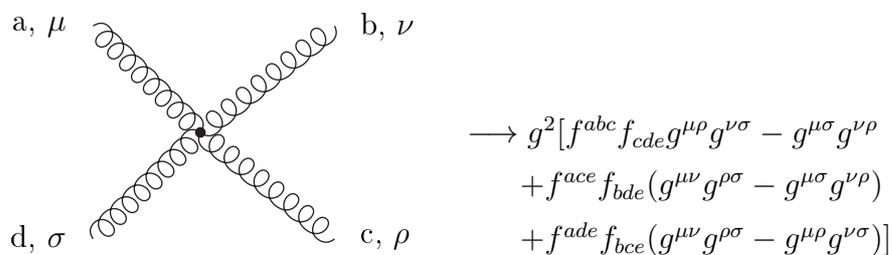altogether. A crucial part of QED and QCD is the evaluation of the Feynman Diagrams which we sum over the polarization states of the fermions.

We define a field as a 3-dimensional 4-vector field, for example is the gravitational field which takes the value of a vector everywhere. Hamilton's Principle of least actions states that particle travels with the least action between two points. The action $\mathcal{S}$ is the integral of the Lagrangian density $\mathcal{L}$, a function of auxiliary fields. Using the Lagrangian of the Klein-Gordon equation as an example, the conserved current can be derived from its E-L equation since there is a global symmetry for the field, undergoing global

gauge transformations. Such transformations do not alter the action. This is due to Noether's theorem which states that the global symmetry is equivalent to the conservation of current.

A field is "relativistically invariant" if an operator acting on the field satisfies $\mathcal{D}\phi = 0$, and when we apply rotations or boosts to the field in different frames of reference, the transformed field will still satisfy $\mathcal{D}\phi' = 0$. We show that the Klein-Gordon equation is relativistically Lorentz invariant under rotations and boosts along the axis. In short, quantity distributed in space time is oriented by performing rotation or boost by expressing them in the form of tensors which also obeys the transformation law. Many examples can be made, a famous one is the Maxwell's equation.

We further showed that the Dirac Lagrangian is invariant under gauge transformations. Demanding invariance under local gauge transformation has introduced an interaction term. Thus, this non linear interaction term is added to the Lagrangian. This interaction term is then absorbed into the Dirac equation since its partial derivative is modified into a covariant derivative. Finally, in order to have a gauge independent and gauge invariant Lagrangian, $-\frac{1}{2\xi}(\partial^\mu A_\mu)^2$ is added to the Lagrangian where the choice of the gauge fixing parameter $\xi$ will not alter the physics. The sets of Feynman Rules can be read directly from the QED Lagrangian.

QED is based on an abelian theory but QCD in contrast is derived from non-abelian theory. In QCD, the existence of the gluon field give rise to triplet and quartic interactions gluon self interactions and ultimately asymptotic freedom. Similarly like in QED, a gauge fixing Lagrangian is also needed but a further complication occurs since unphysical gluon polariztion states can propagate . To remedy this a ghost field is then introduced called the Fadeev-Popov ghost which acts like a scalar field. This also ensures that the unitarity of the S-matrix is not violated. The sets of Feynman Rules can be read directly from the QCD Lagrangian.

# Chapter 2

# Perturbative QCD

## 2.1 Dimensional Regularization

In computing Feynman diagrams beyond the tree-level one inevitably encounters divergences when one integrates over undetermined loop momenta. One encounters both ultraviolet (UV) and infra-red (IR) divergences from the large and small momentum regions, respectively. To control these one needs to "renormalize" the theory, introducing infinite so-called counterterms to convert the infinite parameters (masses, couplings, charges) in the original "bare" Lagrangian to finite "renormalized" parameters. This procedure involves a "renormalization procedure" or renormalization scheme (RS). An essential ingredient is that of "regularization". To handle such divergences the simplest approach is to introduce an upper cutoff on the loop-momenta integrated over. This is referred to as "Pauli-Villars" regularization. We shall work with a more sophisticated approach called "dimensional regularization" which has the major merit of manifestly preserving gauge invariance, which is violated with the naive Pauli-Villars method.

To understand "dimensional regularization", it is best to see how this technique works at the calculational level. A $d$-dimensional space time has 1 time dimension and ($d$-1) space dimensions. We Wick[1]-rotate the Feynman integral over a $d$-dimensional Euclidean space, consider

$$\int \frac{d^d l_E}{(2\pi)^d} \frac{1}{(l_E^2 + \triangle)^2} = \int \frac{d\Omega_d}{(2\pi)^d} \int_0^\infty dl_E \frac{l_E^{d-1}}{(l_E^2 + \triangle)^2}, \qquad (2.1)$$

---

[1]Wick's rotation is a method of solving problem in a Minkowski space from a solution to a problem in an Euclidean space by substituting a real variable with an imaginary variable, example is $ds^2 = -(dt)^2 + dx^2 + dy^2 + dz^2 = dt^2 + dx^2 + dy^2 + dz^2$ by considering $t$ to be imaginary

where $\triangle = m^2 - x(1-x)q^2$. $x$ is the variable that occurs when combining denominators through introduction of Feynman parameter and is related to the shifted momentum $l = k + qx$. The first factor in Eq. (2.1) can be expressed as the area of a unit sphere in $d$ dimensions. We show the proof below

$$
\begin{aligned}
(\sqrt{\pi})^d & = \left(\int dx e^{-x^2}\right)^d = \int d^d x e^{-\sum_{i=1}^d x_i^2} \\
& = \int d\Omega_d \int_0^\infty dx x^{d-1} e^{-x^2} = \left(\int d\Omega^d\right) \frac{1}{2} \int_0^\infty d(x^2)(x^2)^{\frac{d}{2}-1} e^{-x^2} \\
& = \left(\int d\Omega_d\right) \frac{1}{2} \Gamma(d/2).
\end{aligned}
\tag{2.2}
$$

Thus the area of the unit sphere is

$$
\int d\Omega_d = \frac{2\pi^{d/2}}{\Gamma(d/2)}.
\tag{2.3}
$$

The second factor is algebraically derived as follows

$$
\begin{aligned}
\int_0^\infty dl \frac{l^{d-1}}{(l^2 + \triangle)^2} & = \frac{1}{2} \int_0^\infty d(l^2) \frac{(l^2)^{\frac{d}{2}-1}}{(l^2 + \triangle)^2} \\
& = \frac{1}{2} \left(\frac{1}{\triangle}\right)^{2-\frac{d}{2}} \int_0^1 dx x^{1-\frac{d}{2}} (1-x)^{\frac{d}{2}-1},
\end{aligned}
\tag{2.4}
$$

by making the substitution $x = \triangle/(l^2 + \triangle)$. By using the Beta function studied by Euler and Legendre

$$
\int_0^1 dx x^{\alpha-1}(1-x)^{\beta-1} = \frac{\Gamma(\alpha)\Gamma(\beta)}{\Gamma(\alpha+\beta)},
\tag{2.5}
$$

the integral is simply

$$
\int \frac{d^d l_E}{(2\pi)^d} \frac{1}{(l_E^2 + \triangle)^2} = \frac{1}{(4\pi)^{d/2}} \frac{\Gamma(2-\frac{d}{2})}{\Gamma(2)} \left(\frac{1}{\triangle}\right)^{2-\frac{d}{2}},
\tag{2.6}
$$

having evaluated Eq. (2.5) over the variable $x$. Since $\Gamma(z)$ has poles at $z = 0, -1, -2, -3, ....$, this integral also has a pole at $d = 4, 6, 8......$ Using the approximation

$$
\frac{1}{\Gamma(z)} = z e^{\gamma_E z} \prod_{n=1}^\infty \left(1 + \frac{z}{n}\right) e^{-z/n},
\tag{2.7}
$$

and $d = 4 - 2\epsilon =$ with $\gamma_E \approx 0.5722$ (Euler constant), the integral will be of the form

$$\int \frac{d^d l_E}{(2\pi)^d} \frac{1}{(l_E^2 + \triangle)^2} = \frac{1}{(4\pi)^2} \left( \frac{2}{\epsilon} - \log(\triangle) - \gamma_E + \log(4\pi) + \mathcal{O}(\epsilon) \right). \quad (2.8)$$

$1/\epsilon$ will still make the integral divergent when $\epsilon \longrightarrow 0$. This corresponds to a logarithmic divergence in the momentum integral which can be absorbed by using the Modified Minimal Subtraction Scheme ($\overline{MS}$) [5].

## 2.2 RENORMALIZATION THEORY

QCD and QED are renormalizable theories. After divergences are regularized, the troublesome divergent contributions correspond to redefining the fundamental constants of the theory like the coupling $g$ and quark masses $m$ in QCD. In other words, physical quantities are expressed in terms of renormalised parameters and do not involve any UV divergences anymore, examples are $g_{ren}$ and $m_{ren}$. The renormalised constants which depends on $\epsilon$ (dimensional regularization parameter), $g$ (the bare coupling ), $m$ (the bare mass) and $\mu$ (an arbitrary scale) absorb all such divergences.

Rigorously demonstrating the renormalizability of QED is a hard problem, and the non-abelian complications inherent in QCD make this an even harder problem. A good book to refer for a detailed demonstration of QED's renormalizability can be found in [1]. We will not demonstrate anything in detail here but we will provide rather a heuristic physical explanation. Large loop momenta produce UV divergences. In the event that the loop momenta are much larger than the characteristic external momenta, the loop loses its structure and can be considered as a point.
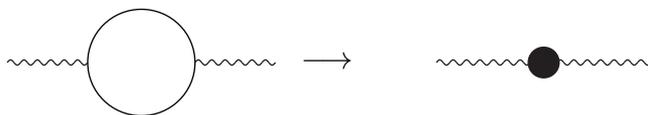


Figure 2.1: *Example of a counterterms*

Figure (2.1) shows the idea of renormalization. By considering the loop as a point, a new quadratic contribution to the Lagrangian emerges. Due to

Lorentz and gauge invariance, the contribution is of the form $\simeq (\partial_\mu A_\nu - \partial_\nu A_\mu)^2$.

Renormalizability is related to the notion of an effective Lagrangian, refer to [6] for more detail. To understand more clearly how this technique works it is useful to consider the QCD effective Lagrangian extracted from the Green's functions which can be obtained from the QCD Feynman diagrams,

$$
\begin{aligned}
\mathcal{L}^{eff} \;=\; & -\frac{1}{4Z_A}(\partial_\mu A_\nu^a - \partial_\nu A_\mu^a)^2 - \frac{g}{Z_{3A}} f^{abc}(\partial_\mu A_\nu^a) A^{b\mu} A^{c\nu} \\
& -\; \frac{g^2}{Z_{4A}} f^{abc} f^{cde} A_\nu^a A_\nu^b A^{\mu c} A^{\nu d} - \frac{1}{2\xi}(\partial^\mu A_\mu^a)^2 + \frac{1}{Z_\eta} \partial_\mu \bar{\eta}^a \partial^\mu \eta^a \\
& +\; \frac{g}{Z_{\bar{\eta}\eta A}} f^{abc} \partial^\mu \bar{\eta}^a A_\mu^b \eta^c + \frac{i}{Z_\psi} \bar{\psi}\,\not{\partial}\psi - \frac{m}{Z_m} \bar{\psi}\psi + \frac{g}{Z_{\bar{\psi}\psi A}} \bar{\psi}\psi A. \quad (2.9)
\end{aligned}
$$

$Z_{3A}$, $Z_{4A}$, $Z_{\bar{\eta}\eta A}$ and $Z_{\bar{\psi}\psi A}$ correspond to the 3-gluon, 4-gluon, ghost-ghost-gluon and quark-quark-gluon vertices renormalization parameters. $Z_A$, $Z_\psi$ and $Z_\eta$ corresponds to the gluon, quark and ghost propagators renormalization parameters while $Z_m$ is the renormalization parameter for quark mass. Ensuring the Kinetic terms are reduced to the standard form, we should redefine the fields

$$
A_{B\mu} \longrightarrow Z_A^{1/2} A_\mu, \qquad \eta_B \longrightarrow Z_\eta^{1/2} \eta, \qquad \psi_B \longrightarrow Z_\psi^{1/2} \psi. \qquad (2.10)
$$

Such renormalization procedure are necessary to ensure the Lagrangian (derived from action) to remain physical and finite. Any infinities that occur corresponding to the vertices and propagators must be renormalized as a consequence. This subsequently result in a sensible and physical quark masses and coupling constants. We will now discuss how renormalization is implemented in practice in QED [2]:

1) Rescaling the fields in the Lagrangian.
2) The Lagrangian is split into 2 pieces to absorb infinities and unobservable shifts into counter-terms.
3) Selecting a specific renormalization conditions which defines the physical mass and coupling constant while ensuring the field-strength renormalizations equal to 1.
4) Introduce new Feynman Rules, then compute its new amplitude.
5) Finally, adjust the counter-terms appropriately.

One of the method of renormalization is regularization. We will present the detail calculation of $\sigma(e^+e^- \longrightarrow q\bar{q}, q\bar{q}g)$ in Section 2.7, now it will be just suffice to quote the result to show how regularization works in general. One of the initially proposed regularization method is the introduction of gluon mass

$$m_g^2 = \epsilon s \tag{2.11}$$

which we will then have,

$$\sigma_{q\bar{q}g} = \sigma_0 C_F \frac{\alpha_s}{2\pi} \left( \log^2 \frac{1}{\epsilon} - 3 \log \frac{1}{\epsilon} + 7 - \frac{\pi^2}{3} + O(\epsilon) \right) \tag{2.12}$$

$$\sigma_{q\bar{q}} = \sigma_0 C_F \frac{\alpha_s}{2\pi} \left( -\log^2 \frac{1}{\epsilon} + 3 \log \frac{1}{\epsilon} - \frac{11}{2} + \frac{\pi^2}{3} + O(\epsilon) \right) \tag{2.13}$$

$$\sigma_{tot} = \sigma_0 C_F \frac{\alpha_s}{2\pi} \left( \frac{3}{2} + O(\epsilon) \right) \tag{2.14}$$

Unfortunately, despite such regularization gives a finite answer as $\epsilon \longrightarrow 0$ in this case, it violates gauge invariance and therefore does not generalize. A much preferred regularization will be touched in Section 2.3 and Section 2.7.

## 2.3 Renormalization Example - One Loop Vacuum Polarization in QED
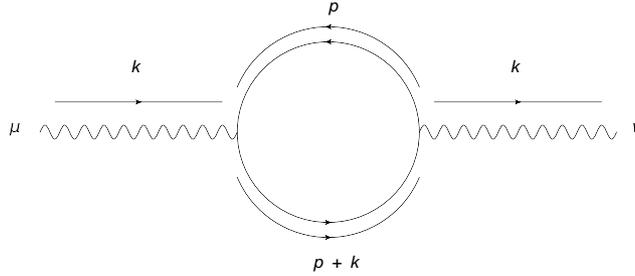


Figure 2.2: *The one loop vacuum polarization diagram*

For revision, we consider a typical QED one loop correction to the photon propagator shown in Fig. (2.2). Using the Feynman Rules for QED in Section 1.8, this particular diagram is represented by the expression

$$-i\Pi^{\mu\nu}(k^2) =$$
$$(-1) \int \frac{d^4p}{(2\pi)^4} (-ie\gamma^\mu)_{\alpha'\beta} \frac{i(\slashed{p}+m)_{\beta\beta'}}{p^2-m^2} (-ie\gamma^\nu)_{\beta'\alpha} \frac{i(\slashed{p}+\slashed{k}+m)_{\alpha\alpha'}}{(p+k)^2-m^2} \tag{2.15}$$

where $\alpha$ and $\beta$ are the spinor indices. Note that we will simplify the expression further by assuming a negligible mass by setting $m = 0$. Note also that $\alpha = \frac{e^2}{4\pi}$ and since that it is a fermion loop, there is a factor of (-1). The integral is divergent and has to be renormalized. The first step in renormalizing ths expression is to regularize the divergent integrals by the common method of "dimensional regularization"[2] in which the integral is performed in $d = 4 - 2\epsilon$ space time dimensions and then the limit $\epsilon \longrightarrow 0$ is taken. Thus, an evaluation of the expression

$$-i\Pi^{\mu\nu}(k^2) = -e^2 \int \frac{d^4p}{(2\pi)^4} \frac{Tr[\gamma^\mu \slashed{p} \gamma^\nu (\slashed{p} + \slashed{k})]}{p^2(p+k)^2} \ . \qquad (2.16)$$

One then needs to use the trace identity given by

$$Tr[\gamma^\mu \gamma^\lambda \gamma^\nu \gamma^\rho] = 4(g^{\mu\lambda}g^{\nu\rho} - g^{\mu\nu}g^{\lambda\rho} + g^{\mu\rho}g^{\lambda\nu}). \qquad (2.17)$$

This further reduces the expression to

$$-i\Pi^{\mu\nu}(k^2) = -4e^2 \int \frac{d^4p}{(2\pi)^4} \frac{[p^\mu(p+k)^\nu - g^{\mu\nu}[p(p+k)] + (p+k)^\mu p^\nu]}{p^2(p+k)^2}. \qquad (2.18)$$

The denominator can be solved using a Feynman parameter

$$\frac{1}{p^2(p+k)^2} = \int_0^1 dx \frac{1}{[(1-x)p^2 + x(p+k)^2]^2}. \qquad (2.19)$$

Changing the variable $l = p + kx$, the numerator is then

$$2l^\mu l^\nu - g^{\mu\nu}l^2 - 2x(1-x)k^\mu k^\nu + g^{\mu\nu}(x(1-x)k^2), \qquad (2.20)$$

where the terms that are odd under $l \to -l$ which vanish on integration have been dropped from the expression. After performing a Wick's rotation where $l^0 = il_E^0$ and applying the identity

$$\int \frac{d^d l_E}{(2\pi)^d} \frac{1}{(l_E^2 + \triangle)^n} = \frac{1}{(4\pi)^{d/2}} \frac{\Gamma(n - d/2)}{\Gamma(n)} (\frac{1}{\triangle})^{n-d/2} \ , \qquad (2.21)$$

and also

$$\int \frac{d^d l_E}{(2\pi)^d} \frac{l_E^2}{(l_E^2 + \triangle)^n} = \frac{1}{(4\pi)^{d/2}} \frac{\Gamma(n - d/2 - 1)}{\Gamma(n)} (\frac{1}{\triangle})^{n-d/2-1}, \qquad (2.22)$$

---

[2] The idea of "dimensional regularization" is such that the Feynman diagrams are computed as an analytic function with space time dimension $d$. Assuming that $d$ is relatively small, the loop-momentum integral will converge, thus the Ward identity proven. Hence, the observable will have a well defined limit as $d \longrightarrow 4$. The reason when to switch from 4 dimensions to $d = 4 - 2\epsilon$ will be shown clearer when introducing Eq. (2.21) and Eq. (2.22).

reduces Eq. (2.18) to

$$-i\Pi^{\mu\nu}(k^2) = [k^\mu k^\nu - g^{\mu\nu}k^2]i\Pi_2(k^2), \qquad (2.23)$$

which we note that $\Gamma(z)$ has isolated poles at $z = 0, -1, -2, -3, ...$ from [2]. Thus for $n = 2$ which has been used for this particular calculation, both integrals Eq. (2.21) and Eq. (2.22) will have poles at $d = 4, 6, 8, ...$. In order to find the behavior near $d = 4$, we therefore define $d = 4 - 2\epsilon$ by using the approximation $\Gamma(\epsilon) = \frac{1}{\epsilon} - \gamma_E + O(\epsilon)$ with $\gamma_E$ being Euler-Mascheroni constant. Continuation to $d$-dimension endows the dimensionless coupling $e$ with a mass dimension, $[e] = 2 - d/2 = \epsilon$, which needs to be replaced with $e \longrightarrow e\mu^\epsilon$. Straightforward calculation of $\Pi_2(k^2)$ yields

$$\Pi_2(k^2) = -\frac{\alpha}{3\pi}\left[ -\frac{1}{\epsilon} + \ln\left(\frac{-k^2}{\mu^2}\right) + \text{finite}\right]. \qquad (2.24)$$

Counterterms are introduced to remove the $\frac{1}{\epsilon}$ divergences, the finite contribution they also cancel is arbitrary and determines the subtraction procedure. Modified minimal subtraction ($\overline{MS}$) absorbs the $\ln(4\pi) - \gamma_E$ term, minimal subtraction (MS) does not. The logarithm in Eq. (2.24) is absolutely crucial in discussing the concept of Renormalons(Chains and Bubbles) with QFT in subsequent chapters, and re-summing powers of logarithms will generate factorial growth of large-order perturbative coefficients.

## 2.4 THE RUNNING COUPLING CONSTANT

In QCD, asymptotic freedom and confinement arise. Confinement explains why no solitary quarks are observed and why quarks are always bound within the hadrons by the strong force carried by gluons. It is important to stress that perturbation theory is a great mathematical tool to analyze QCD . A renormalized coupling constant is said to "run" with energy. As we shall see in QCD the renormalized coupling has a logarithmic running in energy $Q$ and is large at low energy and gradually deceases as energy increases. This physical behavior is called Asymptotic Freedom. This weak coupling at large energy scale property is crucial for the validity of fixed-order perturbative QCD calculations.

Prior to introducing the running coupling, we need to introduce $R$. $R$ has to be a physical observable, dimensionless, a function dependent on the energy scale (which we will denote $Q$). We will assume that the energy $Q$ is much larger than the quark masses and that massless quarks can be assumed.

In QCD, the observable $R$ is expanded as a perturbative series of the fine structure constant $\alpha_S = g^2/4\pi$ where $g$ is the bare coupling. This shows that $R$ has to be renormalized to remove its UV divergences by introducing a second mass scale - a renormalization scale $\mu$ through the renormalization procedure and subtraction scheme discussed previously. Therefore, $R$ in QCD is dependent on the ratio $Q^2/\mu^2$ and the renormalized coupling $\alpha_s$.

The value selected for $\mu$ is part of the specification of the renormalization scheme. In fact, the QCD Lagrangian is independent of $\mu$, but $\mu$ is required to define the theory of QCD. The $\mu$-independence of $R$ is expressed by

$$\mu^2 \frac{d}{d\mu^2} R(Q^2/\mu^2, \alpha_s) \equiv 0,$$

$$\left[\mu^2 \frac{\partial}{\partial\mu^2} + \mu^2 \frac{\partial\alpha_s}{\partial\mu^2}\frac{\partial}{\partial\alpha_s}\right] R = 0. \tag{2.25}$$

Note that the 2nd line just simply shows a transformation of the derivative $d/d\mu^2$ into separate partial derivatives. We rewrite Eq. (2.25) as

$$\left[\frac{\partial}{\partial\tau} - \beta(\alpha_s)\frac{\partial}{\partial\alpha_s}\right] R = 0, \tag{2.26}$$

by introducing the beta function $\beta$ as a derivative of the running coupling with respect to the renormalization scale

$$\beta(\alpha_s) = \mu^2 \frac{\partial\alpha_s}{\partial\mu^2}. \tag{2.27}$$

Note that we can also write

$$\tau = \ln\left(\frac{Q^2}{\mu^2}\right), \tag{2.28}$$

as a function of $Q^2$ as $\tau$ must also be dimensionless. This operation is allowed as

$$\frac{\partial}{\partial\tau} = -\mu^2 \frac{\partial}{\partial\mu^2}, \tag{2.29}$$

remains unchanged by adding an additional term $\ln(Q^2)$ to $\tau$. We will use the same notation $\tau$ and the beta function $\beta$ throughout this thesis. Note that Eq. (2.26) is a 1st order partial differential equation which can be now solved by integrating the bracketed terms

$$\tau = \int_{\alpha_s(\mu^2)}^{\alpha_s(Q^2)} \frac{dx}{\beta(x)}. \tag{2.30}$$

We have to be slightly clearer about what we are doing, we now redefine $\alpha_s(\mu^2) = \alpha_s$ as the lower limit and the *running coupling* as $\alpha_s(Q^2)$ as the upper limit for the integral. Differentiating Eq. (2.28), we have

$$\frac{\partial \alpha_s(Q^2)}{\partial \tau} = \beta(\alpha_s(Q^2)). \tag{2.31}$$

Note that in perturbative QCD, $\beta$ is expanded as a series of $\alpha_s$ and truncated at order $n$.
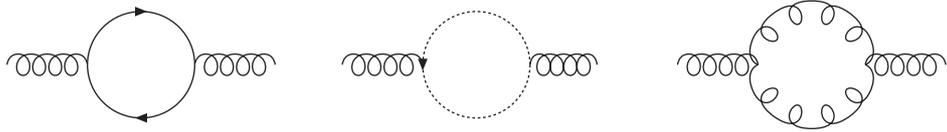


Figure 2.3: *1-loop $\beta$ function contribution*

## 2.5   THE CALLAN−SYMANZIK EQUATION

The Callan−Symanzik equation is a differential equation describing the evolution of the $n$-point correlation Green $G^{(n)}$ functions under different energy scales. The theory involves the definition of the beta-function. This equation has the structure

$$\left[ \mu \frac{\partial}{\partial \mu} + \beta \frac{\partial}{\partial g} + n\gamma \right] G^{(n)}(x_1, ..., x_n; \mu, g) = 0. \tag{2.32}$$

The parameter $\beta$ and $\gamma$ remains unchanged for any $n$ chosen. This simply implies that both $\beta$ and $\gamma$ are independent of the field's momenta denoted by $x_i$. Since the Green's function must be renormalized, $\beta$ and $\gamma$ are both independent of the cut off scale and with dimensional analysis must also be independent of the renormalization mass scale $\mu$. This leads to a universal function namely $\beta(g)$ and an anomalous dimension $\gamma(g)$ which depends on the Green function concerned with $g$ as the renormalized coupling.

This leads on to our discussion on the $\beta$ function in the next section.

## 2.6 THE $\beta$ FUNCTION

We have shown that in renormalization theory, there is a clear distinction between a bare Lagrangian $\mathcal{L}_{Bare}$ and the renormalized effective Lagrangian $\mathcal{L}_{eff}$. Eq. (2.10) shows that such infinite re parameterization is carried out via the introduction of counterterms in Fig. (2.1). As discussed, there is no specific way of choosing a scheme with counterterm coefficients to cancel the $1/\epsilon$ divergences. The $\beta$ function expanded perturbatively on the RHS of Eq. (2.31) is

$$\frac{da}{d\ln(\mu)} = \beta(a) = -ba^2(1 + ca + c_2a^2 + c_3a^3 + ...).  \qquad (2.33)$$

Notice that the LHS of Eq. (2.32) is the coupling $a$ running logarithmically with $\mu$. $a$ will be referred as the coupling throughout this thesis. Here we explicitly relate the coupling with $\mu$, $a(\mu^2) = \alpha_s(\mu^2)/\pi = g^2(\mu^2)/4\pi^2$. The coefficients in the corresponding $\beta$ function have been algebraically derived in the $\overline{MS}$ renormalization scheme [7] and [8], and [9, 10, 11]

$$b = \frac{1}{6}(11C_A - 2N_f),  \qquad (2.34)$$

$$c = \frac{1}{12b}(-\frac{3}{2}C_A[7C_A + 11C_F] + 3b[5C_A + 3C_F]),  \qquad (2.35)$$

$$c_2^{\overline{MS}} = \frac{2857 - \frac{5033}{9}N_f + \frac{325}{27}N_f^2}{64b},  \qquad (2.36)$$

$$c_3^{\overline{MS}} = \left[3564\zeta_3 + \frac{149753}{6} - \left(\frac{6508}{27}\zeta_3 + \frac{1078361}{162}\right)N_f \right. $$
$$\left. + \left(\frac{6472}{81}\zeta_3 + \frac{50065}{162}\right)N_f^2 + \frac{1098}{729}N_f^3\right]/256b.  \qquad (2.37)$$

$b$ and $c$ are Renormalization Scheme (RS) invariant whilst $c_2$ and $c_3$ are RS dependent their values above are calculated in the $\overline{MS}$ scheme. $C_A = N$ ($N$ is the number of colours) and $C_F = (N^2-1)/2N$ are adjoint and fundamental Casimirs, respectively, of the QCD SU(N) theory. Eq. (2.34) to Eq (2.37) can be rewritten as expansions in powers of $b$, a form of expansion that will play a pivotal role in our later discussions of renormalons.

$$c = -\frac{107}{8b} + \frac{19}{4}, \tag{2.38}$$

$$c_2^{\overline{MS}} = -\frac{37117}{768b} + \frac{243}{32} + \frac{325}{192}b, \tag{2.39}$$

$$c_3^{\overline{MS}} = \frac{1218587 + 1389486\xi_3}{13824b} - \frac{5857771 + 932400\xi_3}{27648}$$

$$+ \frac{7761 + 1618\xi_3}{576}b - \frac{1093}{6912}b^2. \tag{2.40}$$

The $N$ color-dependent contribution arises from gluon and ghost vacuum polarization contributions, while the $N_f$ is the number of active quark flavours. If $b$ is required to be positive, corresponding to $N_f < 33/2 \simeq 17$. $a(\mu) \longrightarrow 0$ as $\mu^2 \longrightarrow \infty$ which is a clear indication of Asymptotic Freedom. $\zeta_n$ in the above is the Riemann zeta function. Integrating the beta function, then one obtains

$$\int_0^a \frac{dx}{\beta(x)} = F + \ln(\mu/\Lambda) \tag{2.41}$$

where the constant of integration $F$ contain its infinite part. It is reasonable to make the choice $F = \int_0^\infty dx/(-bx^2(1+cx))$ and the dimensional transmutation parameter $\Lambda$ be replaced by $\tilde{\Lambda}$ defined by [12].

$$\tilde{\Lambda}_{\overline{MS}} = \left(\frac{2c}{b}\right)^{c/b} \Lambda_{\overline{MS}}. \tag{2.42}$$

Using $F$ and $\Lambda$, we have

$$\ln\left(\frac{\mu}{\tilde{\Lambda}}\right) = \int_a^\infty \frac{dx}{bx^2(1+cx)} + \int_0^a \left[\frac{1}{bx^2(1+cx)} + \frac{1}{\beta(x)}\right]dx. \tag{2.43}$$

Eq. (2.43) has two properties, first note that second integral vanishes when $a \longrightarrow 0$, the second property is that the second integral also vanishes again when we choose the a so-called 't Hooft scheme setting $c_2 = c_3... = c_n = 0$.

The solution for Eq. (2.33) at one loop level (retaining just the first term on the RHS of Eq. (2.33)) is

$$a(\mu^2) = \frac{2}{b\ln(\mu^2/\Lambda^2)}, \tag{2.44}$$

and for the two loop level (retaining two terms), the solution may be written in terms of the Lambert W-function

$$a(\mu^2) \;=\; -\frac{1}{c[1 + W(z(\mu))]}, \tag{2.45}$$

$$z(\mu) \;=\; -\frac{1}{e}\left(\frac{\mu}{\Lambda}\right)^{-\frac{b}{c}}, \tag{2.46}$$

defined implicitly by $W(z)e^{W(z)} = z$. For higher loops, $a(\mu^2)$ will be dependent on the choices of $c_2, c_3...c_n$. A useful feature is that in 't Hooft scheme, $a(\mu^2)$ may be written explicitly in terms of $W(z)$ as above. To ensure asymptotic freedom, it is the $W_1$ branch of the Lambert W-Function which is required [13, 14].

## 2.7  $e^+e^-$ INTO HADRONS AND $R_{e^+e^-}$
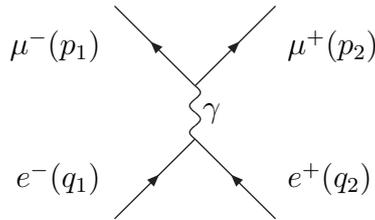


Figure 2.4: $e^+e^- \longrightarrow \mu^+\mu^-$ in QED
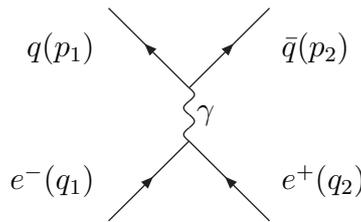


Figure 2.5: *The leading order contribution to the $e^+e^- \longrightarrow$ hadrons in QCD*

Using the Feynman Rules derived in Section 1.8 and Section 1.9, we can at once draw the diagram and write down the amplitude for the $e^+e^- \longrightarrow \mu^+\mu-$ process in QED:

$$M = \{\bar{v}(q_2)e\gamma_\mu u(q_1)\}\frac{-g^{\mu\nu}}{(p_1 + p_2)^2}\{\bar{u}(p_1)e\gamma_\nu v(p_2)\}. \tag{2.47}$$

Rearranging and leaving the spin superscripts implicitly, we have

$$iM(e^+e^- \longrightarrow \mu^+\mu^-) = \frac{ie^2}{s}\left(\bar{v}(q_2)\gamma^\mu u(q_1)\right)\left(\bar{u}(p_1)\gamma_\nu v(p_2)\right), \qquad (2.48)$$

where $s = (p_1 + p_2)^2$. In order to compute the differential cross section, we need $|M|^2$ which require us to find the complex conjugate of $M$. The bi-spinor product of $(\bar{v}\gamma^\mu u)^*$ can be complex conjugated as follows

$$(\bar{v}\gamma^\mu u)^* = u^\dagger(\gamma^\mu)^\dagger(\gamma^0)^\dagger v = u^\dagger(\gamma^\mu)^\dagger\gamma^0 v = u^\dagger\gamma^0\gamma^\mu v = \bar{u}\gamma^\mu v. \qquad (2.49)$$

Thus the squared matrix element is

$$|M|^2 = \frac{e^4}{q^4}\left(\bar{v}(q_2)\gamma_\mu u(q_1)\bar{u}(q_1)\gamma_\nu v(q_2)\right)\left(\bar{u}(p_1)\gamma^\mu v(p_2)\bar{v}(p_2)\gamma^\nu u(p_1)\right). \quad (2.50)$$

Note that we are still free to specify any spinors to any desired spin states of the fermions. In real experiments, it is difficult to retain control over the spin states. In most experiments, the beams are unpolarized, thus the cross section measured is an average over the spins. We will assume to throw away the spin information since muon detectors are normally blind to polarization. The expression for $|M|^2$ simplifies by computing

$$\frac{1}{2}\sum_s \frac{1}{2}\sum_{s'}\sum_r\sum_{r'}|M(s,s' \longrightarrow r,r')|^2. \qquad (2.51)$$

Using the completeness relations Eq (1.26) and Eq (1.27) from Section 1.4, and working with the first half of Eq (2.50) by writing in spinor indices so we can move from one $v$ to the next $v$, we have

$$\begin{aligned}\sum_{s,s'}\bar{v}_a^{s'}(q_2)\gamma_{ab}^\mu u_b^s(q_1)\bar{u}_c^s(q_1)\gamma_{cd}^\nu v_d^{s'}(q_2) &= (\slashed{q}_2 - m)_{da}\gamma_{ab}^\mu(\slashed{q}_1 + m)_{bc}\gamma_{cd}^\nu, \\ &= \text{trace}[(\slashed{q}_2 - m)\gamma^\mu(\slashed{q}_1 + m)\gamma^\nu].\end{aligned}$$
$$(2.52)$$

Evaluating the second half the same manner, we arrived at desired simplification

$$\frac{1}{4}\sum_{spins}|M|^2 = \frac{1}{4}\frac{e^4}{s^2}\text{tr}[(\slashed{q}_2 - m_e)\gamma_\mu(\slashed{q}_1 + m_e)\gamma_\nu]\text{tr}[(\slashed{p}_1 + m_\mu)\gamma^\mu(\slashed{p}_2 - m_\mu)\gamma^\nu].$$
$$(2.53)$$

Thus, we have

$$\frac{1}{4}\sum_{spins}|M|^2 = \frac{8e^4}{s^2}\{p_1.q_2 p_2.q_1 + p_1.q_1 p_2.q_2 + m_\mu^2(q_1.q_2) + m_e^2(p_1.p_2)\}, \quad (2.54)$$

using the cyclic property on Eq (2.53) (and trace identity) by bringing it to the left hand side

$$\text{tr}[(\not{q}_2 - m_e)\gamma_\mu(\not{q}_1 + m_e)\gamma_\nu] = 4[q_{2,\mu}q_{1,\nu} + q_{2,\nu}q_{1,\mu} - g_{\mu\nu}(q_1.q_2 + m_e^2)], \quad (2.55)$$

$$\text{tr}[(\not{p}_1 + m_\mu)\gamma^\mu(\not{p}_2 - m_\mu)\gamma^\nu] = 4[p_1^\mu p_2^\nu + p_1^\nu p_2^\mu - g^{\mu\nu}(p_2.p_1 + m_\mu^2)]. \quad (2.56)$$

Neglecting fermion masses, we obtained

$$\frac{1}{4}\sum_{spins}|M|^2 = \frac{8e^4}{s^2}\{p_1.q_2 p_2.q_1 + p_1.q_1 p_2.q_2\}. \quad (2.57)$$

In order to calculate $\frac{1}{4}\sum|M|^2$ explicitly, suppose

$$q_1^\mu = (E, 0, 0, p) \quad \text{(neglecting fermion mass } p = E) , \quad (2.58)$$
$$q_2^\mu = (E, 0, 0, -E) \quad \text{(center of mass frame)}, \quad (2.59)$$

then the total center of mass energy is

$$s = (q_1 + q_2)^2 = 2q_1.q_2 = 4E^2 \rightarrow E = \frac{1}{2}\sqrt{s}. \quad (2.60)$$

The muon has momentum

$$p_1^\mu = (E', E'\sin(\phi)\sin(\theta), E'\cos(\phi)\sin(\theta), E'\cos(\theta)), \quad (2.61)$$
$$p_1^\mu = (E', E'\sin(\theta), E'\sin(\theta), E'\cos(\theta)), \quad \text{(due to cylindrical symmetry)} \quad (2.62)$$
$$p_2^\mu = q_1^\mu + q_2^\mu - p_1^\mu,$$
$$= (\sqrt{s} - E', 0, -E'\sin(\theta), E'\cos(\theta))). \text{ (by energy conservation) } (2.63)$$

Since the anti-muon is massless

$$p_2^{\mu}.p_{2,\mu} = (s - E')^2 - E'^2\sin^2(\theta) - E'^2\cos^2(\theta) = 0 \rightarrow E' = E = \frac{1}{2}\sqrt{s}. \quad (2.64)$$

Inserting all the relevant expressions into Eq (2.57), the squared matrix element is simply

$$
\begin{aligned}
\frac{1}{4}\sum_{spins}|M|^2 &= \frac{8e^4}{q^4}\{p_1.q_2 p_2.q_1 + p_1.q_1 p_2.q_2\}, \\
&= \frac{e^4}{2}\{(1 + \cos(\theta))^2 + (1 - \cos(\theta))^2\}, \\
&= e^4(1 + \cos^2(\theta)) \quad (2.65)
\end{aligned}
$$

The total cross section will not be possible to be calculated without deriving the two-body phase space, let

$$dPS = \frac{d^3\underline{p_1}}{(2\pi)^3 2E_1}\frac{d^3\underline{p_2}}{(2\pi)^3 2E_2}(2\pi)^4\delta^{(4)}(q_1 + q_2 - p_1 - p_2), \quad (2.66)$$

integrating $d^3\underline{p_2}$ on three spatial $\delta$-functions, yields

$$dPS = \frac{d^3\underline{p_1}}{(2\pi)^3 4E_1 E_2}\delta(\sqrt{s} - E_1 - E_2). \quad (2.67)$$

Expressing $E_1$ and $E_2$ in terms of integration variables, and using spherical coordinates:

$$E_1 = |\underline{p_1}| = p, \ E_2 = |\underline{p_2}| = |-\underline{p_1}| = p, \quad (2.68)$$

$$d^3\underline{p_1} = p^2\,dp\,d\cos(\theta)\,d\phi, \quad (2.69)$$

the two-body phase space can be written as

$$
\begin{aligned}
dPS &= \frac{1}{16\pi}d\cos(\theta)\frac{d\phi}{2\pi}, \quad (2.70) \\
PS &= \frac{d\cos(\theta)}{16\pi}, \quad (2.71)
\end{aligned}
$$

using the integration of $\int \frac{d\phi}{2\pi} = 1$ (due to cylindrical symmetry) and integrating out the final $\delta$-function $\int dp\,\delta(\sqrt{s} - 2p) = \frac{1}{2}$. The phase space $PS$ is related to squared matrix element and differential equation by the relation

$$d\sigma = \frac{1}{2s}\left(\frac{1}{4}\sum|M|^2\right)PS, \tag{2.72}$$

plugging in $|M|^2$ and $PS$, the differential cross section and then the cross section are simply

$$\frac{d\sigma}{d\cos(\theta)} = \frac{1}{2s}\frac{1}{16\pi}\frac{1}{4}\sum|M|^2 = \frac{\pi\alpha^2}{2s}\left(1+\cos^2(\theta)\right), \tag{2.73}$$

$$\sigma(e^+e^- \longrightarrow \mu^+\mu^-, s) = \int_{-1}^{+1} d\cos(\theta)\frac{d\sigma}{d\cos(\theta)} = \frac{4\pi\alpha^2}{3s}. \tag{2.74}$$

For the leading order contribution to Figure (2.5), $\sigma(e^+e^- \longrightarrow \text{hadrons}, s)_{lo}$, intuitively we can replace the muon charge $e$ with the quark charge $Q_f|e|$ ($f$ denotes the flavour) and count each quark three times, one for each color, while finally summing up the relevant flavours:

$$\sigma(e^+e^- \longrightarrow \text{hadrons}, s)_{lo} = \frac{4\pi\alpha^2}{3s}3\sum Q_f^2. \tag{2.75}$$

Here we have not included the emission of real and virtual gluon into the calculations. Figure 2.6 depicts the Feynman diagrams of real gluon emission which leads to 3-jets events in international laboratory.
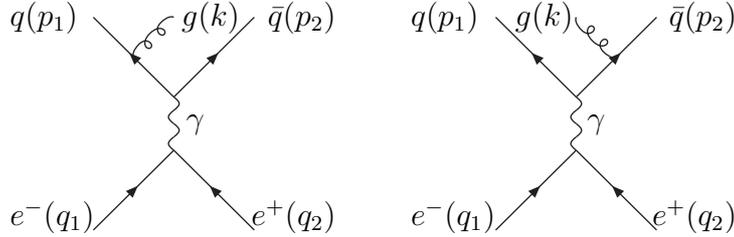


Figure 2.6: *Real gluon emission*

We can now write the amplitude for the real gluon emission (which contributes partially to next leading order correction) by referring to the QCD Feynman Rules

$$\begin{aligned}
M &= e^2 Q_f g T_{ij}^a \{\bar{v}(q_2)\gamma_\mu u(q_1)\}\frac{-g_{\mu\nu}}{s}\\
&\times \left(\bar{u}_i(p_1)\left[\gamma_\sigma\frac{\not{p}_1+\not{k}}{(p_1+k)^2}\gamma_\nu - \gamma_\nu\frac{\not{p}_2+\not{k}}{(p_2+k)^2}\gamma_\sigma\right]v_j(p_2)\right)\epsilon_a^\sigma(k).
\end{aligned} \tag{2.76}$$

Thus, the squared matrix element is

$$
\begin{aligned}
\frac{1}{4}\sum |M|^2 &= \frac{4e^4 Q_f^2 g^2 N}{s} C_F \\
&\times \frac{(p_1.q_1)^2 + (p_1.q_2)^2 + (p_2.q_1)^2 + (p_2.q_2)^2}{(p_1.k)(p_2.k)},
\end{aligned} \tag{2.77}
$$

where we have used the colour algebra $\sum T_{ij}^a (T_{ij}^a)* = T_{ij}^a T_{ji}^a = \frac{1}{2}\delta^{aa} = \frac{1}{2}(N^2 - 1) = N.C_F$. Performing all the necessary steps as discussed in the calculation of $\sigma(e^+ e^- \longrightarrow \text{hadrons}, s)_{lo}$ using phase space integral as well as spinor algebra, we finally arrive at

$$
\begin{aligned}
\sigma(e^+ e^- \longrightarrow q\bar{q}g, s)_{nlo} &= \frac{1}{2s}\frac{s}{16(2\pi)^3}\int dx_1 dx_2 \frac{d\cos(\theta)d(\phi)d(\alpha)}{2(2\pi)^2}\frac{1}{4}\sum |M|^2, \\
&= \frac{4\pi\alpha^2 Q_f^2 N}{3s} C_F \frac{\alpha_s}{2\pi}\int dx_1 dx_2 \frac{x_1^2 + x_2^2}{(1-x_1)(1-x_2)}, \\
&= \sigma_0 C_F \frac{\alpha_s}{2\pi}\int dx_1 dx_2 \frac{x_1^2 + x_2^2}{(1-x_1)(1-x_2)},
\end{aligned} \tag{2.78}
$$

where $x_i = 2p_i/\sqrt{s}$ is the energy fraction and $\alpha_s = g^2/4\pi$ is the strong-interaction analogue of fine structure constant with $g^2$ as the strong interaction coupling. In a 3-jets event, the cross section diverges where the gluon is collinear (results in divergences when the momentum vector of the gluon $k$ is parallel to $p_1$ or $p_2$) with the quark or anti-quark. These events cannot be distinguished experimentally from 2-jets events. To ensure consistency, we have to compute all contributions to quark-anti-quark production of the same order of $g$. This involves also loop diagrams in Figure 2.7
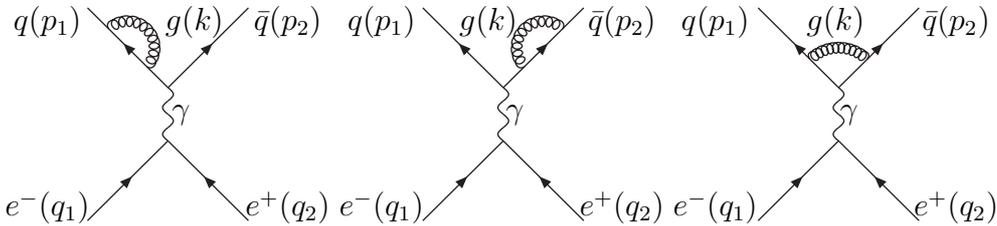


Figure 2.7: *Virtual gluon emission*

in addition to the real gluon emission in Figure 2.6. Naively, one will think since the loop diagrams are of order $e^2 g^2$ or $e^2 \alpha_s$, therefore the contribution must be of order $e^4 g^4$ or $e^4 \alpha_s^2$, implying higher order than the real gluon

emission which of order $e^2g^2$ or $e^2\alpha_s$. Nevertheless, there are interference terms with the leading order diagrams, such interference contributes to the cross section of order $e^2g^2$ or $e^2\alpha_s$ equivalent to real gluon emission. This is because in the loop diagrams, there are contributions which the gluon is almost collinear with the quark and anti-quark. This gives rise to a similar divergence in the infrared region but negative. This gives us some hope in canceling the real divergence to obtain a finite answer. With the fact that both have the same physical origin: soft (soft divergences are divergences which arises from a zero energy gluon $E_g = 0$, implying $x_3 = 0$) and collinear virtual gluons, this furthers increases our hope of cancellation.

The last divergences we will discuss are ultraviolet divergences contribution from the first two diagrams in Figure 2.7.
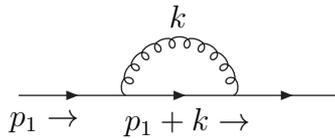


Figure 2.8: *Ultraviolet divergences*

These two diagrams do not contribute as they vanish during renormalization process by introducing a counterterm normally being labeled as $\delta_2$ plus finite terms. The $\delta_2$ is gauge dependent. For example, it has no one loop divergence in Landau gauge $\xi = 0$.
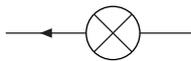


Figure 2.9: *The $\delta_2$ counterterm*

Noticing that the two diagrams do not contribute and regularizing both real and virtual cross sections, adding them together, a finite answer will be obtained and the regularization can be removed later on. This underpin the foundation of Bloch-Nordsieck theorem. This is only true when one sums over the final states that cannot be distinguishable but not in the initial state. Using $d$ space time dimensions $d = 4 - 2\epsilon, \epsilon < 0$,

$$\sigma(e^+e^- \longrightarrow q\bar{q}g, s)_{nlo} = \sigma_0 C_F \frac{\alpha_s}{2\pi} \left( \frac{2^2}{\epsilon} + \frac{3}{\epsilon} + \frac{19}{2} - \pi^2 + O(\epsilon) \right),$$

(2.79)

$$\sigma(e^+e^- \longrightarrow q\bar{q}, s)_{nlo} = \sigma_0 C_F \frac{\alpha_s}{2\pi} \left( -\frac{2^2}{\epsilon} - \frac{3}{\epsilon} - 8 + \pi^2 + O(\epsilon) \right).$$

(2.80)

Note that adding them up together Eq (2.79) and (2.80) yield a finite answer

$$\begin{aligned}
\sigma(e^+e^- \longrightarrow q\bar{q}g + q\bar{q}, s)_{nlo} &= \sigma_0 C_F \frac{\alpha_s}{2\pi} \left( \frac{3}{2} \right), \\
&= \sigma_0 \frac{\alpha_s}{\pi},
\end{aligned}$$

(2.81)

where in the last line, we have made the substitution of $C_F$ for QCD with $N = 3$

$$C_F = \frac{N^2 - 1}{2N} = \frac{3^2 - 1}{2(3)} = \frac{4}{3}.$$

(2.82)

Adding the leading order Eq (2.75) and next leading order contribution Eq (2.81), divided by Eq (2.74), we have the next leading order of the $R_{e^+e^-}$ ratio

$$R_{e^+e^-,nlo} = 3 \sum_f Q_f^2 \left[ 1 + \frac{\alpha_s}{\pi} \right].$$

(2.83)

We have not consider 4-jets and 5-jets events in our calculation, the ratio itself is still a complicated matter at present time of writing and our main study will be the higher order perturbative corrections $R(s)$ denoted by

$$R(s) = a(s) + r_1 a^2(s) + r_2 a^3(s) + r_3 a^4(s) + ...$$

(2.84)

with $r_1$, $r_2$ and $r_3$ computed in the $\overline{MS}$ scheme. $R(s)$ is related to the $R_{e^+e^-}$ ratio by

$$R_{e^+e^-} = 3 \sum_f Q_f^2 \left[ 1 + R(s) \right].$$

(2.85)

Discussions in highlighting the differing approaches to the $R_{e^+e^-}$ ratio will dominate the content of our study. It is worth to note that the $R_{e^+e^-}$ ratio dominates at energies far below the Z pole and for energy on the Z pole,

the analogous quantity is the ratio of the partial decay widths of the Z to hadrons and to $\mu^+\mu^-$ pairs. These results are valid for massless quarks. For $q = u, ..., b$, $R_{e^+e^-} = 11/3$ and $R_Z = 20.09$ while the measured value at LEP is much higher by 3% to 4% due to higher-order QCD corrections. These provide guidances in modifying our $\sigma(e^+e^- \longrightarrow q\bar{q})$ when making comparisons to experimental LEP results to test $\alpha_s$.

## 2.8 SUMMARY

We made in this Chapter a brief introduction into some selective interesting topics of perturbative QCD. We began with dimensional regularization and then moved into renormalization theory and discussed different renormalization schemes. The $\beta$ function was then introduced, which was then used to define the perturbative correction to the $R_{e^+e^-}$ ratio, $R(s)$.

QCD and QED are renormalizable theories. After divergences are regularized, the troublesome divergent contributions can be removed by an infinite redefinition of the fundamental constants of the theory like the coupling and the quark mass in QCD. In other words, physical quantities are expressed in terms of renormalized parameters and do not involve any UV divergences anymore. Demonstrating the renormalizability of QCD can be an extremely rigorous theorem. We provided rather a heuristic physical explanation. Large loop momenta produces UV divergences. In the event that the loop momenta are much larger than its characteristic external momenta, the loop loses its structure and can be considered as a point. We then showed a brief example of how renormalization is implemented in practice in the next section.

We then considered a QED one loop correction to the photon propagator. Using the QED Feynman Rules, we can write its full expression. We then performed some complicated algebraic manipulation and notice that a counterterm needs to be introduced to remove the $1/\epsilon$ divergences. This serves as an early exercise to picture the concept of Renormalons(Chains and Bubbles) with QFT in subsequent chapters.

In QCD, asymptotic freedom and confinement are introduced. Confinement explains why no solitary quarks are observed and why quarks are always bound within the hadrons by the strong force carried by gluons. It is important to stress that perturbation theory is a great mathematical tool to analyze QCD. A coupling constant is said to run by being large at low energy and gradually deceases as energy increases. This physical behavior is called

Asymptotic Freedom. We introduce $R$ a physical observable, dimensionless, a function dependent of energy (which we will denote as $Q$)and we took a zero quark-mass limit. We made the assumption that the energy $Q$ is much larger than the quark masses and that the quark mass can be neglected. $R$ in QCD is dependent on the ratio $Q^2/\mu^2$ and the renormalized coupling $\alpha_S$. The choice of selecting $\mu$ is part of specifying the renormalization scheme.

We finally provide a detail calculation of the $R_{e^+e^-}$ ratio by first calculating the cross section of $e^+e^- \longrightarrow \mu^+\mu^-$ which then generalizes to $R_{e^+e^-,lo}$ ratio at the lowest order by considering $Q_f$ and number of colours. Real and virtual gluon emissions are then considered to wrap up the calculation of $R_{e^+e^-,nlo}$ ratio at the next lowest order before highlighting the importance of perturbative correction $R(s)$.

# Chapter 3

# $\overline{MS}$ and CORGI

## 3.1 Minimal Subtraction Scheme

The most common scheme preferred is the ($\overline{MS}$) modified minimal subtraction scheme [5]. In MS, the factors $\ln(4\pi) - \gamma_E$ which appear together with the pole $1/\epsilon$ are not subtracted, in $\overline{MS}$ these factors are completely removed together with the pole $1/\epsilon$. These two schemes have been popular among particle physicists as they facilitate the calculation and computational procedure. Nevertheless, there are no theoretical arguments to uniquely prefer these schemes over any other. There is a complete democracy in the choice of scheme.

As we shall see in Sec 3.2 the MS and $\overline{MS}$ renormalization schemes can be related exactly to each other given a NLO calculation (e.g. the coefficient $r_1$ in Eq. (2.84)) [15, 16].

$$\Lambda_{\overline{MS}} = \Lambda_{MS} \exp\left[\frac{r_1^{MS}(\mu) - r_1^{\overline{MS}}(\mu)}{b}\right], \qquad (3.1)$$

$$r_1^{MS}(\mu) - r_1^{\overline{MS}}(\mu) = \frac{b}{2}(\ln(4\pi) - \gamma_E), \qquad (3.2)$$

where the relation

$$\Lambda_{\overline{MS}} = \sqrt{4\pi}e^{-\gamma_E/2}\Lambda_{MS}, \qquad (3.3)$$

obtained is completely independent of $N$ and $N_f$. The only difference is the renormalization scale $\mu$ which arises due to the selection of scheme. This implies that by selecting $\mu_{MS}$ in MS, we have

$$\mu_{\overline{MS}} = 2.66\mu_{MS}, \tag{3.4}$$

this emphasises that the meaning of the renormalization scale $\mu$ is correlated with the chosen subtraction procedure. The use of a physical scale choice related to the energy of the process, e.g. $\mu = \sqrt{s}$ for the perturbative correction $R(s)$, does not ,therefore, uniquely specify the scheme.

## 3.2 COMPLETE RENORMALIZATION GROUP IMPROVEMENT

The original idea of complete renormalization group improvement(CORGI) [17] was motivated by the problem of scheme dependence in perturbative QCD. Truncated perturbative series depend on the chosen renormalization scheme (RS), which as we shall discuss below, can be specified by the variable $\tau \equiv b\ln(\mu/\widetilde{\Lambda})$, related to the renormalization scale $\mu$, and by the non-universal beta-function coefficients $(c_2, c_3, \ldots)$. The standard approach used by experimentalists is to use $\overline{MS}$ subtraction with a "physical" scale choice $\mu = Q$ , where $Q$ is a "natural" energy scale of the process, e.g. $\sqrt{s}$ for the $R(s)$ ratio as noted above. Our attitude will be that the scheme-dependence can be avoided if instead of truncating the series one resum to all-orders parts of the higher perturbative coefficients which are renormalization group (RG)-predictable. As we shall discuss this predictability reflects the self-consistency of perturbation theory. This resummation removes the $\tau$ and $c_i$ dependence and leads to unique predictions whose uncertainty is determined by unknown but RS-invariant higher corrections. In contrast theoretical uncertainties in the standard approach are dealt with by arbitrary variation of the scale $\mu$, typically taking $\mu = Q$ as the central value, and $\mu = 2Q$ and $\mu = \frac{1}{2}Q$ to provide upper and lower error estimates. This approach can give extremely misleading estimates of the underlying $\Lambda_{QCD}$ parameter, and the "theoretical error" has no real meaning.

Without loss of generality, consider $R(s)$, Eq. (2.84) as perturbative series where $a \equiv \alpha_s(\mu)/\pi$ is the RG improved coupling satisfying Eq. (2.33). We shall use the notation of Stevenson [18], we label the $\tau \equiv b\ln(\mu/\widetilde{\Lambda})$ which can be obtained as the solution of the transcendental equation

$$\frac{1}{a} + c\ln(\frac{ca}{1+ca}) = \tau - \int_0^a dx(-\frac{1}{B(x)} + \frac{1}{x^2(1+cx)}), \tag{3.5}$$

with the non-universal beta-function coefficients $c_2, c_3, \ldots . a(\tau, c_2, c_3, \ldots)$ and

$$B(x) = x^2(1 + cx + c_2 x^2 + c_3 x^3 + ...). \tag{3.6}$$

Eq. (3.5) is obtained by integrating Eq. (2.33) with a suitable choice of boundary condition. Since $\tau$ is dependent on $\tilde{\Lambda}$, so must be the boundary condition.

As we shall discuss, associated with a given observable $R$ one has a dimensionful parameter $\Lambda_R$ (dependent on the particular observable) which is independent of the renormalization scheme and can be related to the dimensional transmutation parameter in a particular subtraction scheme , e.g. $\Lambda_{\overline{MS}}$ by

$$\Lambda_R \equiv e^{r/b}\tilde{\Lambda}_{\overline{MS}}, \tag{3.7}$$

where we set $r \equiv r_1^{\overline{MS}}(\mu = Q)$ with a preference of $r_1$ (NLO perturbative coefficient) rather than $\tau$. This is possible because [18]

$$\tau - r_1 = \rho_0(Q) \equiv b\ln(Q/\Lambda_R). \tag{3.8}$$

$\rho_0$ is RS invariant which implies that $\tau$ can be traded for $r_1$. By evaluating the RHS of Eq. (3.7) in two different schemes one arrives at the Celmaster Gonsalves relation of Eq. (3.1) [16].

Note that the RHS of Eq. (3.7) is independent of the subtraction scheme applied. Thus we can now define $a(r_1, c_2, c_3, ...)$ using Eqs. (3.5, 3.8). For the perturbative coefficients $r_i$, there must be a cancellation of the RS-dependent $a$ when the series is resummed to all-orders. Perturbation theory requires self consistency during calculation. This results in a demand that the result of a $N^n LO$(truncating at $r_{n+1}a^{n+2}$) calculation in two different schemes should have a difference of $O(a^{n+2})$. This leads to the following dependence of the $r_i$ on the scheme parameters

$$
\begin{aligned}
r_2(r_1, c_2), \\
r_3(r_1, c_2, c_3), \\
.\quad ., \\
.\quad ., \\
r_n(r_1, c_2, c_3, ..., c_n). \quad ., 
\end{aligned}
\tag{3.9}
$$

To find the general structure of $r_n$ on the scheme parameters, we differentiate Eq. (3.5) w.r.t $c_i$,

$$\frac{\partial a}{\partial c_i} = -b\beta(a) \int_0^a \frac{x^{i+2}}{\beta^2(x)} dx. \tag{3.10}$$

Consistency of perturbation theory for an $O(a^n)$ calculation then translates into the statement that

$$\frac{\partial R^{(n)}}{\partial \tau} = O(a^{n+1}), \qquad \frac{\partial R^{(n)}}{\partial c_i} = O(a^{n+1}). \tag{3.11}$$

Using Eq. (3.10) and Eq. (3.11) we have for the $n = 1$ case

$$R^{(1)} = a + r_1 a^2, \qquad \beta(a) = -ba^2(1 + ca), \tag{3.12}$$

$$\frac{\partial R^{(1)}}{\partial \tau} = O(a^2), \qquad \frac{\partial R^{(1)}}{\partial c_i} = O(a^2), \tag{3.13}$$

$$\frac{\partial r_1}{\partial \tau} = 1, \qquad \frac{\partial r_1}{\partial c_2} = 0. \tag{3.14}$$

The last equation is obtained by performing a partial differentiation on Eq. (3.13). Integrating the conditions Eq. (3.14), we have

$$r_1 = \tau - X_0. \tag{3.15}$$

Inserting into Eq. (3.8), we will now have

$$X_0(Q) \equiv b \ln \left( \frac{Q}{\Lambda_R} \right), \tag{3.16}$$

this shows that $X_0$ is an RS-invariant and has a genuine physical significance. Repeating a similar procedure for $n = 2$ we will have a further set of conditions

$$\frac{\partial r_2}{\partial r_1} = 2r_1 + c, \frac{\partial r_2}{\partial c_2} = -1, \frac{\partial r_2}{\partial c_3} = 0. \tag{3.17}$$

Integrating all these conditions and repeating the procedure up to arbitrary $r_n$, one obtains

$$\begin{aligned} r_2(r_1, c_2) &= r_1^2 + cr_1 + X_2 - c_2 \\ r_3(r_1, c_2, c_3) &= r_1^3 + \frac{5}{2}cr_1^2 + (3X_2 - 2c_2)r_1 + X_3 - \frac{1}{2}c_3 \\ &\quad \cdot \qquad \cdot \\ &\quad \cdot \qquad \cdot \\ &\quad \cdot \qquad \cdot \end{aligned} \tag{3.18}$$

where the structure can be generalized as

$$r_n(r_1, c_2, .., c_n) = \widetilde{r}_n(r_1, c_2, ..., c_{(n-1)}) + X_n - c_n/(n-1). \qquad (3.19)$$

$\widetilde{r}_n$ is an nth order polynomial in $r_1$. $\widetilde{r}_n$ can be determined given a complete $N^{n-1}LO$ calculation. These are the "RG-predictable" pieces of higher coefficients that we alluded to earlier.

$X_n$ is a constant of integration and is determined when given a complete $N^n LO$ calculation. $X_n$ is Q-independent and RS-invariant. Given a $N^2 LO$ calculation in the usual $\overline{MS}$ scheme, the RS invariant $X_2$ will be determined as the combination

$$X_2 = r_2^{\overline{MS}}(\mu = Q) - (r_1^{\overline{MS}}(\mu = Q))^2 - c r_1^{\overline{MS}}(\mu = Q) + c_2^{\overline{MS}}, \qquad (3.20)$$

with the renormalization scale $\mu = Q$(energy). A complete $N^n LO$ calculation means we have a set of calculated $c_2$ to $c_n$ and a computed set of $r_1$ up to $r_n$.

Eq. (2.84) can then be written in the form

$$
\begin{aligned}
R(Q^2) &= a + r_1 a^2 + (r_1^2 + c r_1 + X_2 - c_2)a^3 \\
&+ (r_1^3 + \frac{5}{2}c r_1^2 + (3X_2 - 2c_2)r_1 + X_3 - \frac{1}{2}c_3)a^4, \qquad (3.21)
\end{aligned}
$$

where each term exhibits the RS-dependence explicitly. $a$ depends on the scheme parameters such that

$$a \equiv a(r_1, c_2, c_3, ...). \qquad (3.22)$$

Given a Feynman diagram of a given order one should resum all known RG-predictable terms. At $NLO$, $r_1$ is determined but $X_2, X_3, ...$ remain unknown. Setting $R(Q^2) \equiv a_0$ and $X_2, X_3, ..., X_n = 0$, the complete subset of known terms in Eq. (3.21) at NLO is

$$a_0 \equiv a + r_1 a^2 + (r_1^2 + c r_1 - c_2)a^3 + (r_1^3 + \frac{5}{2}c r_1^2 - 2c_2 r_1 - \frac{1}{2}c_3)a^4 + ... \quad (3.23)$$

The justification to sum these terms, $a_0$, can be understood by the following arguments. $a_0$ consist of infinite subsets of terms where summation of all the terms leads to an RS independent result, as the $X_2, X_3, ..., X_n = 0$ dependent

terms cannot cancel their RS-dependence and the fact that Eq. (3.21) is RS-invariant to all-orders. RS-independence allows us to set $r_1 = 0, c_2 = 0, c_3 = 0, ...,$, so that all the terms except the first in Eq. (3.23) vanish and we obtain

$$a_0 = a(r_1 = 0, c_2 = 0, c_3 = 0, ..., c_n = 0). \qquad (3.24)$$

This is equivalent to 't Hooft scheme with $c_2, ...., c_n = 0$ and $r_1 = 0$. Setting $r_1 = 0$ yields the $\overline{MS}$ scale $\mu = e^{-r/b}Q$ by simple manipulation of Eq. (3.8). $a_0$ also immediately satisfies

$$\frac{1}{a_0} + c\ln(\frac{ca_0}{1 + ca_0}) = b\ln(\frac{Q}{\Lambda_R}). \qquad (3.25)$$

Thus $a_0$ is given by Eq. (2.45) and Eq. (2.46) involving the Lambert W-function, with $\Lambda$ replaced by $\Lambda_R$. $\widetilde{\Lambda}$ from Eq (3.7) is based on Stevenson's [17] definition which is different than the standard $\widetilde{\Lambda}_{\overline{MS}}$, so now we redefine

$$\Lambda_R = e^{r/b}(\frac{2c}{b})^{-c/b}\Lambda_{\overline{MS}}. \qquad (3.26)$$

Given a $N^2LO$ calculation, $X_2$ can be computed. Resumming the augmented set of $X_2$-dependent RG-predictable terms using Eq. (3.20), we have

$$X_2a_0^3 = X_2a^3 + 3X_2r_1a^4 + ...., \qquad (3.27)$$

and consequently at $N^2LO$ one has

$$R(Q^2) = a_0 + X_2a_0^3, \qquad (3.28)$$

which the observable $R(Q^2)$ in $N^2LO$ form.

Repeating this procedure continuously, we will have the CORGI version of $R(Q^2)$ given by

$$R(Q^2)_{CORGI} = a_0 + X_2a_0^3 + X_3a_0^4 + ... + X_na_0^{n+1} + ..., \qquad (3.29)$$

which is simply the perturbation series in the RS with $r_1 = c_2 = c_3 = ... = c_n = ... = 0$. This immediately results in

$$a_0(\mu^2) = a(\mu^2). \qquad (3.30)$$

## 3.3 Discussions on CORGI and Effective Charges

A detailed introduction on CORGI and its motivation has been given. It is worthwhile to review the closely related method of Effective Charges discussed by Grunberg [19] and to highlight its relationship with the CORGI approach.

The main idea of the method of Effective Charges is to recognize that there is a choice of RS in which the QCD observable $R(Q^2)$ is equal to the coupling . That is in the Effective Charge (EC) scheme the higher perturbative coeficients vanish, $r_1 = 0, r_2 = 0, r_3 = 0, ....$ The CORGI approach , as we have seen, corresponds to a choice of RS with $r_1 = 0, c_2 = 0, c_3 = 0, ....$ This means that at NLO level CORGI and EC give exactly the same result.

The application of Effective Charges is highlighted in [20] which in the paper considers the dimensionless QCD observable $D(Q) = a + \sum_1^\infty d_n a^{n+1}$ (related to the Adler D-function and to be discussed in Chapter 4) is equivalent to the renormalized coupling itself. The couplings $a$, $\overline{a}$ in the $\overline{MS}$ and EC scheme are related by

$$\overline{\beta}(\overline{a}) = \frac{d\overline{a}}{da}\beta(a(\overline{a})),\tag{3.31}$$

where the beta-function in the EC scheme is given by

$$\overline{\beta}(\overline{a}) = -b\overline{a}^2(1 + c\overline{a} + \rho_2\overline{a}^2 + ... + \rho_k\overline{a}^k + ...),\tag{3.32}$$

with $D = \overline{a}$ ( the QCD observable being the coupling itself ). Note that $c = \rho_1$ ensuring scheme invariance. Then Eq (3.31) gives

$$\rho(D) = \frac{dD}{da}\beta(a(D)),\tag{3.33}$$

where $a(D)$ is the inverted perturbation series. Expanding the above equation on both sides and then making re-arrangements gives

$$
\begin{aligned}
d_2(d_1, c_2) &= d_1^2 + cd_1 + (\rho_2 - c_2)\\
d_3(d_1, c_2, c_3) &= d_1^3 + \frac{5}{2}cd_1^2 + (3\rho_2 - 2c_2)d_1 + \frac{1}{2}(\rho_3 - c_3)\\
&\quad .\qquad .\\
&\quad .\qquad .\\
&\quad .\qquad .
\end{aligned}\tag{3.34}
$$

One finds that the $Q$-independent and RS-invariant EC beta-function coefficients $\rho_2, \rho_3, ...$, are closely related to the CORGI invariants $X_2, X_3, ...$ of Eq.(3.18). One has $\rho_2 = X_2$ and $\rho_3 = 2X_3$. The connection between the two approaches may be further clarified by considering that the coupling in a general RS labelled by $a(r_1, c_2, c_3, ...)$ can be expanded in powers of the CORGI coupling $a_0$ of Eq.(3.24). One has that

$$a(0, c_2, c_3, ...) = a_0 + c_2 a_0^3 + \frac{c_3}{2} a_0^4 + ... \qquad (3.35)$$

Since $a_0$ can be written analytically in terms of the Lambert $W$-function as in eqs.(2.14),(2,15), this enables one to obtain the coupling in a general RS without solving transcendental equations. We shall exploit this approach in our work on tau decays in Chapter 6. In the EC scheme $\overline{a} = a(0, \rho_2, \rho_3, ..)$, and so the above equation reproduces the CORGI expansion of Eq.(3.20). Comparing coefficients one sees that $\rho_2 = X_2$ and $\rho_3 = 2X_3$, as claimed above. This shows in particular that at NNLO the CORGI and EC results differ by $O(a_0^5)$, and that in general they will be close to each other.

## 3.4 SUMMARY

The most common renormalization scheme among phenomenologists is the modified minimal subtraction scheme. In MS, the factor $\ln(4\pi) - \gamma_E$ which appears together with the pole $1/\epsilon$ is preserved. In $\overline{MS}$, this factor is completely removed together with the pole $1/\epsilon$. Nevertheless, there is no compelling theoretical argument to prefer this scheme over any other scheme.

The original idea of a complete renormalization group improvement (CORGI) was motivated by problems arising from renormalization scheme dependence of fixed order perturbative QCD which leads to a dependence of fixed-order predictions on the RS, with consequent large theoretical errors if the standard physical scale approach of choosing $\mu = Q$ is used. An infinite subset of RG-predictable terms should be identified and resummed, resulting in RS-invariant estimates, with the uncertainty due to remaining uncalculated terms in perturbation theory now involving RS-invariant quantities such as $X_2$. In Chapter 6 we shall apply CORGI to the inclusive $\tau$-decay ratio $R_\tau$ where the perturbative corrections are rather large.

At the end of this chapter, we wrap up the similarities and differences between CORGI and Effective Charges.

# Chapter 4

# REVIEW OF RENORMALONS

## 4.1  DIVERGENT SERIES IN PERTURBATION THEORY

Divergent series are common in mathematics and theoretical physics. Feynman argued that QED can be considered equivalently to the theory of the motion of charges acting on each other by direct action from a distant, for example is the interaction between two like charges which is proportional to $e^2$ where $e$ is the electron charge. This led Dyson [21] to propose that suppose the conditions are such to verify Feynman formulation of the theory, let (the series in $e^2$)

$$f(e^2) = \sum_{n=0}^{\infty} f_n e^{2n}, \tag{4.1}$$

be a physical quantity calculated by performing an integration over the equations of motion of the theory over time which can be finite or infinite. $e^2$ is always positive. Suppose that the series prescribed above converges for some $e^2$, $f(e^2)$ is then an analytic function of $e$ at $e = 0$.

Then, we can say that for small values of $e$, $f(-e^2)$ is then a well-behaved analytic function which expands as a convergent power-series. This statement is not true as the argument presented by Dyson was as follows. Consider a system of $N$ interacting electrons, from thermodynamics, it is obvious that the energy of the electrons will be given by

$$E \simeq NT + \frac{1}{2}N^2 V e^2. \tag{4.2}$$

where $T$ is the mean kinetic energy and $V$ is the mean coulomb potential of the particle. The number of interacting particle pairs is equivalent to $\simeq \frac{1}{2} N^2$. $e^2 > 0$ corresponds to the usual world where like charges repel and unlike charges attract. The condition $-e^2 < 0$, however, corresponds to a situation where like charges attract and unlike charges repel resulting in an unstable vacuum state which is prone to the creation of more and more particle pairs. This immediately results in $f(-e^2)$ as being an impossible candidate to be convergent. To find the $N$ which maximizes $E$, we differentiate Eq. (4.2) equation and set it to 0, we will then obtain

$$\frac{dE}{dN} \simeq T + NVe^2 = 0, \tag{4.3}$$

$$N_{max} \simeq \frac{T}{V|e|^2} \simeq \frac{1}{e^2}. \tag{4.4}$$

This implies that there is no stable minimum and the divergent nature of perturbative series emerges when more terms are taken into account. Therefore we have

$$\frac{f_{n+1}}{f_n} \simeq \frac{1}{e^2} \simeq N_{max} \simeq n, \tag{4.5}$$

$$\Rightarrow f_n \simeq n!, \tag{4.6}$$

as the $f_n e^{2n}$ terms decrease for $n < N_{max}$. This can lead us to conclude that perturbation series in QED are divergent with coefficients growing like $n!$ in $n$th order. This $n!$ growth is connected with a "vacuum instability" cut at $e^2 = 0$. It is suffice to end the discussions here on the relationship between energy and divergent series in perturbation theory without discussions on the alternatives prescribed in [21].

## 4.2 ASYMPTOTIC SERIES AND BOREL SUMMATION

Consider the dimensionless observable $R$, a divergent series expanded as

$$R = \sum_{n=0}^{\infty} r_n a^n. \tag{4.7}$$

This series is said to be asymptotic inside the domain $\mathcal{C}$ of the complex $a$-plane if the series diverges for all $a \neq 0$, and there exist coefficients $r_N$ such that

$$|R - \sum_{n=0}^{N} r_n a^n| \leqq r_{N+1}|a|^{N+1}. \tag{4.8}$$

There will be error which arises from the truncation of the series but the error is much less than the neglected terms. This allows us to truncate the series at $n = N_{opt}$ rather than taking $n$ to $\infty$, where $N_{opt}$ corresponds to truncation at one term before the smallest in magnitude. This then provides the optimal approximation.

Discovered by Emile Borel, an asymptotic function can be transformed into a series by using the method of Borel Summation. If $r_n \simeq n!$, the Borel transform of the series is then defined as

$$B[R](z) = \sum_{n=0}^{\infty} \frac{r_n}{n!} z^n. \tag{4.9}$$

We will normally arrange our QCD perturbation series so that $r_0 = 1$. The RHS of this equation will now have a finite radius of convergence, allowing us to write

$$R = \int_0^{\infty} \frac{dz}{a} e^{-z/a} \sum_{n=0}^{\infty} \frac{r_n}{n!} z^n. \tag{4.10}$$

This is permitted since integrating the expression term by term and using the result

$$\int_0^{\infty} dz e^{-z/a} z^n = n! a^{n+1}, \tag{4.11}$$

reproduces the original series for $R$. If this has a finite radius of convergence then $B[R](z)$ will have an infinite radius of convergence. The usual sum of the series for $R$ is then equal to the Borel sum. Borel summation is said to be a "regular" summation method.

$$R = \int_0^{\infty} \frac{dz}{a} e^{-z/a} B[R](z). \tag{4.12}$$

For the case of interest where $R$ has a zero radius of convergence, $B[R](z)$ will have a finite radius of convergence, and may be analytically continued outside of the radius of convergence onto the whole integration range $[0, \infty]$.

$$R \approx \int_0^\infty \frac{dz}{a} e^{-z/a} B[R](z). \tag{4.13}$$

$\approx$ means "asymptotic to". So the idea is that the divergent asymptotic series is asymptotic to the function corresponding to the Borel integral. The application of Borel transformation to the Adler D function will be discussed in the next chapter.

## 4.3 Bubbles and Chains

Renormalons are a certain pattern of divergence of perturbative expansions in quantum field theories present at all orders and arising from a certain class of diagrams, and related to their small and large momentum behavior. To demonstrate the mechanism of how such divergences emerge, we return to the example of a QED one loop correction in Chapter 2 and shown in Fig. (2.2). Fig. (2.2) can be represented by the diagram illustrated in Fig. (4.1), by making clear that we do not include the external gauge QED photon propagator (denoted as chain) coupled to both sides of the fermion loop which we will denote as the (bubble). Fig. (4.1) shows a diagram of a fermion loop and a photon propagator.



$$= -i\Pi_{\mu\nu}(k^2)$$
$$= -i(k^2 g_{\mu\nu} - k_\mu k_\nu)\Pi_0$$

$$= -iP^{\mu\nu}(k^2)$$
$$= -i\left(\frac{g^{\mu\nu}}{k^2} - (1-\xi)\frac{k^\mu k^\nu}{k^4}\right)$$
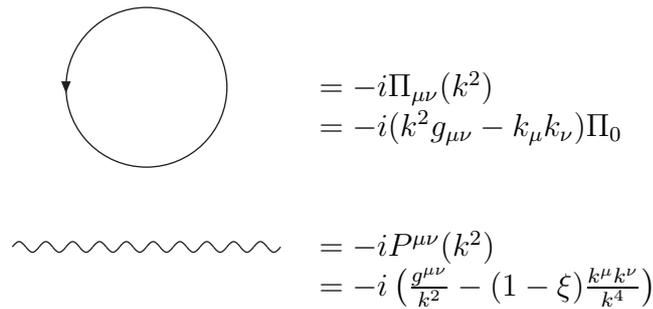
Figure 4.1: *A fermion loop diagram and the photon propagator with their expressions*

Any class of diagrams which contains chains of bubbles were discovered to produce renormalon divergences. Fig. (4.2) gives a clearer picture of an $n$-bubble chain. The complete vacuum polarization function $\Pi(k^2)$ contains

contribution from the diagram containing just a single $n$-bubble chain which is shown in Fig. (4.3).
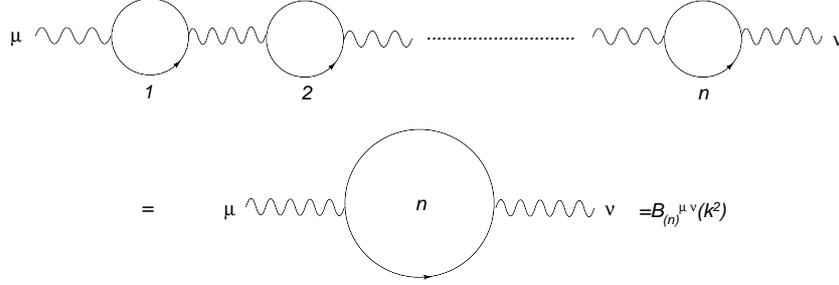


Figure 4.2: *A single n bubble chain*
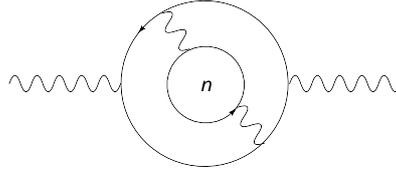


Figure 4.3: *An n-bubble chain inserted into a fermion loop*

Such contributions can be classified as diagrams containing an internal, complete gauge boson propagator. The $n$-bubble chain in Fig. (4.2) can be expressed as

$$B_{(n)}^{\mu\nu}(k^2) =$$
$$(-iP^{\mu\beta_1})(-i\Pi_{\beta_1\alpha_2})(-iP^{\alpha_2\beta_2})(-i\Pi_{\beta_2\alpha_3})...(-iP^{\alpha_n\beta_n})(-i\Pi_{\beta_n\alpha_{n+1}})(-iP^{\alpha_{n+1}\nu}),$$

and then further simplified into

$$B_{(n)}^{\mu\nu}(k^2) = \prod_{k=1}^{n}[(-iP^{\alpha_k\beta_k})(-i\Pi_{\beta_k\alpha_{k+1}})](-iP^{\alpha_{n+1}\nu}). \tag{4.14}$$

Substituting $\mu = \alpha_1$ and after some simple algebra, it is obvious that

$$P^{\alpha_k\beta_k}\Pi_{\beta_k\alpha_{k+1}} = \frac{1}{k^2}\Pi_{\alpha_{k+1}}^{\alpha_k}. \tag{4.15}$$
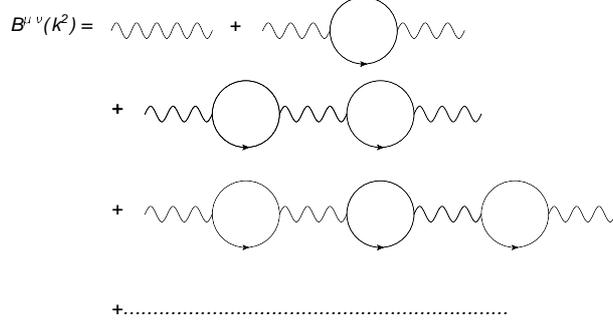
Figure 4.4: *Summing bubble chains from $n = 0$ to $\infty$*

Note that the product $P^{\alpha_k \beta_k} \Pi^{\beta_k \alpha_{k+1}}$ is gauge-independent despite the fact that it consists of strings of propagators which are gauge $\xi$-dependent. Evaluating the product of Eq. (4.15) yields

$$\prod_{k=1}^{n}[\Pi^{\alpha_k}_{\alpha_{k+1}}] = \Pi^{\alpha_1}_{\alpha_{n+1}} \Pi_0^{n-1}(k^2)^{n-1}. \tag{4.16}$$

Thus, Eq. (4.14) can be expressed as

$$
\begin{aligned}
B^{\mu\nu}_{(n)}(k^2) &= \frac{-1^n}{k^2}\Pi^{\alpha_1}_{\alpha_{n+1}} \Pi^{n-1}_{\alpha_0}(-iP^{\alpha_{n+1}\nu}) \\
&= (-1)^n (\Pi_0)^n (\frac{i}{k^2})[g^{\mu\nu} - \frac{k^\mu k^\nu}{k^2}],
\end{aligned}
\tag{4.17}
$$

which in fact corresponds to evaluation in the Landau gauge, $\xi = 0$. One has

$$B^{\mu\nu}_{(n)}(k^2) = (-1)^n (\Pi_0)^n (\frac{i}{k^2})[-iP^{\mu\nu}(k^2, \xi = 0)] \tag{4.18}$$

This is the complete gauge boson propagator. It is the sum of all possible diagrams with two external photon lines only and such exact calculations would corresponds to truncating the perturbative series at the $\infty$th order. This is something which we will not do. Therefore, we restrict the calculation to just include one loop diagrams without considering any higher-loop diagrams for simplicity. This means performing the construction of diagrams with only the above "bubble' corrections to the "bare" gauge boson propagator. As demonstrated in Fig. (4.4), summing over $B^{\mu\nu}_{(n)}(k^2)$ from $n = 0$ to $\infty$ and including one loop contributions only, the complete photon propagator.

$B^{\mu\nu}(k^2)$ can be expressed as

$$
\begin{aligned}
B^{\mu\nu}(k^2) &= -iP^{\mu\nu}(k^2) + \sum_{n=1}^{\infty} B_{(n)}^{\mu\nu}(k^2) \\
&= (\frac{-i}{k^2})[g^{\mu\nu} - \frac{k^\mu k^\nu}{k^2}] \sum_{n=0}^{\infty} (-1)^n (\Pi_0)^n + (\frac{-i}{k^2}) \frac{k^\mu k^\nu}{k^2} \xi \\
&= (\frac{-i}{k^2})[g^{\mu\nu} - \frac{k^\mu k^\nu}{k^2}] \frac{1}{1 + \Pi_0} + (\frac{-i}{k^2}) \frac{k^\mu k^\nu}{k^2} \xi. \tag{4.19}
\end{aligned}
$$

It is interesting to see how a single fermion bubble diagram containing a single internal, complete gauge boson propagator contributes to the vacuum polarization function $\Pi(q^2)$ as represented in Fig. (4.5). This represents the entire set of diagrams with the nth order contribution of Fig. (4.3). The diagram in Fig. (4.5) has an $n$th order term associated with an $n!$ factor, this contributes to what we have discussed in length as "renormalon divergences".

## 4.4 LARGE-NF APPROXIMATION FOR VACUUM PO-LARIZATION

Instead of considering the vacuum polarization function itself, it is useful to study a closely related object known as the Adler D function. The Adler D function plays a crucial role in providing a theoretical description of strong interaction processes like the $e^+ e^-$ annihilation into hadrons which is heavily based on this function. At high energies, perturbation theory remains the most reliable tool for calculating the Adler D function. The Adler D-function is proportional to the logarithmic derivative of $\Pi(s)$ with respect to $s$. This allows us to avoid an unspecified constant associated with $\Pi(s)$. We shall define it more carefully in Chapter 5. Expanded in the coupling $a$ in perturbative QCD we have

$$
D = a + \sum_{n=1}^{\infty} d_n a^{n+1}. \tag{4.20}
$$

We will explain its relation to the parton model result and $R(s)$ in Chapter 6.

Note that the nth term in $D(q^2)$ and $\Pi(q^2)$ are derived from the same diagram. So $d_n a^{n+1}$ will contain contributions from diagram in Fig. (4.6) the calculation of which simply involves combining the expression for an $n$-bubble chain, $B_{(n)}^{\mu\nu}(k^2)$ with the relevant fermion propagators of the loop and

then integrating over the loop momentum of the fermion loop $p$ and that of the photon momentum $k$. This leads to
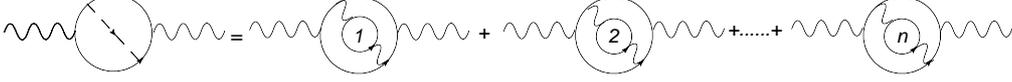


Figure 4.5 *Diagram of a complete photon propagator inserted into a bubble*

$$
\begin{aligned}
d_n a^{n+1} &\sim a \int \frac{d^4 k}{(2\pi)^4} \frac{d^4 p}{(2\pi)^4} \\
&\times \left[ B_{(n)}^{\sigma\rho}(k^2) Tr(\gamma_\nu \frac{1}{\not p + \not q + \not k} \gamma_\rho \frac{1}{\not p + \not q} \gamma_\mu \frac{1}{\not p} \gamma_\sigma \frac{1}{\not p + \not k}) \right. \\
&+ \left. 2 B_{(n)}^{\sigma\rho}(k^2) Tr(\gamma_\nu \frac{1}{\not p + \not q} \gamma_\mu \frac{1}{\not p} \gamma_\sigma \frac{1}{\not p + \not k} \gamma_\rho \frac{1}{\not p}) \right] \qquad (4.21) \\
&\sim a \int \frac{d^4 k}{(2\pi)^4} \frac{d^4 p}{(2\pi)^4} \left[ B_{(n)}^{\sigma\rho}(k^2) X_{\nu\rho\mu\sigma} + 2 B_{(n)}^{\sigma\rho}(k^2) \overline{X}_{\nu\mu\sigma\rho} \right]. \,(4.22)
\end{aligned}
$$

X and $\overline{X}$ are the tensor structures found by evaluating

$$
\begin{aligned}
X_{\nu\rho\mu\sigma} &= Tr(\gamma_\nu \frac{1}{\not p + \not q + \not k} \gamma_\rho \frac{1}{\not p + \not q} \gamma_\mu \frac{1}{\not p} \gamma_\sigma \frac{1}{\not p + \not k}), & (4.23) \\
\overline{X}_{\nu\mu\sigma\rho} &= Tr(\gamma_\nu \frac{1}{\not p + \not q} \gamma_\mu \frac{1}{\not p} \gamma_\sigma \frac{1}{\not p + \not k} \gamma_\rho \frac{1}{\not p}). & (4.24)
\end{aligned}
$$

Each coefficient $d_n$ may be expanded in powers of $N_f$

$$
d_n = d_n^{[n]} N_f^n + d_n^{[n-1]} N_f^{n-1} + \ldots + d_n^{[0]}. \qquad (4.25)
$$

The leading $d_n^{[n]} N_f^n$ term corresponds to evaluating the one-chain diagrams of Fig(4.6). The sub-leading $N_f^{n-1}$ term arises from two-chain diagrams as in Fig. (4.7) , which generates a contribution of order $a^{l+m+2} N_f^{l+m} \sim a^{n+1} N_f^{n-1}$ .
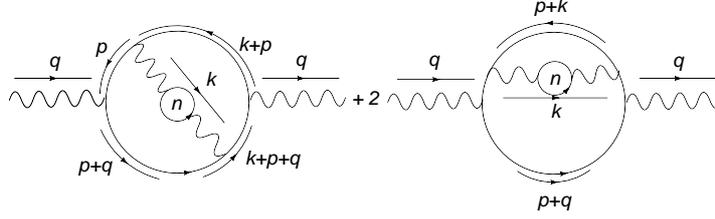
Figure 4.6 : *Contribution to $d_n a^{n+1}$*

The large-$N_f$ all-orders result can describe QED vacuum polarization, but for QCD the corrections to the gluon propagator involve gluon and ghost loops (see Fig(2.3)), and are gauge ($\xi$)-dependent. The result for $\Pi_0(k^2)$ cf. Eq. (2.24) is proportional to $-N_f/3$ which is the first QED beta-function coefficient, $b$. In QCD one expects large-order behaviour of the form $d_n \sim K n^\gamma (b/2)^n n!$ ($\gamma$ is the fractional exponent related to the anomalous dimension) involving the QCD beta-function coefficient $b = (33 - 2N_f)/6$ [22], it is natural to replace $N_f$ by $(33/2 - 3b)$ to obtain an expansion in powers of $b$

$$d_n = d_n^{(n)} b^n + d_n^{(n-1)} b^{n-1} + \ldots + d_n^{(0)}. \tag{4.26}$$

The leading-$b$ term $d_n^{(L)} \equiv d_n^{(n)} b^n = (-3)^n d_n^{[n]} b^n$ can then be used to approximate $d_n$ to all-orders. One imagines that the fermion bubble chains in QED are replaced by chains of effective QCD bubbles involving gauge invariant combinations of gluon and ghost contributions, so that for both QED and QCD

$$\Pi_0(k^2) = \frac{ba}{2} (\ln \frac{-k^2}{\mu^2} + C), \tag{4.27}$$

with either $b = -\frac{2N_f}{3}$, or $b = (33 - 2N_f)/6$. It is convenient to use a particular choice of RS, the $V$-scheme which corresponds to using the $\overline{MS}$ scheme with a scale $\mu^2 = Q^2 e^{-5/3}$. This ensures that $C = 0$, so that

$$\Pi_0(k^2) = \frac{ba}{2} \ln \frac{-k^2}{Q^2}. \tag{4.28}$$

We have

$$
\begin{aligned}
d_n^{[n]} N_f^n a^{n+1} &\sim a \\
&\times \int \frac{d^4 k}{(2\pi)^4} \frac{d^4 p}{(2\pi)^4} [B_{(n)}^{\sigma\rho}(k^2) X_{\nu\rho\mu\sigma} + 2 B_{(n)}^{\sigma\rho}(k^2) \overline{X}_{\nu\mu\sigma\rho}] (4.29) \\
&= a \int \frac{d^2 \tilde{k}}{\tilde{k}^2} F(\tilde{k}^2) (-\Pi_0)^n. \tag{4.30}
\end{aligned}
$$

where we integrate over fermion loop momenta $p$ and the angle of the gluon momentum $k$. $F(\tilde{k}^2)$ itself is complicated and its exact expression can be found in [23]. Here we have introduce the notation $\tilde{k}^2 = -k^2/Q^2$. The coefficient $d_n^{[n]}(V)$ is explicitly given by [24, 25]

$$
\begin{aligned}
d_n^{[n]}(V) &= \frac{-2}{3}(n+1)\left(\frac{-1}{6}\right)^n \\
&\times \left[ -2n - \frac{n+6}{2^{n+2}} + \left( \frac{16}{n+1} \sum_{\frac{n}{2}+1>m>0} m(1-2^{-2m})(1-2^{2m-n-2})\zeta_{2m+1} \right) \right] n!.
\end{aligned}
$$
(4.31)

This has $n!$ growth and can be resummed using Borel summation as we shall see in Chapter 5. Hence, using the presentation in [26],

$$
d_n^{[n]} N_f^n a^{n+1} = a \int \frac{d^2\tilde{k}}{\tilde{k}^2} F(\tilde{k}^2) \left( \frac{ba}{2} \ln \frac{\tilde{k}^2 Q^2 e^{-5/3}}{\mu^2} \right)^n, \quad (4.32)
$$

$$
\Rightarrow D \simeq \sum_{(n=0)}^{\infty} d_n^{[n]} N_f^n a^{n+1} = \sum_{(n=0)}^{\infty} a \int \frac{d^2\tilde{k}}{\tilde{k}^2} F(\tilde{k}^2) \left( \frac{ba}{2} \ln \frac{\tilde{k}^2 Q^2 e^{-5/3}}{\mu^2} \right)^n.
$$
(4.33)
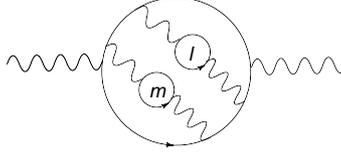


Figure 4.7 : *A double chain contribution to* $D(\tilde{k}^2)$

Provided that the renormalization scale $\mu$ is kept fixed to the order of perturbation theory, the dominant contributions to the integral come from both regions of small $k \ll Q$ and large $k \gg Q$ behavior of $F(\tilde{k}^2)$.

$$
F(\tilde{k}^2) = 3C_F \tilde{k}^4 + O(\tilde{k}^6 \ln(\tilde{k}^2)) \tag{4.34}
$$

$$
F(\tilde{k}^2) = \frac{2C_F}{3} \frac{1}{\tilde{k}^2} \left( \ln(\tilde{k}^2) + \frac{5}{6} \right) + O\left( \frac{\ln(\tilde{k}^2)}{\tilde{k}^4} \right) \tag{4.35}
$$

This concludes that the ultraviolet and infrared finiteness of the Adler D function implies that $F(\tilde{k}^2)$ must have a power like approach to zero in both

regions. Splitting the integral of Eq. (4.33) at $\tilde{k}^2$ in both regions, we will obtain

$$D = C_F \sum_{(n=0)}^{\infty} a^{n+1} \left[ \frac{3}{4} \left( \frac{Q^2}{\mu^2} e^{-5/3} \right)^{-2} \left( -\frac{b}{2} \right)^n n! + \frac{1}{3} \left( \frac{Q^2}{\mu^2} e^{-5/3} \right) \left( n + \frac{11}{6} \right) b^n n! \right].$$
(4.36)

The first term from small $\tilde{k}$ and the second from large $\tilde{k}$. The singularities in the Borel plane lie at $t = -2/b$ for IR renormalon and $t = 1/b$ for UV renormalon with the Borel transform given by

$$
\begin{aligned}
B[D](u) \; = \; & \frac{3C_F}{2} \left( \frac{Q^2}{\mu^2} e^{-5/3} \right)^{-2} \frac{1}{2-u} \quad \text{(1st IR Renormalon)} \\
+ \; & \frac{C_F}{3} \left( \frac{Q^2}{\mu^2} e^{-5/3} \right) \left[ \frac{1}{(1+u)^2} + \frac{5}{6} \frac{1}{1+u} \right] \quad \text{(1st UV Renormalon)}
\end{aligned}
$$
(4.37)

Here we define $u = -bt$. Note that this is not the exact Borel transform for Fig. (4.6). The exact Borel transform for the Adler D function will be defined in Chapter 5.

Multi-chain diagrams in QED have been analyzed that higher order corrections in $1/N_f$ do not modify renormalon singularities except their strength indicated by $b$. As the location of the singularities are a function of $b$, we will have different location of UV and IR renormalons in QED and QCD. We will highlight a few important characteristics of UV renormalons, IR renormalons as well as their differences with instantons in QCD briefly.

Ultraviolet renormalons are located at $t = m/b$, $m$ are positive integers implying $u = -1, -2, \ldots$ UV renormalons produce alternating sign factorial divergences. All UV renormalons are double poles, restricting oneself to the bubble diagram of Fig. (4.6). The first singularity $u = -1$ has been analyzed in detail using renormalization group method, which turned out to be a complicated branch point structure attaching to it. They are theory-specific but process-independent (process-dependence factorizes and is calculable). In 4-dimensions, UV renormalons are always located at positive integer multiples of $1/b$ although there are exceptional cases if the theory contains power divergences (begins at some negative integer multiples of $1/b$) or in the case of heavy quark effective theory (can occur at half-integer u).

Infrared renormalons are located at $t = -m/b$, with $m = 2, 3, ...$ implying $u = 2, 3, ...$ This result in the minimal term associated with this subseries is of order $(\Lambda/Q)^4$ (this will be clearer as we go along Chapter 5 and 7) due to the first IR renormalon. Contrary to UV renormalons, IR renormalons are $\mu$-independent suggesting that its ambiguities might have physical significance. For the Adler function, we can associate them with the absence of dimension-2 condensate in the OPE as the $u = 1$ singularity is absent. All IR renormalons are double poles except for $u = 2$, which is a single pole. The first singularity has been analyzed in detail using renormalization properties of gluon condensate which it was concluded that the pole turned into a branch cut with structure simpler than the first UV renormalon.

Instantons are also known to produce divergent series but as they carry topological charge, they are unrelated to perturbative expansion in QCD. In QCD, instanton singularities are far away from the origin of Borel plane implying that it plays insignificant role in large-order behaviour of perturbative expansion in QCD.
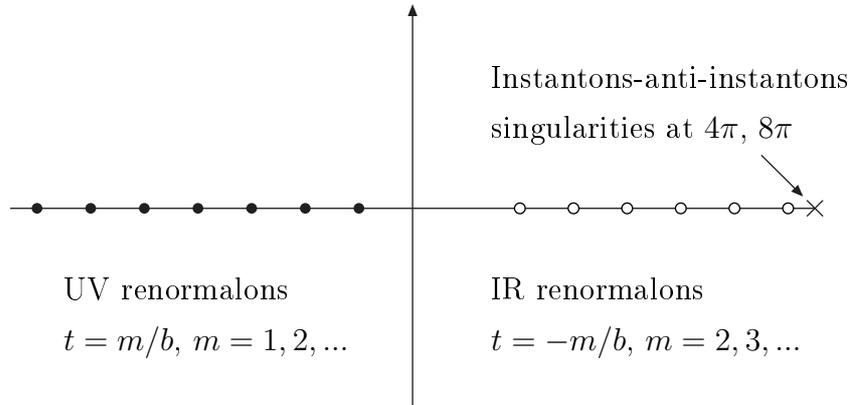


Figure 4.8: Singularities in the Borel plane of $\Pi(k^2)$, the correlator function in QCD. Shown are UV renormalons, IR renormalons and instantons

## 4.5 SUMMARY

We began this chapter by introducing divergent series in perturbation theory and the application of the Borel method to define an asymptotic series as a function. We later explained bubbles and chains in a very informal manner showing all the details step by step and its relation to the Adler D function. A brief introduction to the Adler D function as a divergent series was made and we finally pointed out what a "renormalon" is, distinguishing between

UV and IR renormalons corresponding to large and small momenta- $k$ flowing through the fermion or effective QCD bubble chains.

We end the chapter by highlighting the theoretical analysis on UV and IR renormalons while making a brief introduction to instantons.

# Chapter 5

# IR Freezing of Euclidean QCD Observables

## 5.1 Introduction

Fixed-Order Perturbation Theory in QCD has proved successful in making accurate approximations to physical observables at large energies, $Q^2$. Nevertheless, such a perturbative approach breaks down below the Landau pole $Q^2 = \Lambda^2$, this is due to non-perturbative effects in the Infrared region. Non-perturbative information is essential to make perturbation theory sensible as higher perturbative coefficients exhibit factorial growth making the series not convergent. Resummed perturbation series can be represented by a Borel integral which is ambiguous due to singularities on the positive real axis (also known as Infrared Renormalons) of the Borel plane. These ambiguities are in the form of powers of $\Lambda^2/Q^2$ and we will discuss them in more detail in Chapter 7. In this chapter, we will demonstrate how to use Borel summation to resum the "leading-b" terms in perturbative corrections to the Polarized Bjorken Sum Rule $K_{pBj}$, Unpolarized Bjorken Sum Rule $U_{uBJ}$ and the Adler D function to all orders. We begin by defining the three Euclidean quantities of interest but firstly with a heuristic detailed description on deep inelastic scattering, structure functions, parton distribution function and an overview of sum rules.

## 5.2 DIS and Sum Rules

Deep inelastic scattering (DIS) or high energy lepton-nucleon scattering plays a role in understanding the partonic structure of the proton. We will not touch on the detailed kinematics of DIS. Deep inelastic structure functions

68

provide not only some of the most precise test to the theory but also momentum distributions of partons in hadrons. The structure function $F_i(x, Q^2)$ (where $Q^2 = -q^2$ with $q$ as the four-momentum transfer from an exchanged particle like photon or $Z$ to the nucleon and $x$ is the fraction of nucleon's momentum carried by struck quark) which parameterize the structure of the target as 'seen' by the virtual photon - are defined in terms of lepton scattering cross sections. In the hadronic region $Q^2 << \Lambda^2$, the wavelength of the photon is too small to resolve the structure of the nucleon and the nucleon simply undergoes elastic scattering. At higher values of $Q^2$, $Q^2 > \Lambda^2$, the scattering becomes inelastic as the photon starts to resolve the substructure of the nucleon and, in particular, the momentum fraction carried by the partons.

The Bjorken limit (or Bjorken scaling) is defined as the independence of the structure function on $Q^2$ where $F_1(x, Q^2) \longrightarrow F_1(x)$ and $F_2(x, Q^2) \longrightarrow F_2(x)$ implying scattering from point-like constituents within the proton. In this limit, the structure function obey an approximate scaling law. The participating structure function for an unpolarized (neutral- and charged-current DIS on unpolarized nucleons) proton target are $F_2^\nu$, $xF_3^\nu$, $F_2^{\bar\nu}$, $xF_3^{\bar\nu}$, $F_2^{em}$ and $2xF_1 = F_2$. *em* denotes neutral current arises from neutral current $eN \longrightarrow eX$ ($N$ denotes nucleon and $X$ denotes hadrons) processes which involves photons and $Z$ exchange. $\nu$ denotes charge current structure functions which exclusively derived from $W$ exchange processes like $eN \longrightarrow \nu X$ or $\nu N \longrightarrow eX$. Polarized DIS involve the helicities ($\pm 1$) of the incoming lepton and nucleon with five structure functions $g_{1,...5}(x, Q^2)$. For $e^-$ or $\nu$ initiated processes, the difference to the polarized cross section arises from the difference of anti-parallel minus parallel spin, for $e^+$ or $\bar\nu$ initiated processes, this is the opposite. Note that there is the same tensor structure between the spin-dependent and spin-independent parts of hadronic tensor, thus the substitution of $F_1 \longrightarrow -g_5$, $F_2 \longrightarrow -g_4$ and $F_3 \longrightarrow -2g_1$ in calculation of the cross section is allowed. $g_2$ and $g_3$ are suppressed by powers of $M^2/Q^2$ ($M$ denotes nucleon mass) for longitudinal nucleon while for transverse nucleons, the cross section difference vanishes as $M/Q \longrightarrow 0$. Using the Callan-Gross relations $F_L^i = 0$ and the Dicus relations $g_L^i = 0$, there are two independent polarized structure functions $g_1$ (conserves parity) and $g_5$ (violates parity), in analogy to $F_1$ and $F_3$.

In quark-parton model, $F_i$ and $g_i$ are expressed in parton distribution functions $q(x, Q^2)$ of the proton where $q = u, \bar{u}, d, \bar{d}, s, c, b$ and $g$. $q(x, Q^2)dx$ is the number of that particular parton carrying a momentum fraction between $x$ and $x + dx$ of the proton's momentum in a frame in which the proton

momentum is large.

Integrals over certain combinations of parton distribution functions had particular values in the parton model, such integrals are called sum rules. In QCD, these sum rules remain valid up to perturbative corrections. This sum rules provide constraints on parton distributions and tests of conservation law up to the measurement of $\alpha_s$. Most of the famous sum rules are combination of these sum rules

$$
\int_0^1 u_v(x)dx = 2, \qquad \int_0^1 d_v(x)dx = 1,
$$

$$
\sum_q \int_0^1 x[q(x) + \bar{q}(x)]dx = \int_0^1 x[u_v(x) + d_v(x) + 6S(x)]dx \approx 0.5.
$$

Here, we have assumed the sea of quarks of the particle (in this case a proton) to be symmetric in quark flavors (which the particle has an infinite sea of light $q\bar{q}$ pairs) where we have $u(x) = u_v(x) + S(x)$, $d(x) = d_v(x) + S(x)$ and $S(x) = \bar{u}(x) = \bar{d}(x) = s(x) = \bar{s}(x)$. The subscript $v$ denotes the word valence. Note the last sum rule $\sum_q \int_0^1 x[q(x) + \bar{q}(x)]dx$ is obtained through experiment. The interpretation of the sum rule indicates the percentages of the particle's momentum (in this case a proton) carried by the partons (in this case quarks) which is equivalent to 50%. And the rest are carried away by gluons.

In the partonic region $Q^2 >> \Lambda^2$, the shape of the quark and gluon distributions changes quickly at very low $x$. The sea becomes more flavour symmetric. This is because at low $x$, the evolution is flavour-independent, and there are more and more sea quarks and gluons. This confirms the foundational prediction of QCD which was verified by the HERA experiments at DESY.

However, there is not a unique set of Parton Distribution Functions being commonly accepted. There are several groups competing to provide the best parametrization of the parton distributions. They do not use the same input data, parameterisation, treatment of heavy quarks, value of the coupling constant as well as the way the estimation of the experimental and theoretical errors are treated. A recommended on line program written by professional groups is at the link:

http://hepdata.cedar.ac.uk/pdf/pdf3.html

By changing the parameters set in the program, we did not just verify all the facts on the parton distribution function but also from the shape and area under the curve, we can predict the expectation values of the sum rules.

## 5.3 THE GROSS-LLEWELLYN-SMITH SUM RULE

The GLS Sum Rule applies to the $F_3$ structure function measured in neutrino-and antineutrino-proton scattering, in the parton model, it has a value of 3. The sum rule is defined as

$$G_{GLS} = \frac{1}{2} \int_0^1 F_3^{\bar{\nu}p + \nu p}(x, Q^2) dx. \tag{5.1}$$

In the parton model this is given by,

$$G_{GLS} = \int_0^1 \left( u(x) - \bar{u}(x) + d(x) - \bar{d}(x) \right) dx,$$

but incorporating QCD corrections we have,

$$G_{GLS} = 3(1 - \frac{3}{4} C_F G(Q^2)),$$

where $G(Q^2)$ is defined as,

$$G(Q^2) = a + G_1 a^2 + G_2 a^3 + \dots \tag{5.2}$$

$G_1$, $G_2$ and $G_3$ are the coefficients calculated in the $\overline{MS}$ scheme.

## 5.4 THE GERASIMOV-DRELL-HEARN SUM RULE

The GDH Sum Rule is explicitly discussed in [27]. The GDH Sum Rule relates the helicity structure of the cross sections in the inelastic region with ground state properties. Base on the physics law like Lorentz and gauge invariance, causality and unitarity, GDH Sum Rule is important for us to check our understanding on the hadronic structure. There are many forms of GDH Sum Rule written in different forms and notations. In general, the GDH Sum Rule is expressed as

$$I_1(Q^2) = \frac{2M^2}{Q^2} \int_0^1 \left[ g_1(x, Q^2) - \frac{4x^2 M^2}{Q^2} g_2(x, Q^2) \right] dx, \tag{5.3}$$

where $x = Q^2/2M\nu$ with $M$ being the nucleon mass and $\nu$ being the energy transfer. Note that the quark distribution function are related to densities for longitudinal and transverse quark polarization denoted by $f_i^{\uparrow,\downarrow}$ and $f_i^{\rightarrow,\leftarrow}$. $e$ denotes the value of the charges of the quarks while $i$ denotes the quark flavour

$$g_1(x, Q^2) \quad \longrightarrow g_1(x) = \frac{1}{2} \sum_i e_i^2 \left( f_i^{\uparrow} - f_i^{\downarrow} \right), \tag{5.4}$$

$$g_2(x, Q^2) \quad \longrightarrow g_2(x) = \frac{1}{2} \sum_i e_i^2 (f_i^{\rightarrow} - f_i^{\leftarrow}) - g_1(x). \tag{5.5}$$

We will revisit GDH Sum Rule in Chapter 7 under usual experiment condition by neglecting $g_2(x, Q^2)$ contribution and relating it to the polarized Bjorken Sum Rule.

## 5.5 POLARIZED BJORKEN SUM RULE

The polarized Bjorken Sum Rule is defined via the spin-dependent proton and neutron structure functions $g_1^{ep}$, $g_1^{en}$ with $x = Q^2/2M\nu$, $\nu$ denotes the energy transfer and $M$ is the nucleus mass. At extremely large $Q^2$, $K_{pBj}$ arrived at its renowned value of $= |g_A/6g_V|$. At finite $Q >> \Lambda$, $K_{pBj}$ is dominated by perturbative corrections $K(Q^2)$ to the parton model sum rule in $a^n$

$$
\begin{aligned}
K_{pBj} &\equiv \int_0^1 g_1^{ep-en}(x, Q^2)dx \\
&= \frac{1}{6} \left| \frac{g_A}{g_V} \right| \left( 1 - \frac{3}{4} C_F K(Q^2) \right), 
\end{aligned}
\tag{5.6}
$$

where $g_V$ and $g_A$ are the nucleon vector and axial vector couplings. $K(Q^2)$ is defined as,

$$K(Q^2) = a + K_1 a^2 + K_2 a^3 + \dots\dots \tag{5.7}$$

$K_1$, $K_2$ and $K_3$ are the coefficients calculated in the $\overline{MS}$ scheme. Higher-twist terms are not taken into account. [28, 29]

## 5.6 Unpolarized Bjorken Sum Rule

The unpolarized Bjorken Sum Rule for $F_1$ structure function of $\nu N$ deep inelastic scattering still remains experimentally unchecked. However at Neutrino Factories, there is a possibility to determine the $xF^{\nu N}$ and $xF^{\bar{\nu} N}$ structure functions which provides the first experimental determination of the unpolarized Bjorken Sum Rule. The unpolarized Bjorken Sum Rule is given by

$$U_{uBj} \equiv \int_0^1 F_1^{\nu n - \nu p}(x, Q^2) dx.$$

In the parton model, this is given by

$$U_{uBj} = \int_0^1 \left( u(x) - \bar{u}(x) - d(x) + \bar{d}(x) \right) dx.$$

$U_{uBJ}$ is related to the Adler isospin Sum Rule $U_{uBj2}$ and the Callan-Gross relation for $\nu N$ deep inelastic scattering $U_{uBjL}$ by

$$U_{uBj}(Q^2) = U_{uBj2}(Q^2) + U_{uBjL}(Q^2),$$

where,

$$U_{uBj2}(Q^2) = \int_0^1 F_2^{\nu n - \nu p}(x, Q^2) \frac{dx}{2x} = 1,$$

$$U_{uBjL}(Q^2) = \int_0^1 F_L^{\nu p - \nu n}(x, Q^2) \frac{dx}{2x}.$$

Incorporating QCD corrections we have [30],

$$U_{uBj}(Q^2) = \left( 1 - \frac{1}{2} C_F U(Q^2) \right), \tag{5.8}$$

where higher-twist terms are neglected and

$$U(Q^2) = a + U_1 a^2 + U_2 a^3 + \ldots\ldots \tag{5.9}$$

$U_1$, $U_2$ and $U_3$ are coefficients also calculated in the $\overline{MS}$ scheme [28, 29].

## 5.7 $Q^2-$DEPENDENCE OF THE EUCLIDEAN OBSERVABLES

We follow the presentation and notation of [31] [32] very closely, and refer the reader there for more details. The Adler D function $D(Q^2)$ is defined as the logarithmic derivative of $\Pi(Q^2)$ with respect to the energy $Q^2$

$$\tilde{D}(Q^2) = -\frac{3}{4}Q^2\frac{d}{dQ^2}\Pi(Q^2), \tag{5.10}$$

where $\Pi(Q^2)$ is the QCD vacuum polarization function. $\Pi(Q^2)$ is related to the correlator of the two vector currents

$$(q_\mu q_\nu - g_{\mu\nu}q^2)\Pi(Q^2) = 16\pi^2\int d^4xe^{iq.x} < 0|T[J_\mu(x),J_\nu(0)]|0 >, \tag{5.11}$$

where $q^\mu$ is a vector satisfying $q^2 = Q^2$. The function $\Pi(Q^2)$ can be calculated from the diagrams in Fig. (5.1).

Eq. (5.10) consists of the parton model result and the QCD corrections, $D(Q^2)$,

$$\tilde{D}(Q^2) = N\sum_f Q_f^2(1 + \frac{3}{4}C_F D(Q^2)). \tag{5.12}$$

$N$ is the number of colours and $Q_f$ is the charge of quark flavour $f$. We neglect here "light-by-light" terms which will be mentioned in Chapter 6. Here $D(Q^2)$ is given by two terms

$$D(Q^2) = D_{PT}(Q^2) + D_{NP}(Q^2), \tag{5.13}$$

where the first term is the perturbative term and the second term is the non-perturbative term. The perturbative term is given by

$$D_{PT}(Q^2) = a(Q^2) + \sum_{n>0} d_n a^{n+1}(Q^2), \tag{5.14}$$

where $a(Q^2) = \alpha_s(Q^2)/\pi$ is the renormalized coupling and for one loop approximation (which we have discussed in Section 2.6)

$$a(Q^2) = \frac{2}{b\ln(\frac{Q^2}{\Lambda^2})} \tag{5.15}$$

as the plots in this chapter will just be a simple model using just one loop approximation. Use of the one loop coupling together with the "leading-b"

contributions to the perturbative coefficients automatically ensures that the all-orders resummations are independent of the RS scale $\mu$, which is the only source of RS-dependence at the one loop level. $Q^2 = -q^2 > 0$ is the single space like energy scale. $D(Q^2) \longrightarrow 0$ as $Q^2 \longrightarrow \infty$ thanks to asymptotic freedom. We will not take into account non-perturbative contributions arising from the OPE (Operator Product Expansion). These will be covered in Chapter 7. In this chapter we shall be concerned with trying to resum to all-orders the perturbative "leading-$b$" terms discussed in Chapter 4 Eq. (4.26).

The polarized Bjorken ($K_{pBj}$) Sum Rule is defined in Eq. (5.6) and the corresponding GLS Sum Rule in Eq. (5.1). $G(Q^2)$ and $U(Q^2)$ are split into perturbative (PT) and non-perturbative (NP) parts just like the case for $D(Q^2)$. Note that contributions due to "light-by-light" diagrams are omitted for the perturbative corrections to the $G_{GLS}$ and $K_{pBj}$.
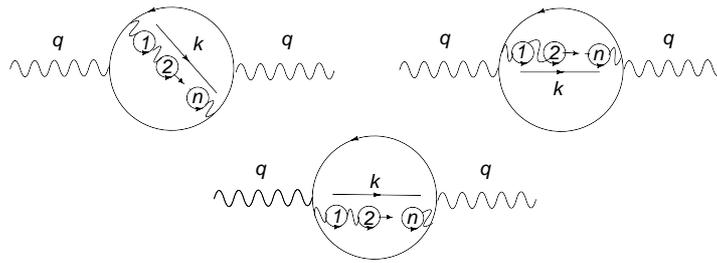


Figure 5.1: *Leading large $N_f$ contributions of $\Pi(Q^2)$ at nth order*
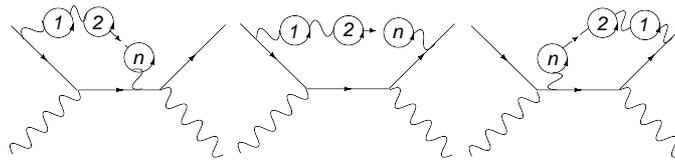


Figure 5.2: *Leading large $N_f$ contributions to $K_{pBJ}$, $U_{uBJ}$ and $G_{GLS}$ at nth order*

Fig. (5.2) provides the leading $N_f$ contributions to all these sum rules. These large $N_f$ results will be used to compute the leading-$b$ all-orders resummation of these perturbative corrections denoted by $D_{PT}^{(L)}(Q^2)$, $K_{PT}^{(L)}(Q^2)$ and $U_{PT}^{(L)}(Q^2)$.

We recall from Chapter 4 that in the large $N_f$ limit, we can expand $d_n$ as

$$d_n = d_n^{[n]} N_f^n + d_n^{[n-1]} N_f^{n-1} + ... + d_n^{[0]}, \tag{5.16}$$

where $d_n^{[n]}$ is the leading large $N_f$ coefficient which can be computed to all-orders from a set of Feynman diagrams Fig(5.1). Replacing $N_f = (33/2 - 3b)$, we will then obtain an expansion of the form

$$d_n = d_n^{(n)} b^n + d_n^{(n-1)} b^{n-1} + ... + d_n^{(0)}, \tag{5.17}$$

where computation of the "leading-$b$", $d_n^{(L)} \equiv d_n^{(n)} b^n$ to all-orders based on large-$N_f$ results is possible. One can then arrive at an all-orders leading-$b$ result by resumming the $d_n^{(L)} a^{n+1}$ terms using a Borel transform technique.

We will now write the Borel transform of $D_{PT}^{(L)}$ found in [33],

$$\begin{aligned}
B[D_{PT}^{(L)}](z) &= \sum_{n=1}^{\infty} \frac{A_0(n) - A_1(n) z_n}{(1 + \frac{z}{z_n})^2} + \frac{A_1(n) z_n}{(1 + \frac{z}{z_n})} \\
&+ \sum_{n=1}^{\infty} \frac{B_0(n) + B_1(n) z_n}{(1 - \frac{z}{z_n})^2} - \frac{B_1(n) z_n}{(1 - \frac{z}{z_n})},
\end{aligned} \tag{5.18}$$

where

$$\begin{aligned}
A_0(n) &= \frac{8}{3} \frac{(-1)^{n+1}(3n^2 + 6n + 2)}{n^2(n+1)^2(n+2)^2} \\
A_1(n) &= \frac{8}{3} \frac{b(-1)^{n+1}(n + \frac{3}{2})}{n^2(n+1)^2(n+2)^2} \\
B_0(1) &= 0, \\
B_0(2) &= 1, \\
B_0(n) &= -A_0(-n), n \geq 3 \\
B_1(1) &= 0, \\
B_1(2) &= -\frac{b}{4}, \\
B_1(n) &= -A_1(-n), n \geq 3 \\
z_n &= \frac{2n}{b}
\end{aligned} \tag{5.19}$$

Here $z_n \equiv \frac{2n}{b}$ give the positions of IR renormalons at $z = z_n$ and UV renormalons at $z = -z_n$ in the Borel plane. We will derive the Borel transform of $D_{PT}^{(L)}$ explicitly in the next section by using a skeleton expansion and converting it to the Borel representation by a change of variable. This turns out to be much easier than evaluating the result using the two loop one-chain

result for $d_n^{[n]}(V)$ in Eq. (4.31). The Borel transform of $K_{PT}^{(L)}$ and $U_{PT}^{(L)}$ which have a simpler structure structure than that for the Adler D function can be written as [34]

$$B[K_{PT}^{(L)}](z) = \frac{4}{9}\frac{1}{1+\frac{z}{z_1}} - \frac{1}{18}\frac{1}{1+\frac{z}{z_2}} + \frac{8}{9}\frac{1}{1-\frac{z}{z_1}} - \frac{5}{18}\frac{1}{1-\frac{z}{z_2}}, \qquad (5.20)$$

and

$$B[U_{PT}^{(L)}](z) = \frac{1}{6}\frac{1}{1+\frac{z}{z_2}} + \frac{4}{3}\frac{1}{1-\frac{z}{z_1}} - \frac{1}{2}\frac{1}{1-\frac{z}{z_2}}. \qquad (5.21)$$

They are much simpler as they come from inserting chain of $n$-bubbles into a tree level diagram shown in Fig. (5.2), rather than inserting into a quark loop. Eq. (5.20) has 4 poles while Eq. (5.21) has three poles in contrast to Eq. (5.18) which has an infinite amount of poles.

The following resummed expressions for $D_{PT}^{(L)}(Q^2)$,$K_{PT}^{(L)}(Q^2)$ and $U_{PT}^{(L)}(Q^2)$

$$
\begin{aligned}
D_{PT}^{(L)}(Q^2) &= \sum_{n=1}^{\infty} z_n \left\{ e^{(z_n/a(Q^2))}\mathrm{Ei}\left(\frac{-z_n}{a(Q^2)}\right)\left[\frac{z_n}{a(Q^2)}(A_0(n) - z_1 A_1(n) - z_n A_1(n))\right]\right. \\
&+ \left. (A_0(n) - z_n A_1(n))\right\} + \sum_{n=1}^{\infty} z_n \left\{ e^{(-z_n/a(Q^2))}\mathrm{Ei}\left(\frac{z_n}{a(Q^2)}\right)\left[\frac{z_n}{a(Q^2)}(B_0(n) + z_1 B_1(n)\right.\right. \\
&- \left.\left. z_n B_1(n))\right] - (B_0(n) + z_n B_1(n))\right\}, \qquad (5.22)
\end{aligned}
$$

$$
\begin{aligned}
K_{PT}^{(L)}(Q^2) &= \frac{1}{9b}\left[-8e^{(-z_1/a(Q^2))}\mathrm{Ei}\left(\frac{-z_1}{a(Q^2)}\right) + 2e^{(-z_2/a(Q^2))}\mathrm{Ei}\left(\frac{-z_2}{a(Q^2)}\right)\right. \\
&+ \left. 16e^{(-z_1/a(Q^2))}\mathrm{Ei}\left(\frac{z_1}{a(Q^2)}\right) - 10e^{(-z_2/a(Q^2))}\mathrm{Ei}\left(\frac{z_2}{a(Q^2)}\right)\right], \qquad (5.23)
\end{aligned}
$$

$$
\begin{aligned}
U_{PT}^{(L)}(Q^2) &= \frac{1}{3b}\left[8e^{(-z_1/a(Q^2))}\mathrm{Ei}\left(\frac{z_1}{a(Q^2)}\right)\right. \\
&- \left. 6e^{(-z_2/a(Q^2))}\mathrm{Ei}\left(\frac{z_2}{a(Q^2)}\right) - 2e^{(z_2/a(Q^2))}\mathrm{Ei}\left(\frac{-z_2}{a(Q^2)}\right)\right], \qquad (5.24)
\end{aligned}
$$

can easily be obtained using the standard integrals involving the $Ei(x)$ function

$$\int_0^\infty dz\left(\frac{e^{-\frac{z}{a}}}{1+\frac{z}{z_n}}\right) = -z_n e^{\frac{z_n}{a}} Ei(-z_n/a), \tag{5.25}$$

$$\int_0^\infty dz\frac{e^{-\frac{z}{a}}}{(1+\frac{z}{z_n})^2} = z_n[1+\frac{z_n}{a}e^{\frac{z_n}{a}} Ei(-z_n/a)]. \tag{5.26}$$

The $Ei(x)$ function known as the exponential integral function [35] is defined as

$$Ei(x) = -\int_{-x}^\infty dt\frac{e^{-t}}{t}, \tag{5.27}$$

for $x < 0$. For $x > 0$, only the principal value of the integral is considered and can be expanded such that

$$Ei(x) = \ln|x| + \gamma_E + O(x), \tag{5.28}$$

for small values of $x$. For the region $Q^2 < \Lambda^2$, the one loop coupling Eq. (5.15) changes sign on passing through $Q^2 = \Lambda^2$ and we need to introduce a modified Borel representation introduced and motivated in [31], expanded in powers of $|a|$ given by

$$D_{PT}^{(L)}(Q^2) = -\int_0^\infty dze^{-z/|a(Q^2)|}B[D_{PT}^{(L)}](-z), \tag{5.29}$$

by making a change of sign on

$$a(Q^2) \longrightarrow -a(Q^2),$$
$$z_n \longrightarrow -z_n,$$

and then adding an overall (-) in Eqs. (5.22), (5.23) and (5.24). It is straightforward to see that these equations are invariant under these changes. We explicitly checked this by making these alteration to the codes in Maple required to plot Eqs. (5.22), (5.23) and (5.24). This worked successfully.

Changing $A_1 \longrightarrow -A_1$ and $B_1 \longrightarrow -B_1$ in Eq. (5.22) are necessary as they contain $z_n$ in their definitions. $1/b$ also needs to change sign since it has been factorized from $z_1$, $z_2$ in Eqs. (5.23) and (5.24).

[31] provides a deeper analytical discussion on Eqs. (5.20), (5.21) and (5.18). Our plots of Eqs. (5.22), (5.23) and (5.24) obtained with Maple are shown in Fig. (5.3). [31] and [32] clearly explains and discusses the analytical

behavior of Eqs. (5.22), (5.23) and (5.24) such that they obey the following relations when $Q^2 \longrightarrow \Lambda^2$.

$$
\begin{aligned}
D_{PT}^{(L)}(Q^2 = \Lambda^2) &= \sum_{n=1}^{\infty} z_n [A_0(n) - B_0(n)] - \sum_{n=1}^{\infty} z_n^2 [A_1(n) - B_1(n)] \ln(n) \\
&\approx \frac{0.679938}{b}
\end{aligned}
$$

(5.30)

$$
K_{PT}^{(L)}(Q^2 = \Lambda^2) \approx -\frac{8}{9b} \ln 2 \tag{5.31}
$$

$$
U_{PT}^{(L)}(Q^2 = \Lambda^2) \approx -\frac{8}{3b} \ln 2 \tag{5.32}
$$

These leading-$b$ results change sign in the vicinity of $Q^2 = \Lambda^2$, where they remain finite , and as $Q^2 \to 0$ they approach the freezing limit of 0. The $Q$-dependence is only piecewise analytic, with only the first three derivatives $\frac{d}{d\ln Q}$ for $D^{(L)}(Q^2)$ being finite, and only the first derivative for the sum rules. The full result including non-perturbative effects must be an analytic function of $Q^2$. This will be further discussed in Chapter 7.

## 5.8   SKELETON EXPANSION AND BOREL REPRESENTATIONS FOR THE ADLER FUNCTION

We begin by re-writing the leading Adler D function expressed in leading term of the skeleton expansion which arises from the integral corresponding to a chain of bubbles

$$
D_{PT}^{(L)} = \int_0^{\infty} dt \omega(t) a(e^C t Q^2). \tag{5.33}
$$

Here $t = k^2/Q^2$. $\omega(t)$ is the characteristic function and $C$ is the standard $\overline{MS}$ subtraction scheme constant $= -5/3$. In this thesis, we will set $C = 0$. This corresponds to the V-scheme with the renormalization scale

$$
\mu^2 = e^{-5/3} Q^2. \tag{5.34}
$$

The characteristic function $\omega(t)$ is normalised such that

$$
\int_0^{\infty} dt \omega(t) = 1. \tag{5.35}
$$
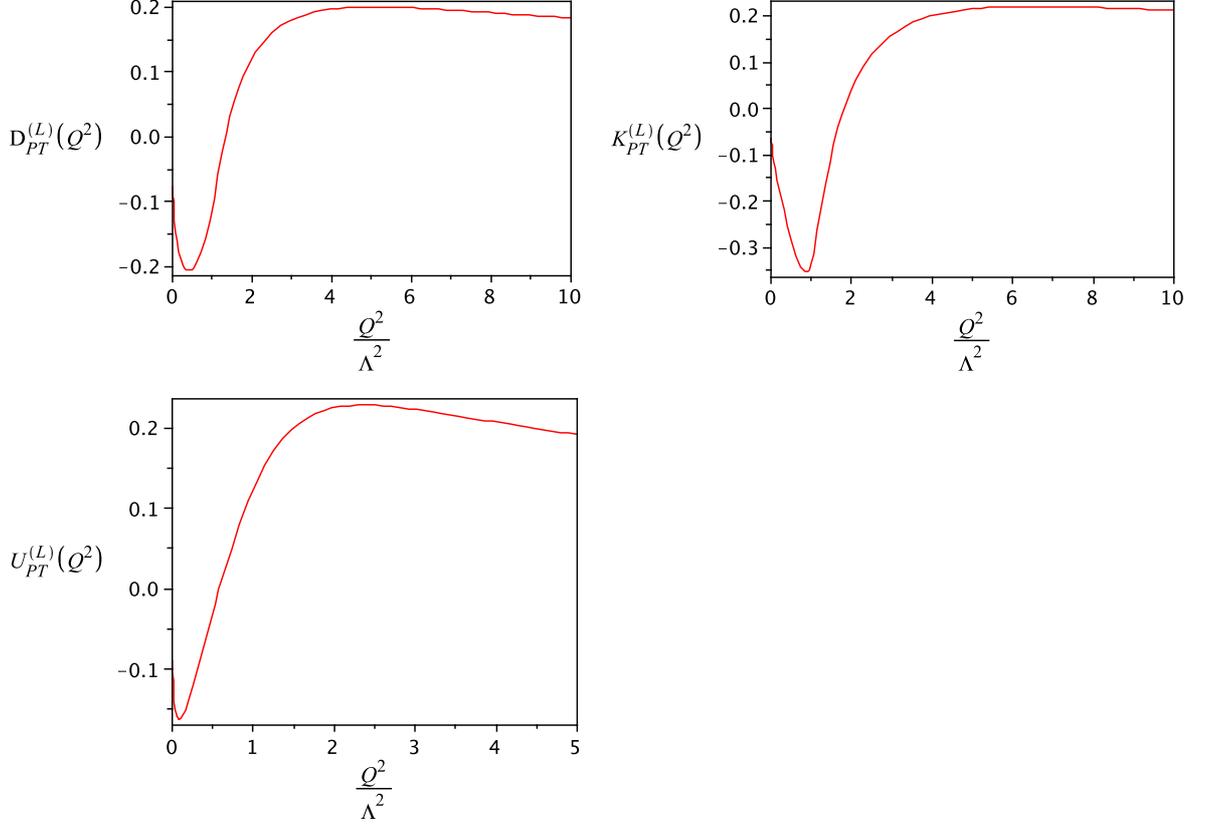
Figure 5.3: $Q^2$-*dependence of the perturbative corrections to the observables in Eqs. (5.22), (5.23)and (5.24), resummed to all orders in the leading-b approximation. All plots by Maple 11*

We will now demonstrate how to convert the skeleton expansion into a Borel representation by introducing the vacuum polarization function $\Pi(Q^2)$ of Eq. (5.11) being re-defined as,

$$\Pi(Q^2) = \int_0^\infty dt\,\omega_\Pi(t)a(tQ^2). \tag{5.36}$$

where the characteristic function $\omega_\Pi(t)$ in the $t \leq 1 \longleftrightarrow IR$ region is given by

$$\omega_\Pi(t) = -t\frac{4}{3}t\Xi(t), \tag{5.37}$$

and for the $t \geq 1 \longleftrightarrow UV$ region

$$\omega_\Pi(t) = -\frac{1}{t}\frac{4}{3}t\Xi(\frac{1}{t}). \tag{5.38}$$

Nevertheless, these 2 regions are related by the conformal symmetry $t \longrightarrow 1/t$.

Classic QED work in [36] shows that Eq. (5.36) can be obtained simply by adding appropriate color factors. This is related to the Bethe-Salpeter kernel for the scattering light-by-light. It is also the first term in a well-defined QED skeleton expansion. Fig. (5.4) is the diagram of the relevant kernel
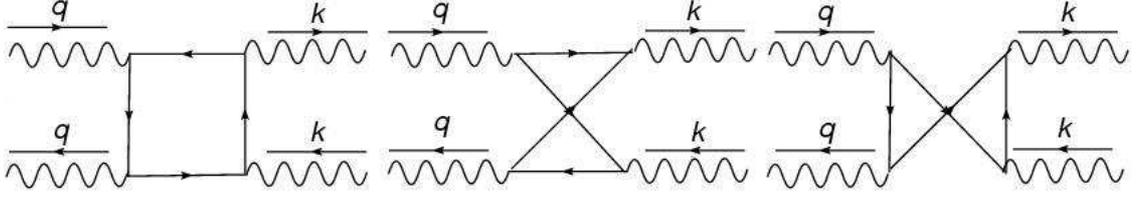


Figure 5.4: *Light-by-light scattering diagrams for* $\omega_\Pi(t)$ *calculation*

The diagrams in Fig. (5.4) can reproduce the topology of Fig. (5.1). The QCD skeleton expansion is problematic and we will avoid its detailed discussion completely. Let us define $\Xi(t)$

$$\Xi(t) = \frac{4}{3t}[1 - \ln(t) + (\frac{5}{2} - \frac{3}{2}\ln(t))t + \frac{(1+t)^2}{t}[L_2(-t) + \ln(t)\ln(1+t)]], \quad (5.39)$$

with $L_2(x)$ as the dilogarithmic function given by

$$L_2(x) = -\int_0^x dy \frac{\ln(1-y)}{y}. \quad (5.40)$$

The relation between the Adler D function and the vacuum polarization function $\Pi(Q^2)$ given by Eq. (5.5) will have a one-chain skeleton expansion term associated with $\omega_D(t^2)$ where

$$D_{PT}^{(L)}(Q^2) = \int_0^\infty dt\omega_D(t)a(tQ^2). \quad (5.41)$$

$\omega_D(t)$ is obtained by applying Eq. (5.5) on $\omega_\Pi(t)$

$$
\begin{aligned}
D_{PT}^{(L)}(Q^2) &= -\frac{3}{4}Q^2\frac{d}{dQ^2}\int_0^\infty dt\omega_\Pi(t)t\left(\frac{a(tQ^2)}{t}\right), \\
&= +\frac{3}{2b}Q^2\frac{d}{dQ^2}\int_0^\infty dt\frac{d}{dt}[\omega_\Pi(t)t]\ln[a(tQ^2)],
\end{aligned}
$$

$$(5.42)$$

and then integrating by parts

$$= -\frac{3}{4} \int_0^\infty dt [\omega_\Pi(t) + t\frac{d}{dt}\omega_\Pi(t)] a(tQ^2).$$

This induces a transformation in $\omega_\Pi(t)$ such that

$$\Pi(Q^2) \longrightarrow Q^2 \frac{d}{dQ^2}\Pi(Q^2) = -\frac{4}{3}D(Q^2) \Rightarrow \omega_\Pi(t)$$

$$\longrightarrow \omega_\Pi(t) + t\frac{d}{dt}\omega_\Pi(t) = -\frac{4}{3}\omega_D(t), \tag{5.43}$$

spoiling the conformal symmetry present in $\omega_\Pi(t)$. $\omega_D(t)$ are more complicated in the UV and IR regions

$$\omega_D^{IR}(t) = \frac{8}{3}[(\frac{7}{4} - \ln(t))t + (1+t)[L_2(-t) + \ln(t)\ln(1+t)]], \tag{5.44}$$

$$\omega_D^{UV}(t) = \frac{8}{3}[1 + \ln(t) + (\frac{3}{4} - \frac{1}{2}\ln(t))\frac{1}{t} + (1+t)[L_2(-t^{-1}) - \ln(t)\ln(1+t^{-1})]]. \tag{5.45}$$

We will now expand $\omega_\Pi(t)$ in powers of $t$. The expressions in both the IR and UV regions consists of expansion in $t$ and an expansion multiplied by a logarithm which is

$$\omega_\Pi^{IR}(t) = -\frac{4}{3}(\sum_{n=1}^\infty \xi_n t^n + \ln(t)\sum_{n=2}^\infty \hat{\xi}_n t^n). \tag{5.46}$$

By the conformal symmetry expressed in Eq. (5.37) and Eq. (5.38) implies that the UV part can be written in terms of $\xi_n$ and $\hat{\xi}_n$

$$\omega_\Pi^{UV}(t) = -\frac{4}{3}(\sum_{n=1}^\infty \xi_n t^{-n} - \ln(t)\sum_{n=2}^\infty \hat{\xi}_n t^{-n}). \tag{5.47}$$

This steps are necessary to ensure us to write the Borel representations of

$$D_{PT}^{(L)}(Q^2) = \int_0^\infty dz e^{-z/a(Q^2)} B[D_{PT}^{(L)}](z), \tag{5.48}$$

in the region $Q^2 > \Lambda^2$ and

$$D_{PT}^{(L)}(Q^2) = -\int_0^\infty dz e^{-z/|a(Q^2)|} B[D_{PT}^{(L)}](-z), \tag{5.49}$$

in the region $Q^2 < \Lambda^2$, converted from skeleton expansion. This is done by making a change of variables.

$\xi_n$ and $\hat{\xi}_n$ are extracted by comparing Eq. (5.39) to Eq. (5.47) and Eq. (5.48) and are found to be

$$
\begin{aligned}
\xi_{n>1} &= \frac{4}{3} \frac{(2 - 6n^2)(-1)^n}{(n-1)^2 n^2 (n+1)^2}, \\
\hat{\xi}_{n>1} &= \frac{4}{3} \frac{2(-1)^n}{(n-1)n(n+1)}, \\
\xi_1 &= 1, \\
\hat{\xi}_1 &= 0.
\end{aligned}
\tag{5.50}
$$

As we have discussed previously an induced transformation through Eq. (5.44) is necessary, this permits us to express $\omega_D(t)$ in a similar expansion

$$
\omega_D^{IR}(t) = \sum_{n=1}^{\infty} [\xi_n(1+n) + \hat{\xi}_n] t^n + \ln(t) \sum_{n=2}^{\infty} \hat{\xi}_n (n+1) t^n,
\tag{5.51}
$$

$$
\omega_D^{UV}(t) = \sum_{n=1}^{\infty} [\xi_n(1-n) - \hat{\xi}_n] t^{-n} + \ln(t) \sum_{n=2}^{\infty} \hat{\xi}_n (n-1) t^{-n}.
\tag{5.52}
$$

With the above expansions, we can now represent $D_{PT}^{(L)}(Q^2)$ in terms of a Borel integral. Expressing $D_{PT}^{(L)}(Q^2)$ in terms of $\omega_D(t)$ which is then split into the IR and UV regions

$$
\begin{aligned}
D_{PT}^{(L)}(Q^2) &= \int_0^{\infty} dt \omega_D(t) a(tQ^2) \\
&= \sum_{k=0}^{\infty} a(Q^2) \int_0^1 dt \omega_D^{IR}(t) (-\frac{ba(Q^2)}{2} \ln(t))^k \\
&+ \sum_{k=0}^{\infty} a(Q^2) \int_1^{\infty} dt \omega_D^{UV}(t) (-\frac{ba(Q^2)}{2} \ln(t))^k \\
&= a(Q^2) \sum_{k=0}^{\infty} (-\frac{ba(Q^2)}{2})^k [\int_0^1 dt (\sum_{n=1}^{\infty} [\xi_n(1+n) + \hat{\xi}_n] t^n \\
&+ \ln(t) \sum_{n=2}^{\infty} \hat{\xi}_n (n+1)) \ln(t)^k + \int_1^{\infty} dt (\sum_{n=1}^{\infty} [\xi_n(1-n) - \hat{\xi}_n](t)^{-n} \\
&+ \ln(t) \sum_{n=2}^{\infty} \hat{\xi}_n (n-1) t^{-n}) (\ln(t))^k].
\end{aligned}
\tag{5.53}
$$

We have used the mathematical relation below in deriving the above expression

$$a(xy) = a(y) \sum_{k=0}^{\infty} (-\frac{ba(y)}{2} \ln(x))^k. \tag{5.54}$$

Using the fact that at $n = 1$

$$[\xi_n(1 - n) - \hat{\xi}_n] = 0,$$

this allows us to omit the term from the $D_{PT}^{(L)}(Q^2)$.

$D_{PT}^{(L)}(Q^2)$ can be transformed into a Borel integral of the form Eq. (5.49) with a changes of variables

$$
\begin{aligned}
z &= -a(Q^2) \times (n+1) \ln(t) &&\longrightarrow IR, \\
z &= a(Q^2)(n-1) \ln(t), &&\longrightarrow UV,
\end{aligned}
$$

in their respective regions. Using integration by parts, we manage to remove the extra $\ln(t)$ term in the integral. The standard Borel representation should be of the form

$$
\begin{aligned}
D_{PT}^{(L)}(Q^2) &= \int_0^{\infty} dz e^{-z/a(Q^2)} [\sum_{n=1}^{\infty} \frac{[\xi_n(1+n) + \hat{\xi}_n]}{n+1} \frac{1}{1 - \frac{bz}{2(n+1)}} \\
&\quad - \sum_{n=2}^{\infty} \frac{\hat{\xi}_n(n+1)}{(n+1)^2} \frac{1}{(1 - \frac{bz}{2(n+1)})^2}] \\
&\quad + \int_0^{\infty} dz e^{-z/a(Q^2)} [\sum_{n=2}^{\infty} \frac{[\xi_n(1-n) - \hat{\xi}_n]}{n-1} \frac{1}{1 + \frac{bz}{2(n-1)}} \\
&\quad + \sum_{n=2}^{\infty} \frac{\hat{\xi}_n(n-1)}{(n-1)^2} \frac{1}{(1 + \frac{bz}{2(n-1)})^2}], \tag{5.55}
\end{aligned}
$$

for $Q^2 > \Lambda^2$, $a(Q^2) > 0$ of Eq. (5.49), and for $Q^2 < \Lambda^2$, $a(Q^2) < 0$, we will have the modified Borel representation of Eq. (5.50) with its upper limit at $-\infty$. Making contact with Eq. (5.18), the following relations can be identified

$$\frac{\xi_n(1+n) + \hat{\xi}_n}{n+1} = -B_1(n+1)z_{n+1}, \tag{5.56}$$

for $n \geq 1$

$$\frac{\xi_n(1-n) - \hat{\xi}_n}{n-1} = A_1(n-1)z_{n-1}, \tag{5.57}$$

for $n \geq 2$, for the single pole residues and

$$-\frac{\xi_n(1+n)}{(n+1)^2} = B_0(n+1) + B_1(n+1)z_{n+1}, \tag{5.58}$$

for $n \geq 2$

$$\frac{\xi_n(1-n)}{(n-1)^2} = A_0(n-1) - A_1(n-1)z_{n-1}, \tag{5.59}$$

for $n \geq 2$, for the double pole residues. The equations above are verified by substituting $\xi_n$ and $\hat{\xi}_n$ given by Eq. (5.19) into Eq. (5.51).

Note that explicit derivation of all relations have been performed with pencil and paper as well as solved in Maple for exercise.

For further details, please refer to [31] whose calculational steps we have largely followed.

## 5.9 SUMMARY

We begin with a brief introduction on deep inelastic scattering, structure functions, sum rules and then discussing the significance of fixed-order Perturbation Theory in QCD which has been very successful in making accurate approximations to physical observables at large energies, $Q^2$. Nevertheless, such a fixed-order perturbative approach breaks down below the Landau pole. Non-perturbative information is essential to make perturbation theory sensible as higher perturbative coefficients exhibit factorial growth making the series not convergent. Resummed perturbation series can be represented by a Borel integral which is ambiguous due to singularities on the positive real axis (also known as Infrared Renormalons) of the Borel plane.

We then moved on to introduce the Polarized Bjorken Sum Rule $K_{pBJ}$ and the Unpolarized Bjorken Sum Rule $U_{uBJ}$, relating them to the Parton model and their corresponding perturbative corrections.

The Adler D function is first introduced as a logarithmic derivative of the QCD vacuum polarization function with respect to the energy. The function itself is calculated from a set of diagrams in Fig. (5.1). It is then fairly straightforward that from the parton model result, the QCD corrections can be split into perturbative PT and non perturbative NP parts. Let us just focus on the PT part for now whilst discussion of the physical interpretation of the NP part will be made in Chapter 7. Fig. (5.2) shows the leading $N_f$

contributions for the $K_{pBJ}$, $U_{uBJ}$ and $G_{GLS}$ sum rules at leading order. A very brief introduction on leading-b approximation is then made which is essential because all these large $N_f$ results will be used to compute leading-b all orders resummations of the perturbative corrections discussed. We then write the Borel transform of $B[D_{PT}^{(L)}](z)$, $B[K_{PT}^{(L)}](z)$ and $B[U_{PT}^{(L)}](z)$ where the structure for the last two are simpler with a finite number of poles in contrast to $B[D_{PT}^{(L)}](z)$ which has an infinite number. The reason that they are much simpler comes from the fact that one is inserting a chain of $n$-bubbles into a tree level diagram shown in Fig. (5.2) which is much simpler than insertion into a quark loop. A brief analysis of its mathematical behavior makes a completion to the section. Fig(5.3) shows the leading-b approximations for $D_{PT}^{(L)}$, and the $K_{PT}^{(L)}$ and $U_{PT}^{(L)}$ Sum Rules.

The rigorous mathematical derivation of the Borel transform for $D_{PT}^{(L)}$ was performed by using a one-chain skeleton expansion. We begin this task by re-writing the leading Adler D function expressed in leading term of the skeleton expansion which arises from the integral corresponding to the chain of bubbles. The computation has been carried out in the V-scheme where $C = 0$ which we were using throughout this thesis. The characteristic function is then introduced for IR and UV regions which they also fulfill the renormalization condition setting them equal to 1 when integrated from 0 to $\infty$. The vacuum polarization function is dependent on the characteristic function and upon completing certain equations, direct comparisons could be made to verify the Borel transform of the Adler D function discussed in the previous section. We finally show the existence of single and double pole behavior in its corresponding Borel transform.

The Borel transform of the Adler D function is the main ingredient of this thesis for our $N^3LO$ Renormalon resummations and our derivation for fully analytic perturbative QCD.

# Chapter 6

# NUMERICAL CALCULATION OF $R(s)$ AND $R_\tau$

## 6.1 $R_{e^+e^-}$ IN 4 SCHEMES

We begin with the definition of the dimensionless observable the $R_{e^+e^-}$ ratio for some value of the center of mass energy $\sqrt{s}$

$$R_{e^+e^-}(s) = \frac{\sigma_{TOT}(e^+e^- \longrightarrow hadrons)}{\sigma(e^+e^- \longrightarrow \mu + \mu -)} = 3 \sum_f Q_f^2 [1+R(s)] + \left( \sum_f Q_f \right)^2 \mathcal{R}(s),$$
(6.1)

where $Q_f$ is the electric charge of each quark flavour and the sum is over the different flavours. $R(s)$ denotes the QCD perturbative corrections to the parton model result and can be expressed as

$$R(s) = a + \sum_{n>0} r_n a^{n+1},$$
(6.2)

where quarks produced in electromagnetic interactions become part of the final-state hadrons. $a = \alpha_s(\mu^2)/\pi$ is the renormalized coupling. The coefficients $r_1$, $r_2$ and $r_3$ are computed in the $(\overline{MS})$ scheme using the renormalization scale $\mu^2 = s$. Full expressions of the coefficients will be provided in the next section. $\mathcal{R}(s)$ comes from the "light-by-light" part in the figure below, and has a $(\sum Q_f)^2$ dependence.
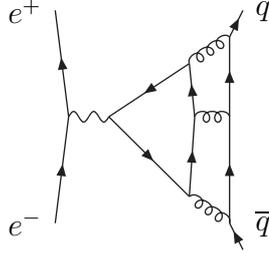
Figure 6.1 :  *Light-by-light corrections diagram*

The ratio $R_{e^+e^-}$ is related directly to the transverse part of the correlator of two vector currents in the Euclidean region with the condition that $s = -q^2 > 0$. In order to avoid an unspecified constant, the logarithmic derivative with respect to $s$ was considered and the Adler D function was defined and given by Eq. (5.12). We now can replace the perturbative correction $R(s)$ with $D(s)$ written as a perturbative series

$$D(s) = a + \sum_{n>0} d_n a^{n+1}. \tag{6.3}$$

By analytical continuation from Euclidean to Minkowskian, one may notice that the Minkowskian observable $R(s)$ can be related to $D(-s)$ by the dispersion relation,

$$R(s) = \frac{1}{2\pi i} \int_{s-i\epsilon}^{s+i\epsilon} dt \frac{D(-t)}{t}. \tag{6.4}$$

It is very clear from the expression above that the 'landau pole' in the coupling $a(s)$ laying along the positive real $s$-axis can now be well-defined. Thus $R(s)$ will be defined for all $s$. The dispersion relation can now be explicitly expressed as

$$R(s) = \frac{1}{2\pi} \int_{-\pi}^{\pi} d\theta D(se^{i\theta}), \tag{6.5}$$

where we perform an integration around a circular contour in the complex energy-squared $s$-plane. It is worth noting that the dispersion relation of Eq. (6.5) is valid for values of $s > \Lambda^2$ above the 'Landau pole'. The idea which leads to the 'contour-improved' perturbation series comes from the expansion of $D(se^{i\theta})$ as a power series in $\overline{a} \equiv a(se^{i\theta})$, and performing the integration of $\theta$ term-by-term, where at each order, an infinite subset of analytical continuation terms present in Eq. (6.2) are resummed. This complete analytical continuation, as we shall see, serves to freeze $R(s)$ with an infrared limit as $s \to 0$ of $R(0) = 2/b$.

As an example, we begin by considering the 'contour-improved' series for a one loop coupling. The one loop coupling which we have introduced in the

$\beta$ function section is given by

$$a(s) = \frac{2}{b \ln(s/\Lambda_{\overline{MS}}^2)}. \tag{6.6}$$

Now, we will consider the "contour-improved" perturbation series for $R(s)$ by rewriting

$$R(s) = A_1(s) + \sum_{n=1}^{\infty} d_n A_{n+1}(s), \tag{6.7}$$

where the function $A_n(s)$

$$A_n(s) = \frac{1}{2\pi} \int_{-\pi}^{\pi} d\theta \overline{a}^n = \frac{1}{2\pi} \int_{-\pi}^{\pi} d\theta \frac{a^n(s)}{[1 + ib\theta a(s)/2]^n}, \tag{6.8}$$

are obtained by applying the contour integration on the coupling. Such integral are evaluated in closed-form as

$$\begin{aligned} A_1(s) &= \frac{2}{\pi b} arctan(\frac{\pi b a(s)}{2}), \\ A_n(s) &= \frac{2 a^{n-1}(s)}{\pi b (1-n)} Im[(1 + \frac{ib\pi a(s)}{2})^{1-n}]. \end{aligned} \tag{6.9}$$

We can then obtain the one loop "contour improved" series for R(s),

$$R(s) = \frac{2}{\pi b} arctan(\frac{\pi b a(s)}{2}) + d_1 [\frac{a^2(s)}{(1 + b^2 \pi^2 a^2(s)/4)^2}] + d_2 [\frac{a^3(s)}{(1 + b^2 \pi^2 a^2(s)/4)^2}] + ... \tag{6.10}$$

As $s \to 0$ one has $A_1(0) = 2/b$ as the freezing limit, whereas $A_i(0) = 0$ for the higher $i > 1$ functions. We see that this procedure resum in each order an infinite set of terms involving powers of $\pi^2 b^2$, which arise from the analytical continuation. Since these terms are large they should be resummed to all-orders to achieve accurate approximations, and this is precisely what the Contour Improved (CIPT) approach achieves.

We will move now to a consideration of the two loop "contour improved" perturbation series to calculate results in the $\overline{MS}$, CIPT, CORGI and CIPT + CORGI scheme. Further discussions on the physical behavior of the one loop "contour improved" perturbation series are presented in Ref. [37, 38].

Beyond the simple one loop approximation, the freezing could be analyzed by selecting a renormalization scheme with the beta function equation written in its two loop form

$$\frac{\partial a(\mu^2)}{\partial \ln \mu^2} = -\frac{b}{2} a^2(\mu^2)(1 + ca(\mu^2)). \tag{6.11}$$

This is the 't Hooft scheme in which we set all the non-universal beta-function coefficients to zero. Here $c = (153 - 19N_f)/12b$ is the second universal beta function coefficient. In these schemes, the coupling can be expressed analytically in closed form in terms of the Lambert W function where $W(z)exp(W(z)) = z$ [13]. Note that $\ln(z)$, as all logarithms has different branches, thus the branches can be selected so that $Re(W)$ has the interval $[-\infty, \infty]$ and $Im(W)$ with the interval $[-i\pi, i\pi]$. The other branches has the same interval for $Re(W)$ with the imaginary part taking a set of intervals $[i\pi, 3i\pi]$, $[-i\pi, -3i\pi]$ and etc. These corresponds to the branches having a branch cut along the negative real axis in the $z$-plane. The Lambert-W function has a similar structure assuming the function is large and real. For the limit $Re(W) \longrightarrow \infty$ and $Im(W)$ with the interval $[-i\pi, i\pi]$ corresponds to the principal branch denoted by $W_0$. In the similar limit $Re(W) \longrightarrow \infty$, $W_{\pm 1}$ have the interval $[\pm i\pi, \pm 3i\pi]$. Analogously, $W_{\pm n}$ have the interval $[\pm ni\pi, \pm(n + 2)i\pi]$ where $n$ is a positive integer for $Re(W) \longrightarrow \infty$. Nevertheless, for the limit $Re(W) \longrightarrow -\infty$, $W_{\pm 1}$ have another imaginary intervals running from $[0, \pm 2i\pi]$ with $[\pm 2i\pi, \pm 4i\pi]$ for $W_{\pm 2}$ and so on. The principal branch $W_0$ closes up at the point on the real axis where $Re(W) = -1$ and is the only branch with a branch cut along the negative real axis starting at $z = -\frac{1}{e}$ while the other branches have their branch cuts along the negative real $z$ axis in the $z$ plane. One of the important characteristic is $W_n(z) = W_{-n}^*(z^*)$. Other important properties essential to the algebraic manipulation will be pointed out as the thesis proceeds.

Solving, the two loop beta function, one will then have

$$a(\mu^2) = -\frac{1}{c[1 + W_{-1}(z(\mu))]}, \qquad (6.12)$$

$$z(\mu) = -\frac{1}{e}(\frac{\mu}{\widetilde{\Lambda}_{\overline{MS}}})^{(-b/c)}, \qquad (6.13)$$

by solving the beta function. $\widetilde{\Lambda}_{\overline{MS}}$ is defined conventionally in Ref. [39] and is related to the standard definition

$$\widetilde{\Lambda}_{\overline{MS}} = (2c/b)^{-c/b}\Lambda_{\overline{MS}}, \qquad (6.14)$$

provided in [12]. The "-1" subscript corresponds to the branch cut of the Lambert W function and is the branch cut which will preserve asymptotic freedom. Intuitively, the selection was made based on the necessity to have a real coupling with large $\mu$. The only 3 branches of the Lambert-W function which can take real values are $W_0$ and $W_{\pm 1}$. $W_0$ will not provide asymptotic freedom as $\longrightarrow 0$, $\mu \longrightarrow 0$ giving a non-zero coupling. $W_{-1}$ is chosen as we

demand $W(z(\mu))$ to be continuous against $\mu$ in the complex plane. The $W_1$ branch will return non-zero imaginary part for $\mu = |\mu|$ when expecting a real coupling. For a detail technical discussion on the selection of the branches, we advise reader to refer [14]. Reader can also convince themselves by making a plot of Eq. (6.12) with real positive coupling in different branches to understand the selection of the branches better.

We select the renormalization scale $\mu^2 = xs$, where $x$ is an arbitrary dimensionless constant, for the perturbation series of $D(s)$ in Eq. (6.2). Expanding the integrand in Eq. (6.4) for $R(s)$ in powers of $\overline{a} \equiv a(xse^{1\theta})$ expressed in terms of Lambert W function using Eq. (6.12), we will obtain

$$\overline{a} = \frac{-1}{c[1 + W(A(s)e^{iK\theta})]}, \tag{6.15}$$

where

$$A(s) = -\frac{1}{e}\left(\frac{\sqrt{xs}}{\widetilde{\Lambda_{\overline{MS}}}}\right)^{-b/c}, K = \frac{-b}{2c}. \tag{6.16}$$

Using Eqs. (6.12), (6.13) and (6.15), the function $A_n(s)$ in the "contour improved" series are computed

$$\begin{aligned}
A_n(s) &= \frac{1}{2\pi}\int_\pi^\pi d\theta \overline{a}^n = \frac{1}{2\pi}\int_{-\pi}^0 d\theta \frac{(-1)^n}{c^n}[1 + W_1(A(s)e^{iK\theta})]^{-n} \\
&+ \frac{1}{2\pi}\int_0^\pi d\theta \frac{(-1)^n}{c^n}[1 + W_{-1}(A(s)e^{iK\theta})]^{-n}.
\end{aligned} \tag{6.17}$$

It is necessary to apply the appropriate branches of the Lambert-W function in the two different regions of integration and by making a change of variable $w = W(A(s)e^{iK\theta})$, one will obtain

$$A_n(s) = \frac{(-1)^n}{2iKc^n\pi}\int_{W_1(A(s)e^{iK\pi})}^{W_{-1}(A(s)e^{iK\pi})} \frac{dw}{w(1+w)^{n-1}}. \tag{6.18}$$

Noting the relationship between the +1 and the -1 branch cuts in the Lambert-W function $W_1(A(s)e^{-iK\theta}) = [W_{-1}(A(s)e^{iK\theta})]^*$, we can then evaluate the elementary integral

$$A_1(s) = \frac{2}{b} - \frac{1}{\pi Kc}Im[\ln(W_{-1}(A(s)e^{iK\pi}))], \tag{6.19}$$

for $n = 1$, where $2/b$ is the residue of the pole at $w = 0$. For $n > 1$, we have

$$A_n(s) = \frac{(-1)^n}{c^n K\pi}Im[\ln(\frac{W_{-1}(A(s)e^{iK\pi})}{1 + W_{-1}(A(s)e^{iK\pi})}) + \sum_{k=1}^{n-2}\frac{1}{k(1 + W_{-1}(A(s)e^{iK\pi}))^k}], \tag{6.20}$$

where the first four functions $A_1(s)$, $A_2(s)$, $A_3(s)$ and $A_4(s)$ are plotted versus $sx/\widetilde{\Lambda}^2_{\overline{MS}}$ in Fig. (6.2) with $N_f = 5$ flavours of quark. Note that the figures show that the $A_i(Q)$ all show the behavior of asymptotic freedom, approaching zero as $Q \to \infty$. $A_1(0) = 2/b$, whereas for $i > 1$ one has $A_i(0) = 0$.

Note that we only compute $A_n(s)$ in the 't Hooft scheme where we only consider a two loop beta function. To avoid confusions with $n > 2$ loops, we set the two loop $A_n(s)$ function as

$$A_{(0)1}(s) = A_1(s), \tag{6.21}$$
$$A_{(0)n}(s) = A_n(s). \tag{6.22}$$

For higher loops beta function, our current interest is the 4 loop beta function to match the latest calculation for $d_3$ given in Ref. [40], we have

$$\frac{\partial a(\mu^2)}{\partial \ln \mu^2} = -\frac{b}{2}a^2(\mu^2)(1 + ca(\mu^2) + c_2 a^2(\mu^2) + c_3 a^3(\mu^2)). \tag{6.23}$$

Theoretically, the solution for $a(\mu^2)$ in a 4 loop beta function can be solved by considering $a(\mu^2)$ as a perturbative series of $a(\mu^2) = -1/c[1 + W_{-1}(z(\mu))]$ (the solution for $a(\mu^2)$ in a 2 loop beta function) which for convenience and to avoid confusion is set such that $a(\mu^2) = -1/c[1 + W_{-1}(z(\mu))] = a_0$. Thus $a_4(\mu^2)$ (the solution of a in 4 loop beta function) is

$$a_4(\mu^2) = a_0(\mu^2) + k_1 a_0^2(\mu^2) + k_2 a_0^3(\mu^2) + k_3 a_0^4(\mu^2) + k_4 a_0^5(\mu^2). \tag{6.24}$$

By equating the coefficients of the beta function on both sides of this expression we can fix the $k_i$ as

$$
\begin{aligned}
k_1 &= 0, \\
k_2 &= c_2, \\
k_3 &= \frac{1}{2}c_3, \\
k_4 &= \frac{1}{3}c_2^2 + \frac{1}{2}c_3 + \frac{4}{3}cc_2 - \frac{2}{3}cc_3.
\end{aligned}
\tag{6.25}
$$

Expressions for $c_2$, $c_3$ and all the corresponding variables required to fit for $\alpha_s$ using the $\overline{MS}$, CIPT, CORGI and the CIPT + CORGI versions of PT will be given in the next section. Since we can expand $a_4(\mu^2) = a_0(\mu^2) + k_1 a_0^2(\mu^2) + k_2 a_0^3(\mu^2) + k_3 a_0^4(\mu^2) + k_4 a_0^5(\mu^2)$, we can write our 4-loop coupling as a sum of $a_0$ terms. Since $a_0$ is known analytically in terms of the Lambert-$W$ function we avoid having to solve the transcendental 4-loop beta-function

equation, which makes calculations more straightforward. Similarly a 4-loop $A_{(4)n}(s)$ function can be expanded perturbatively with a two loop $A_{(0)n}(s)$ function such that

$$A_{(4)1}(s) = A_{(0)1}(s) + k_2 A_{(0)1}^3(s) + k_3 A_{(0)1}^4(s) + k_4 A_{(0)1}^5(s), \quad (6.26)$$

$$A_{(4)n}(s) = A_{(0)n}(s) + k_2 A_{(0)n}^3(s) + k_3 A_{(0)n}^4(s) + k_4 A_{(0)n}^5(s). \quad (6.27)$$

Note that Eqs. (6.21) and (6.22) are essential for the calculation in the CORGI and CIPT + CORGI version while Eqs. (6.26) and (6.27) are needed for the CIPT version. Thus, the correction $R(s)$ to the 4-loop $R_{e^+e^-}$ in the $\overline{MS}$ (version 2) and CIPT (version 3) are

$$R(s)_{\overline{MS}} = a_4(\mu^2) + r_1 a_4^2(\mu^2) + r_2 a_4^3(\mu^2) + r_3 a_4^4(\mu^2) \quad (6.28)$$

$$R(s)_{CIPT} = A_{(4)1}(s) + d_1 A_{(4)2}(s) + d_2 A_{(4)3}(s) + d_3 A_{(4)3}(s) \quad (6.29)$$

while the correction $R(s)$ to the 4-loop $R_{e^+e^-}$ in the CORGI(version 1) derived with great detail in Chapter 3 and CIPT + CORGI (version 4) is given by

$$R(s)_{CORGI} = a(\mu^2) + X_{2R} a(\mu^2)^3 + X_{3R} a(\mu^2)^4 \quad (6.30)$$

$$R(s)_{CIPT+CORGI} = A_{(0)1}(s) + X_{2D} A_{(0)3}(s) + X_{3D} A_{(0)4}(s) \quad (6.31)$$

The last equation is the application of the "contour improved technique" in the CORGI scheme (version 1).
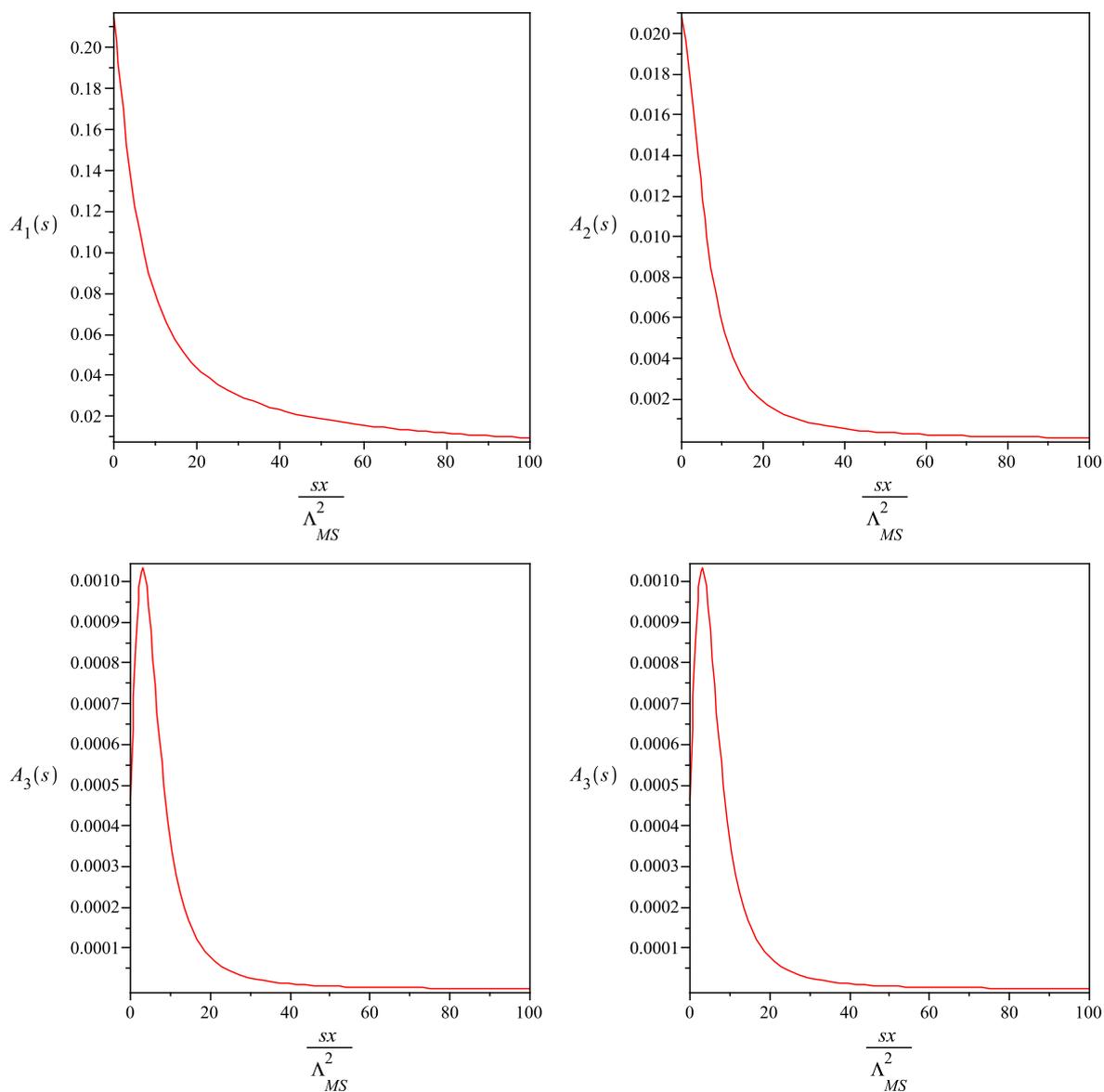
Figure 6.2 :   The function $A_1(s)$, $A_2(s)$, $A_3(s)$ and $A_4(s)$ against $sx/\widetilde{\Lambda}_{\overline{MS}}$ - showing asymptotic freedom behaviour. All plots by Maple 11

## 6.2 ANALYTICAL PREDICTIONS OF $\tau$ IN 4 VERSIONS

It is useful to fit data for $R(s)$ to the parameter $\tau_s \equiv b\ln(\sqrt{s}/\tilde{\Lambda}_{\overline{MS}})$. This is a convenient choice which can easily be converted into $\alpha_s(M_Z)$ or $\tilde{\Lambda}_{\overline{MS}}$ as required. As discussed, we shall consider four versions of perturbation theory for $R(s)$, and make fits for the corresponding values of $\tau$ which we denote $\tau_{\overline{MS}}$, $\tau_{CIPT}$, $\tau_{CORGI}$ and $\tau_{CIPT+CORGI}$ which can be extracted from Eqs. (6.28), (6.29), (6.30) and (6.31). Regrouping all the essential equations

$$
\begin{aligned}
R(s)_{\overline{MS}} &= a_4(\mu^2) + r_1 a_4^2(\mu^2) + r_2 a_4^3(\mu^2) + r3 a_4^4(\mu^2) \\
R(s)_{CIPT} &= A_{(4)1}(s) + d_1 A_{(4)2}(s) + d_2 A_{(4)3}(s) + d_3 A_{(4)3}(s) \\
R(s)_{CORGI} &= a(\mu^2) + X_{2R} a(\mu^2)^3 + X_{3R} a(\mu^2)^4 \\
R(s)_{CIPT+CORGI} &= A_{(0)1}(s) + X_{2D} A_{(0)3}(s) + X_{3D} A_{(0)4}(s)
\end{aligned}
$$

$R(s = M_Z^2)$=0.03904±0.00087 is the value considered by Baikov and collaborators [40] using the value of $\alpha_s(M_Z^2)^{NNLO}$ extracted from the working group of [41] including terms up to $O(\alpha_s^3)$. The main reason we are considering to use this value is to ensure the consistency with the latest $d_3$ calculation as well as to check in the later Section 6.5 if the value of $\alpha_s(M_Z^2)$ we obtained will be agreeable with value obtained by Baikov and collaborators by performing a shift of $\delta\alpha_s(M_Z^2) = 0.0005$ implying $\alpha_s(M_Z^2)_{Baikov}^{NNNLO} = 0.1190 \pm 0.0026^{exp}$. We believe that using the latest $d_4$ calculation will not change the result significantly or changing the conclusion of our predictions. Ignoring the error, we will set $R(s) = R(s = M_Z^2) = 0.03904$ and the rest of the versions having the equivalent value to test the value of $\alpha_s$ extracted from its version,

$$R(M_Z^2)_{\overline{MS}} = R(M_Z^2)_{CIPT} = R(M_Z^2)_{CIPT+CORGI} = R(M_Z^2)_{CIPT+CORGI} = 0.03904$$
$$(6.32)$$

This will be the value we use throughout our calculation to extract $\tau$ from each of the 4 versions. All 4 taus are solved with Maple 11 by using approriate commands and techniques. The coefficients $b$, $c$, $c_2$, $c_3$, $r_1$, $r_2$, $r_3$, $d_1$, $d_2$, $d_3$,

$X_{2R}$, $X_{3R}$, $X_{2D}$, $X_{3D}$ are

$$b = \frac{1}{6}(11C_A - 2N_f) \tag{6.33}$$

$$c = \frac{1}{12b}(-\frac{3}{2}C_A[7C_A + 11C_F] + 3b[5C_A + 3C_F]) \tag{6.34}$$

$$c_2 = \frac{2857 - \frac{5033}{9}N_f + \frac{325}{27}N_f^2}{64b} \tag{6.35}$$

$$c_3 = \frac{1218587 + 1389486\xi_3}{13824b} - \frac{5857771 + 932400\xi_3}{27648}$$

$$+ \frac{7761 + 1618\xi_3}{576}b - \frac{1093}{6912}b^2 \tag{6.36}$$

$$r_1 = d_1 - \frac{1}{12}\pi^2 b^2 \tag{6.37}$$

$$r_2 = d_2 - \frac{1}{24}(6d_1 + 5c)\pi^2 b^2 \tag{6.38}$$

$$r_3 = d_3 - \frac{1}{24}(12d_2 + 14cd_1 + 3c^2 + 6c_2)\pi^2 b^2 + \frac{1}{80}\pi^4 b^4 \tag{6.39}$$

$$d_1 = (\frac{11}{4} - 2\xi_3)b + \frac{C_A}{12} - \frac{C_F}{8} \tag{6.40}$$

$$d_2 = (\frac{151}{18} - \frac{19}{3}\xi_3)b^2 + C_A(\frac{31}{6} - \frac{5}{3}\xi_3 - \frac{5}{3}\xi_5)b$$

$$+ C_F(\frac{29}{32} - \frac{19}{2}\xi_3 + 10\xi_5)b + C_A^2(\frac{799}{288} - \xi_3)$$

$$+ C_A C_F(-\frac{827}{192} + \frac{11}{2}\xi_3) + C_F^2(-\frac{23}{32}) \tag{6.41}$$

$$d_3 = N_f^3[-\frac{6131}{5832} + \frac{203}{324}\xi^3 + \frac{5}{18}\xi_5]$$

$$+ N_f^2[-\frac{1045381}{15552} - \frac{40655}{864}\xi^3 + \frac{5}{6}\xi_3^2 - \frac{260}{27}\xi_5]$$

$$+ N_f[-\frac{13044007}{10368} + \frac{12205}{12}\xi^3 - 55\xi_3^2 + \frac{29675}{432}\xi_5 + \frac{665}{72}\xi_7]$$

$$+ \frac{144939499}{20736} - \frac{5693495}{864}\xi^3 + \frac{5445}{8}\xi_3^2 + \frac{65945}{288}\xi_5 - \frac{7315}{48}\xi_7 \tag{6.42}$$

$$X_{2R} = r_2 - r_1^2 - cr_1 + c_2 \tag{6.43}$$

$$X_{3R} = r_3 - r_1^3 - \frac{5c}{2}r_1^2 - (3X_{2R} - 2c_2)r_1 + \frac{c_3}{2} \tag{6.44}$$

$$X_{2D} = d_2 - d_1^2 - cd_1 + c_2 \tag{6.45}$$

$$X_{3D} = d_3 - d_1^3 - \frac{5c}{2}d_1^2 - (3X_{2D} - 2c_2)d_1 + \frac{d_3}{2} \tag{6.46}$$

Having all these equations, fits to $\tau$ of each version (performed with Maple 11 to 100 digit precision) could be obtained where in this particular case, we

set $N_f = 5$. We find fitting to $R(M_Z) = 0.03904$

$$\tau_{\overline{MS}} = 22.561 \tag{6.47}$$
$$\tau_{CIPT} = 22.569 \tag{6.48}$$
$$\tau_{CORGI} = 22.544 \tag{6.49}$$
$$\tau_{CIPT+CORGI} = 22.574 \tag{6.50}$$

The value of $\tau$'s show that all four versions are quite consistent to one another as might be expected for a $N^3LO$ calculation at a large $\sqrt{s}$. All the values are consistent with $\alpha_s(M_Z) = 0.119$. Clearly the impact of resumming analytical continuation terms $\pi^2 b^2$ is not great at this order and energy. We will see much larger differences when we go on to apply similar fits to the much lower energy inclusive $R_\tau$ observable.

## 6.3 CONTOUR INTEGRAL REPRESENTATION OF MINKOWSKI OBSERVABLES

Among all the leptons, only the tau particle can decay into hadrons as it is the heaviest lepton and therefore has the necessary mass. Some of the common leptonic decays are into a tau neutrino, electron and electron anti neutrino ($\tau^- \longrightarrow \nu_\tau e^- \bar{\tau}_e$) or tau neutrino, muon and muon anti neutrino ($\tau^- \longrightarrow \nu_\tau \mu^- \bar{\tau}_\mu$). The possibility for the decay of tau into a tau neutrino, electron and electron anti neutrino is only slightly higher than the decay of tau into tau neutrino, muon and muon anti neutrino [42]. The creation of a tau neutrino is due to the conservation of lepton number in weak interaction whereas the creation of electron or muon is due to the conservation of charge by the emission $W^-$ gauge boson. The Feynman diagram below represents the possibility of some of the decay modes.
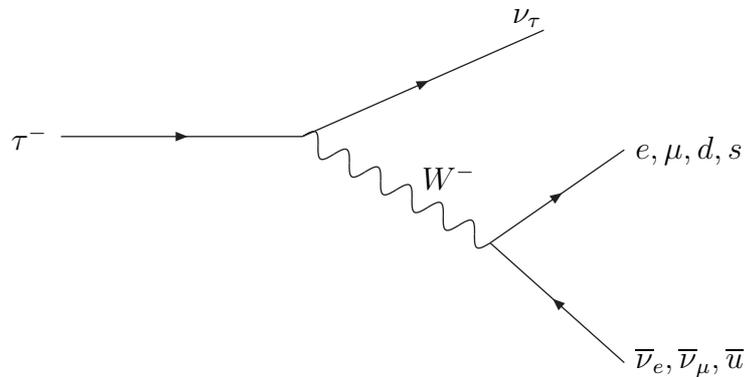


Figure 6.3: *Feynman diagram of the tau decay*

While the hadronic decay modes($\tau^- \longrightarrow \nu_\tau d_\theta \bar{u}$) will produce quark-antiquark pairs dominated by $\bar{u}$, $d$ and $s$ where $d_\theta = cos(\theta_C)d + sin(\theta_C)s$. Note that since mesons must be colorless, the pair must have the color anti-color combination. Thus, the possible mesons that can be created are $\pi^-(\bar{u}d)$, $K^-(\bar{u}s)$, $\rho^-(\bar{u}d)$ and $K^{*-}(\bar{u}s)$. Despite that $\rho^-(\bar{u}d)$ and $K^{*-}(\bar{u}s)$ have the same quark content as $\pi^-(\bar{u}d)$ and $K^-(\bar{u}s)$, they differ by parity. Other mesons involved are $\eta(\frac{u\bar{u}+d\bar{d}-2s\bar{s}}{\sqrt{6}})$ and $\omega(\frac{u\bar{u}+d\bar{d}}{\sqrt{2}})$. There are other decay modes which required detail explanation which will not be discussed here like 3 charged tracks and 5 charged tracks decay modes. Hence, the branching ratios for the different channels are expected to be approximately [43]:

$$B_l = Br(\tau^- \longrightarrow \nu_\tau l\bar{\nu}_l) = \frac{1}{5} = 20\% \quad (l = e, \mu), \qquad (6.51)$$

$$\tilde{R}_\tau = \frac{\Gamma(\tau^- \longrightarrow \nu_\tau + \text{hadrons})}{\Gamma(\tau^- \longrightarrow \nu_\tau e^- \nu_e)} \approx N = 3, \qquad (6.52)$$

which are consistent with experimental averages [44]. The agreements are relatively good and taking notice that the measured $\tau$ hadronic width provides evidence for the color degree of freedom. Note the measured value of $\tilde{R}_\tau$ at its lowest order prediction $\tilde{R}_\tau \approx N$ and the branching ratio of the leptonic channel $B_l$ is dominated by the dynamics of QCD perturbative correction $R_\tau = 0.2038$ (the leading order + other orders, which the leading order contributes most) show that the tau decay is a good choice to extract QCD strong coupling. For reviews of tau decays into hadrons see [45, 46].

The ratio $\tilde{R}_\tau$ is defined analogously to $R(s)$ as the ratio of the total $\tau$ hadronic decay width to its leptonic decay width,

$$\tilde{R}_\tau \equiv \frac{\Gamma(\tau \to \nu_\tau + \text{hadrons})}{\Gamma(\tau \to \nu_\tau e^- \bar{\nu}_e)} . \qquad (6.53)$$

$\tilde{R}_\tau$ involves 2 two-point correlation functions

$$\Pi_{ij,V}^{\mu\nu}(q) = i \int d^4x e^{iqx} \langle 0|T(V_{ij}^\mu(x)V_{ij}^\nu(0)^\dagger)|0\rangle, \qquad (6.54)$$

$$\Pi_{ij,A}^{\mu\nu}(q) = i \int d^4x e^{iqx} \langle 0|T(A_{ij}^\mu(x)A_{ij}^\nu(0)^\dagger)|0\rangle, \qquad (6.55)$$

where $V_{ij}^\mu = \bar{\psi}_j \gamma^\mu \psi_i$ is the vector and $A_{ij}^\mu = \bar{\psi}_j \gamma^\mu \gamma_5 \psi_i$ is the axial vector with the indices $i, j$ correspond to the flavour $u, d, s$. We will then have the Lorentz decompositions

$$\Pi^{\mu\nu}_{ij,V/A}(q) = (-g_{\mu\nu}q^2 + q^\mu q^\nu)\Pi^1_{ij,V/A}(q^2) + q^\mu q^\nu \Pi^0_{ij,V/A}(q^2), \qquad (6.56)$$

where 0 and 1 are the angular momentum J in the hadronic rest frame. Note that the imaginary part of the two-point functions are proportional to the spectral functions for hadrons with the quantum numbers 0 and 1. Thus the tau decay rate can be written as the integral of these spectral functions over the invariant mass of the final-state hadrons

$$\tilde{R}_\tau = 12\pi \int_0^{m_\tau^2} \frac{ds}{m_\tau^2} \left(1 - \frac{s}{m_\tau^2}\right)^2 \left[\left(1 + 2\frac{s}{m_\tau^2}\right) Im\Pi^{(1)}(s) + Im\Pi^{(0)}(s)\right]. \tag{6.57}$$

The combinations of correlators are

$$\Pi^J(s) = |V_{ud}|^2[\Pi^{(J)}_{ud,V}(s) + \Pi^{(J)}_{ud,A}(s)] + |V_{us}|^2[\Pi^{(J)}_{us,V}(s) + \Pi^{(J)}_{us,A}(s)]. \tag{6.58}$$

The inclusive contributions associated to different quarks can be separated:

$$\tilde{R}_\tau = \tilde{R}_{\tau,V} + \tilde{R}_{\tau,A} + \tilde{R}_{\tau,S}. \tag{6.59}$$

$\tilde{R}_{\tau,V}$ and $\tilde{R}_{\tau,A}$ are the first two terms of Eq. (6.58). $\tilde{R}_{\tau,S}$ is the suppressed Cabbibo contribution. $\tilde{R}_{\tau,V}$ and $\tilde{R}_{\tau,A}$ are measured experimentally from the even or odd pions in the hadronic final state while $\tilde{R}_{\tau,S}$ is measured from the number of odd kaons. The hadronic spectral function is sensitive towards non-perturbative effects of QCD, this makes the calculation of integral Eq. (6.57) to be impossible at present. The best approach is to analyze the analytic properties of the correlators $\Pi^{(J)}(s)$. For more detail, [43] will be a recommended reference, at the moment it will be suffice to express $\tilde{R}_{\tau,V/A}$ and $\tilde{R}_{\tau,S}$ as

$$\tilde{R}_{\tau,V/A} = \frac{3}{2}|V_{ud}|^2 S_{EW} \left(1 + \frac{5}{12}\frac{\alpha(m_\tau^2)}{\pi} + R_\tau + \delta_{PC}\right), \qquad (6.60)$$

$$\tilde{R}_{\tau,S} = 3|V_{us}|^2 S_{EW} \left(1 + \frac{5}{12}\frac{\alpha(m_\tau^2)}{\pi} + R_\tau + \delta_{PC}\right). \qquad (6.61)$$

Adding all the three terms, the total ratio $\tilde{R}_\tau$ can be expressed perturbatively as

$$\tilde{R}_\tau = N(|V_{ud}|^2 + |V_{us}|^2)S_{EW} \left[1 + \frac{5}{12}\frac{\alpha(m_\tau^2)}{\pi} + R_\tau(s) + \delta_{PC}\right], \qquad (6.62)$$

with $V_{ud}$ and $V_{us}$ are elements extracted from the CKM mixing matrix. $s = m_\tau^2$ lies below the threshold for charmed hadron production. Therefore, only three flavours $u$,$d$ and $s$ which are active. The electroweak correction is given by $\frac{5}{12}\frac{\alpha(m_\tau^2)}{\pi} \simeq 0.001$ with the factor $S_{EW} = 1.0194$ [43]. $\delta_{PC}$ are power corrections which arises from the leading quark-mass corrections which are extremely small for up and down quarks but extremely large for strange decays ($\delta_{us}^{(2)} \approx 20\%$). Nevertheless, the value was suppressed by the factor $\sin\theta_C^2$ which affects the total $\tilde{R}_\tau$ ratio only by $\approx -1\%$. The value of such non-perturbative corrections can be obtained from the invariant-mass distribution of the final hadrons in tau decay, although it is still unpredictable currently, it can be calculated the same way like $\tilde{R}_\tau$. $R_\tau(s)$ is the purely perturbative correction ignoring quark masses, which can be expanded as

$$R_\tau(s) = a(1 + \sum_{n>0} r_n^\tau a^n) \ . \tag{6.63}$$

Since summation over the $u$,$d$ and $s$ quarks leads to $(\sum Q_f)^2 = 0$, there will be no "light-by-light". This permits us to directly express both $R$ and $R_\tau$ in terms of the transverse part of the correlator of two vector currents in the Euclidean region.

We can now relate both Minkowskian observables denoted by $\hat{R}(s_0)$ to $D(-s)$ by analytical continuation from the Euclidean to Minkowskian region which is formulated as an integration around a circular contour in the complex energy squared $s$-plane [47],

$$\hat{R}(s_0) = \frac{1}{2\pi}\int_{-\pi}^{\pi} W(\theta)D(s_0 e^{i\theta})d\theta \ , \tag{6.64}$$

$W(\theta)$ is the weight function which is dependent on the observable $\hat{R}$ with $s_0$ as the initial energy extracted from $\tau$ then inserting into the initial coupling $a(s_0)$ (which is required for recursion relation). Evaluating the above equation with $W(\theta) = 1$ one will produce $\hat{R}(s_0) = R(s_0)$ while using the expression $W(\theta) = (1 + 2e^{i\theta} - 2e^{3i\theta} - e^{4i\theta})$, one will then have $\hat{R}(m_\tau^2) = R_\tau$. Expanding $\tilde{D}(s_0 e^{i\theta})$ perturbatively in $\bar{a} \equiv a(s_0 e^{i\theta})$ and performing numerically the $\theta$ integration term-by-term, one will then obtain "contour-improved" perturbative results. Note that at each order, an infinite subset of analytical continuation terms present in $R(s)$ and $R_\tau$ are resummed. We have discussed in the previous sections that such terms must not be ignored as they are potentially quite large, involving powers of $\pi^2$ and other beta-function coefficients. This is easily seen by expanding $\bar{a}$ in powers of $a(s_0)$ and then performing integration. We shall focus on this "contour-improved" version

of perturbation theory throughout this thesis. Comparisons of the two versions were made in great detail and length together with an emphasis of the importance of resummation of the analytical continuation terms, in [47].

The basic numerical algorithm we shall use for the evaluation of the integral in Eq. (6.65) is to split the range from $\theta = 0$ to $\pi$ into $K$ steps of size $\Delta\theta = \pi/K$ and then perform a sum over the integrand evaluated at $\theta_n = n\Delta\theta$ where $n = 0, 1, ..., K$. Thus the integral can represented as

$$\hat{R}(s_0) \simeq \frac{\Delta\theta}{2\pi}[W(0)D(s_0) + 2Re\sum_{n=1}^{K}W(\theta_n)D(s_n)], \qquad (6.65)$$

where $s_n \equiv s_0 e^{in\Delta\theta}$. In practice, we perform such trivial algorithm with all sorts of numerical packages as well as coding manually in Mathematica 6.0 and Maple 11. Rewriting $\tilde{D}(s_n)$ as a perturbative expansion, one will then have

$$\tilde{D}(s_n) = \bar{a}_n + d_1\bar{a}_n^2 + d_2\bar{a}_n^3 + \dots . \qquad (6.66)$$

Here $\bar{a}_n$ is defined as $a(s_n)$. Using Taylor's theorem in evolving $\bar{a}_n$ to $\bar{a}_{n+1}$, we will begin with $\bar{a}_0 = a(s_0)$, the following recursion relation is then given by

$$\begin{aligned}\bar{a}_{n+1} &= \bar{a}_n - i\frac{\Delta\theta}{2}bB(\bar{a}_n) - \frac{\Delta\theta^2}{8}b^2B(\bar{a}_n)B'(\bar{a}_n) + i\frac{\Delta\theta^3}{48}b^3[B(\bar{a}_n)B'(\bar{a}_n)^2 \\ &\quad + B(\bar{a}_n)^2B''(\bar{a}_n)] + O(\Delta\theta^4) + ..,\end{aligned} \qquad (6.67)$$

with $B(x)$ being defined as

$$B(x) = x^2 + cx^3 + c_2x^4 + \dots , \qquad (6.68)$$

so that $\bar{a}$ will satisfy

$$\frac{\partial\bar{a}}{\partial lns} = -\frac{b}{2}(\bar{a}^2 + c\bar{a}^3 + c_2\bar{a}^4 + ...) = -\frac{b}{2}B(\bar{a}) . \qquad (6.69)$$

$b = (33 - 2N_f)/6$, and $c = (153 - 19N_f)/12b$ are the first two universal beta-function coefficients with the subsequent coefficients $c_i, i > 1$ being scheme-dependent. We will now move on to the application of CORGI to the contour integral representation of the Minkowski observables.

## 6.4 ALL ORDERS AND FIXED-ORDER $D(s)$ IN THE CORGI APPROACH

Our previous discussion has shown that in the CORGI approach, the renormalization scale $\mu$-dependence could be avoided completely by performing a complete resummation of the UV logarithms. It is such a resummation which builds the dependence of the observable on the physical energy scale [48]. [49] demonstrates the direct relation between the observable and the direct transmutation parameter of the theory $\Lambda_{\overline{MS}}$. This allows us to define the CORGI version of $D(s)$,

$$D(s) = a_0(s) + X_2 a_0^3(s) + X_3 a_0^4 + \ldots + X_n a_0^{n+1} + \ldots . \tag{6.70}$$

Here $a_0(s)$ is the CORGI coupling in terms of the Lambert $W$-function,

$$
\begin{aligned}
a_0(s) &= -\frac{1}{c[1 + W(z(s))]}, \\
z(s) &\equiv -\frac{1}{e}\left(\frac{\sqrt{s}}{\Lambda_D}\right)^{-b/c},
\end{aligned}
\tag{6.71}
$$

where $\Lambda_D \equiv e^{d/b}(2c/b)^{-c/b}\Lambda_{\overline{MS}}$. $d$ is defined as the NLO perturbative coefficient $d_1$ for $D(s)$ in the $\overline{MS}$ scheme with $\mu^2 = s$. $a_0(s)$ is the coupling in the scheme with $\mu^2 = e^{-2d/b}s$ with all the other coefficient $c_i$, $(i > 1)$ set to zero in the 't Hooft scheme. In the CORGI scheme $d_1 = 0$, and is exactly equivalent at NLO to the Effective Charge approach discussed in [50] whereas conventional RG-improvement in this scheme completely resum all ultraviolet logarithms. This is equivalent to the CORGI approach and can be formulated in any scheme [48]. $X_2$ and $X_3$ are the $N^2LO$ and $N^3LO$ scheme-invariant coefficients

$$
\begin{aligned}
X_2 &= c_2 + d_2 - cd_1 - d_1^2, \\
X_3 &= \frac{c_3}{2} + d_3 - d_1^3 - \frac{5c}{2}d_1^2 - (3X_2 - 2c_2)d_1 ,
\end{aligned}
\tag{6.72}
$$
$$
\tag{6.73}
$$

built from the coefficients $d_1$ and $d_2$ and beta-function coefficients. Note that $X_2$ and $X_3$ are equivalent to $X_{2D}$ and $X_{3D}$ in Section 6.1. $d_1$, $d_2$ and $d_3$ are known exactly and have been calculated in [40]. Therefore, the $N^3LO$ contour-improved CORGI model can be obviously constructed for Minkowski observables $\hat{R}(s_0)$, using the numerical approach described in Section 6.3.

The fact that knowing $a_0(s)$ in closed form expressed in terms of the Lambert $W$-function, which has a well-defined branch structure in the complex plane, one can evaluate it directly avoiding the numerical approach of evolving $\bar{a}_n$ in Eq. (6.71). It is worth mentioning again that the selection of the $W_{-1}$ branch of the function on the range of integration $[0, \pi]$, and the $W_1$ branch on the range $[-\pi, 0]$ are necessary to ensure asymptotic freedom as well as a sensible value of integration. We will not discuss the possibility of avoiding the use of Simpson's Rule integration in the $R_{e^+e^-}$ ratio for $W(\theta) = 1$ in this thesis, for interest, one can refer to [51].

We will now test the accuracy of the fixed-order perturbative approximation by attempting to approximate the still uncalculated coefficients $d_i$, $(i > 2)$ in $D(s)$ using the suggested "leading-$b$" approximation. As we have previously discussed, $d_n$ can be written as an expansion in powers of $N_f$, given by Eq. (5.16). These large-$N_f$ coefficients $d_n^{[n]}$ are calculated exactly to all-orders. We are motivated by the structure of renormalon singularities in the Borel plane which lead to find it possible to convert this expansion into the leading-$b$ expansion described in Eq. (5.17) by using $N_f = (33/2 - 3b)$.

We will construct an all-orders "leading-b" resummation as discussed in Chapter 5. One can use the exact *V-scheme* leading-b result of [24].

$$
\begin{aligned}
d_n^{(L)}(V) \;=\; & \frac{-2}{3}n!\frac{(n+1)}{2^n}[-2n - \frac{n+6}{2^{n+2}} \\
& + \frac{16}{n+1}\sum_{\frac{n}{2}+1>s>0} s(1-2^{-2s})(1-2^{2s-n-2}\zeta_{2s+1})]b^n \;.
\end{aligned}
\tag{6.74}
$$

The resulting leading-$b$ resummation of $D(s)$ can be expressed as

$$
D^{(L)} = a(1 + \sum_{k=0}^{\infty} d_k^{(L)} a^k),
\tag{6.75}
$$

where the principal value (PV) is regulated by the Borel Sum,

$$
\tilde{D}^{(L)}(1/a) = PV \int_0^\infty dz e^{-z/a} B[D^{(L)}](z) \;,
\tag{6.76}
$$

where $B[\tilde{D}^{(L)}](z)$ is the Borel transform which behaviour has been discussed extensively in Chapter 5, where its structure is Eq. (5.18)

$$
B[\tilde{D}^{(L)}](z) = \sum_{j=1}^{\infty} \frac{A_0(j) + A_1(j)z}{(1+\frac{z}{z_j})^2} + \frac{B_0(2)}{(1-\frac{z}{z_2})} + \sum_{j=3}^{\infty} \frac{B_0(j) + B_1(j)z}{(1-\frac{z}{z_j})^2} \;.
\tag{6.77}
$$

Note that the residues of these poles can be computed from the exact all-orders large-$N_f$ result which makes it easy to compute the $UV$ and $IR$ renor-malon contributions, expressed in terms of the exponential integral function,

$$Ei(x) = -\int_{-x}^{\infty} dt \frac{e^{-t}}{t} \ . \tag{6.78}$$

We recall that for $IR$ renormalons where $x > 0$, the $Ei(x)$ function is defined by taking the Cauchy principal value of the integral. Such arbitrariness in regulating the $IR$ renormalon contributions implies that the perturbative series is lacking the power corrections of the operator product expansion (OPE) which are essential in order to have a sensible result. There is no relevant operator in dimension of two in the Operator Product Exapansion for the vector correlator. This is therefore in accordance with the fact that the singularity $IR_1$ is absent , and the nearest singularity to the origin in the Borel plane is $UV_1$. This generates the leading $d_n^{(L)}$ asymptotic behaviour [49],

$$d_n^{(L)}(V) \approx \frac{(12n + 22)}{27} n! \left(-\frac{1}{2}\right)^n b^n \ . \tag{6.79}$$

The $UV$ renormalon and $IR$ renormalon can be expressed as the contribu-tions of infinite sums of the $Ei$ functions,

$$
\begin{aligned}
D^{(L)}(F)|_{UV} \ = \ & \sum_{j=1}^{\infty} z_j \{ e^{F(a)z_j} Ei(-Fz_j)[Fz_j(A_0(j) - z_j A_1(j)) - z_j A_1(j)] \\
& + (A_0(j) - z_j A_1(j))) \} \ ,
\end{aligned} \tag{6.80}
$$

and

$$
\begin{aligned}
D^{(L)}(F)|_{IR} \ = \ & e^{-Fz_2} z_2 B_0(2) Ei(Fz_2) \\
& \sum_{j=3}^{\infty} z_j \{ e^{-Fz_j} Ei(Fz_j)[Fz_j(B_0(j) + z_j B_1(j)) - z_j B_1(j)] \\
& - (B_0(j) + z_j B_1(j)) \} \ ,
\end{aligned} \tag{6.81}
$$

where we have used $F \equiv 1/a_V$ with $a_V$ denoted as the coupling in the V-scheme. Referring to [49], $A_0(j), A_1(j)$ are related to the residues of the $UV_j$ poles by

$$A_0(j) = \frac{8}{3} \frac{(-1)^{j+1}(3j^2 + 6j + 2)}{j^2(j+1)^2(j+2)^2}, \quad A_1(j) = \frac{4}{3} \frac{b(-1)^{j+1}(2j+3)}{j^2(j+1)^2(j+2)^2} \ . \tag{6.82}$$

The *UV* residues are related to the *IR* residues with $B_0(j) = -A_0(-j)$ and $B_1(j) = -A_1(-j)$ for $j>2$, and $B_0(1) = B_1(1) = B_1(2) = 0$, and $B_0(2) = 1$ [49] by conformal symmetry [52] of the vector correlator . The contour integral is then evaluated using the $D^{(L)}(F)$ result by modifying the definition of the $Ei$ functions in accord to their argument involving $1/a_V(s_0 e^{i\theta})$ which is complex for $\theta$ not equal to zero. Therefore, it is best to generalize the $Ei$ function $Ei(n, z)$ such that

$$Ei(n, z) = \int_1^\infty dt \frac{e^{-tz}}{t^n}, \tag{6.83}$$

which is analytic in the complex $z$-plane with a branch cut along the negative real axis as what we required. The replacement of the $Ei(-Fz_j)$ in the *UV* contribution with $-Ei(1, Fz_j)$, and $Ei(Fz_j)$ in the *IR* contribution with $-Ei(1, -Fz_j) + i\pi sign(Im(Fz_j))$ are necessary as this is where the discontinuities across the branch cut are removed with the final $i\pi$ contribution [49]. The final result for $\tilde{D}^{(L)}(F)$ is simply the sum of the *UV* and *IR* contributions. Eqs. (6.80) and (6.81) have rapidly convergent behavior since the $A(j)$ and $B(j)$ coefficients have a $j^{-4}$ dependence for large $j$. For the numerical computation which will be discussed in Section 6.5, we will truncate Eq. (6.80) and Eq. (6.81) at $N_{UV} = 15$ and $N_{IR} = 17$ respectively. Such an arrangement $N_{IR} = N_{UV} + 2$ is sensible as the symmetry properties imply that $A_0(j) = -B_0(j + 2)$ ensuring that the first O($a$) term in the perturbation series has the correct unit coefficient $B_0(2) = 1$.

Our last step is to use the results above to perform an all-orders CORGI resummation which can formally be expressed as

$$D_{CORGI} = a_0 + X_2 a_0^3 + X_3 a_0^4 + \sum_{n>3} X_n^{(L)} a_0^{n+1} , \tag{6.84}$$

where the exactly known $N^2LO$ $X_2$ and $N^3LO$ $X_3$ coefficients are included and the remaining unknown coefficients are approximated at leading-$b$, $X_4^{(L)}$ ,$X_5^{(L)}$,.... Note that $a_0$ is the full CORGI coupling of Eq. (6.71) in which all the Renormalization Group-predictable UV logarithms containing the exact $d_1$ are resummed. Note that such a resummation is achieved by taking note of the combination suggested in [39]

$$\rho_0 = bln\left(\frac{\mu}{\tilde{\Lambda}}\right) - d_1(\mu) , \tag{6.85}$$

which is scheme-independent. The coupling $a^{(L)}(s)$ is defined as

$$a^{(L)}(s) = \frac{1}{b\ln(\sqrt{s}/\tilde{\Lambda})} \,, \tag{6.86}$$

at the leading-$b$ level for a simple case of one loop. Note that in the CORGI scheme, $d_1^{(L)} = 0$, and by evaluating the invariant $\rho_0$ in the $V$ scheme and the CORGI scheme, the relations between the couplings in the two schemes are clear and can be expressed as

$$\frac{1}{a_V^{(L)}} = \frac{1}{a_0} + d_1^{(L)}(V) \,. \tag{6.87}$$

Now it is straightforwardly follows that the formal resummation in Eq. (6.84) is simply

$$D_{CORGI} = D^{(L)}\left(\frac{1}{a_0} + d_1^{(L)}(V)\right) + (X_2 - X_2^{(L)})a_0^3 + (X_3 - X_3^{(L)})a_0^4 \,, \tag{6.88}$$

where the $D^{(L)}$ term with the exact $X_2$ and $X_3$ are replaced by $X_2^{(L)}$ and $X_3^{(L)}$. This expression is corrected by the corresponding second and third term. Now it is possible to approximate N$^4$LO and higher CORGI results by the truncation of Eq. (6.84). The $X_n^{(L)}$ can then be evaluated immediately by using the leading-$b$ of Eq. (6.87) where one will then find

$$X_n^{(L)} = \mathcal{C}_{n+1}\left[\sum_{k=0}^{\infty} d_n^{(L)}(V)\left(\frac{a}{1 + ad_1^{(L)}(V)}\right)^{k+1}\right] \,. \tag{6.89}$$

The symbol $\mathcal{C}_n[f(a)]$ is the coefficient of $a^n$ expanded in power series of $f(a)$ which the expression of $d_n^{(L)}(V)$ can be directly obtained from Eq. (6.74).

With the above results of Eq. (6.89), we can generate all-orders resummed and fixed-order contour-improved CORGI results for the Minkowski observable $R_\tau$ to perform phenomenological studies in the next two sections.

## 6.5 ALL-ORDERS CORGI VERSUS $NLO$, $N^2LO$ AND $N^3LO$ CORGI RESULTS

The observable $R_\tau$ has been the subject of experimental study by the ALEPH collaboration via $e^+e^- \to \tau^+\tau^-$ on the $Z$ resonance [53]. If data consisting of
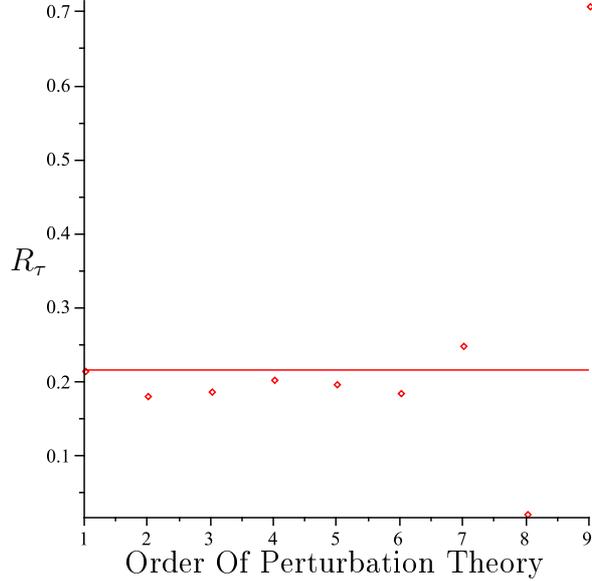
Figure 6.4 :  *All Orders CORGI resummation versus $N^n LO$ fixed order*

strange quarks are omitted (this is necessary as the strange quarks are much heavier than the up and down quarks, thus its inclusion will affect our prediction) from the data. The latest value is given by $\tilde{R}_\tau = 3.479 \pm 0.011$ [54]. We use the values of the variables $V_{us} = 0$, and $V_{ud} = 0.97418 \pm 0.00027$ [55] from the CKM matrix. The estimated power correction contribution  is given by $\delta_{PC} = -0.003 \pm 0.004$ [54]. Plugging in all the values collected, one finds from Eq. (6.62) that the experimental value is then given by $R_\tau = 0.2038 \pm 0.004$. Note that we have neglected the QED contribution to the experimental value. By doing so, we will be able to obtain an all-orders "leading-b" resummation of the contour-improved CORGI as well as the fixed-order version where we will truncate the series at corresponding terms of $NLO$, $N^2 LO$ and $N^3 LO$ described in Sections 6.3 and 6.4. As a generalization, we will set $N_f = 3$ permanently throughout the calculations except when making flavour threshold calculations. We will fix $\Lambda_{\overline{MS}}^{(3)}$ where our goal is to make a theoretical comparison of the all-orders CORGI versus fixed-order truncated CORGI result in reproducing the measured central value $R_\tau = 0.2038$. We present the results in Fig. (6.4) with the solid red line representing the all-orders CORGI result fixed to the data, and the red points are the $N^n LO$ fixed-order CORGI results. In this case, we select the $N^3 LO$ ($n = 3$) fixed-order result as a comparison, which is the highest order exactly known to date. It turns out to be in exceptionally good agreement with the all-orders CORGI resummation. Nevertheless, such a leading-$b$ approximation $N^n LO$ eventually shows an oscillatory behavior which becomes more and more explosive for $n > 7$. This is
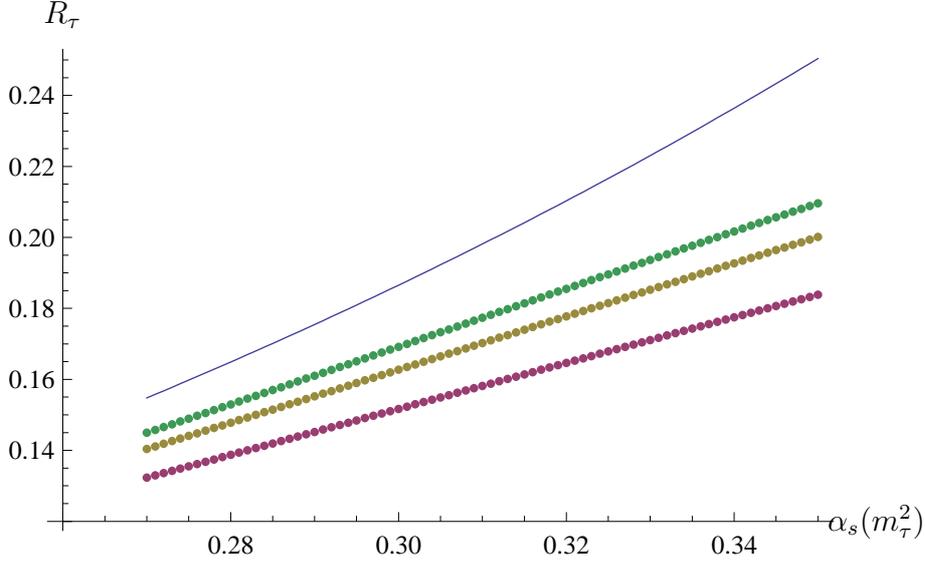
Figure 6.5 :   $R_\tau$ *as a function of* $\alpha_s(m_\tau^2)$. *All Orders CORGI (solid blue curve), dense dotted lines are the NLO, $N^2LO$ and $N^3LO$ truncated fixed-order CORGI result.*

when fixed-order CORGI eventually breaks down. Such oscillatory behavior is exactly what we could predict from the alternating positive and negative sign factorial growth of the contribution from the leading $UV_1$ renormalon of Eq. (6.82).

We will now make an attempt to estimate the uncertainty in $\alpha_s(m_\tau^2)$ extracted from $R_\tau$ measurements. The difference between the all-orders CORGI and the exact $N^3LO$ fixed-order CORGI results will be used in the estimation of uncalculated higher order terms.  Fig. (6.5) represents $R_\tau$ versus $\alpha_s(m_\tau^2)$ where the upper solid curve is the all-orders CORGI result while dense dotted lines are the $NLO$, $N^2LO$ and $N^3LO$ truncated fixed-order CORGI result. From the plot, we can deduce that by having more of the exact higher $n$ order terms will lead us to conclude that the fixed-order CORGI gets closer to the all-orders CORGI result. Note also that the separation between the curves increases rapidly as $R_\tau$ increases. As the experimentally measured $R_\tau \simeq 0.2038$, we are therefore quite fortunate that the separation of the curves is reasonably small in this region. Using data collected from ALEPH, we extract $\alpha_s(m_\tau^2)$ for all-orders CORGI and the fix order CORGI in Table 6.1. Note that the right hand column of Table 6.1 represents the value of $\alpha_s(m_\tau^2)$ extracted from the standard $\overline{MS}$ fixed-order perturbation theory calculation which we denote as FOPT, which clearly shows that it is badly defined at the $N^3LO$ truncation as well as the all-orders FOPT which
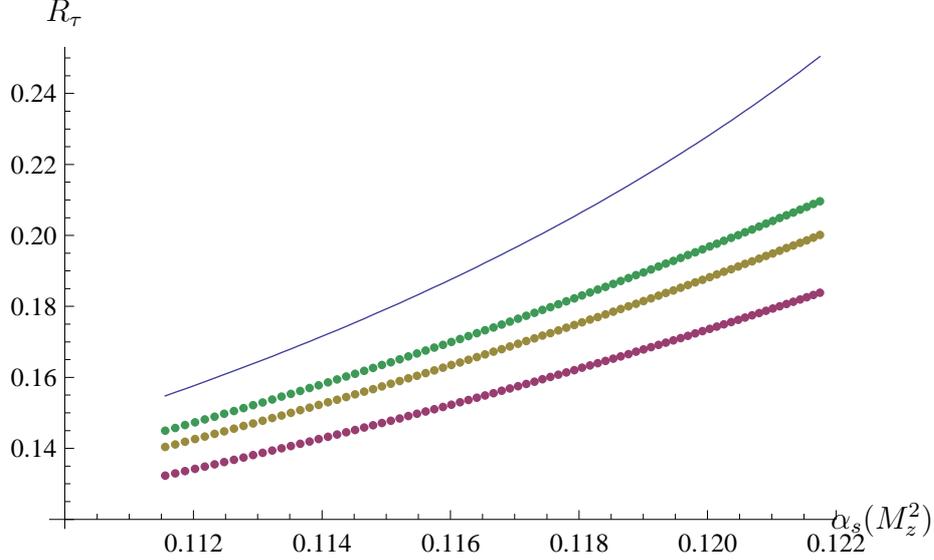
Figure 6.6 :   $R_\tau$ *as a function of* $\alpha_s(M_z^2)$*.All Orders CORGI (solid blue curve), dense dotted lines are the NLO, $N^2LO$ and $N^3LO$ truncated fixed-order CORGI result.*

settles at a higher value than the all-orders CORGI. This clearly shows the motivation of CORGI as a substitute to the standardized FOPT. Now, evolving these $\alpha_s(m_\tau^2)$ results through flavour thresholds up to $\mu = M_Z$ using the three-loop matching conditions [56], we present values of $\alpha_s(M_Z^2)$ in Table 6.2.

| | |
|---|---|
| $\alpha_s(m_\tau^2)^{CORGI}_{allorders} = 0.315^{+0.0033}_{-0.0033}$ | $\alpha_s(m_\tau^2)^{FOPT}_{allorders} = 0.321^{+0.0032}_{-0.0033}$ |
| $\alpha_s(m_\tau^2)^{CORGI}_{N^3LO} = 0.343^{+0.0051}_{-0.0051}$ | $\alpha_s(m_\tau^2)^{FOPT}_{N^3LO} = 0.263$ |
| $\alpha_s(m_\tau^2)^{CORGI}_{N^2LO} = 0.351^{+0.0053}_{-0.0052}$ | $\alpha_s(m_\tau^2)^{FOPT}_{N^2LO} = 0.316$ |
| $\alpha_s(m_\tau^2)^{CORGI}_{NLO} = 0.376^{+0.0063}_{-0.0063}$ | $\alpha_s(m_\tau^2)^{FOPT}_{NLO} = \text{N/A}$ |

Table 6.1 $\alpha_s(m_\tau^2)$ extracted from All-orders CORGI(red) versus Fixed-Order $NLO$, $N^2LO$ and $N^3LO$ CORGI with comparison to Fixed Order Perturbation Theory(blue)

| | |
|---|---|
| $\alpha_s(M_Z^2)_{allorders}^{CORGI} = 0.118_{-0.0004}^{+0.0004}$ | $\alpha_s(M_Z^2)_{allorders}^{FOPT} = 0.119_{-0.0004}^{+0.0004}$ |
| $\alpha_s(M_Z^2)_{N^3LO}^{CORGI} = 0.121_{-0.0007}^{+0.0005}$ | $\alpha_s(M_Z^2)_{N^3LO}^{FOPT} = 0.110$ |
| $\alpha_s(M_Z^2)_{N^2LO}^{CORGI} = 0.122_{-0.0006}^{+0.0005}$ | $\alpha_s(M_Z^2)_{N^2LO}^{FOPT} = 0.118$ |
| $\alpha_s(M_Z^2)_{NLO}^{CORGI} = 0.125_{-0.0006}^{+0.0006}$ | $\alpha_s(M_Z^2)_{NLO}^{FOPT} = \text{N/A}$ |

Table 6.2 $\alpha_s(M_Z)$ extracted from All-orders CORGI(red) versus Fixed-Order $NLO$, $N^2LO$ and $N^3LO$ CORGI with comparison to Fixed Order Perturbation Theory(blue)

Our main interest is in the estimation of the uncertainty in $\alpha_s(M_Z^2)$ due to missing higher-order corrections. We can take this to be $\alpha(M_Z^2)_{N^3LO}^{CORGI} - \alpha(M_Z^2)_{allorders}^{CORGI} = \delta\alpha_s(M_Z^2){\approx}0.003$. A plot showing the resummed all-orders CORGI versus the fixed-orders CORGI results for $R_\tau$ versus $\alpha_s(M_Z^2)$ is shown in Fig. (6.6). We should compare our fit for $\alpha_s(m_\tau^2)_{N^3LO}^{CORGI} = 0.343 \pm 0.0051$ in Table 6.1 with other comparable $\alpha_s(m_\tau^2)$ determinations based on the use of CIPT and FOPT. Baikov et al [40] find $0.332 \pm 0.0043$, Davier et al [54] find $0.344 \pm 0.009$, Menke [57] gives $0.342 \pm 0.010$ while Pich [58] reports $0.342 \pm 0.012$. Our determination is seen to be consistent with these. There are other determinations not using CIPT, but using FOPT augmented by renormalon or power correction models [59, 60, 61]. These tend to find lower values of $\alpha_s(m_\tau^2)$, but these values are highly dependent on the models used. The values found are actually similar to our all-orders leading-$b$ CORGI result $\alpha_s(m_\tau^2)_{allorders}^{CORGI} = 0.315 \pm 0.0033$ found in Table 6.1. We would stress that our CORGI result uses CIPT and so all RG-predictable terms and all analytical continuation terms known at $N^3LO$ are resummed to all-orders.

We define the quantity $\tilde{R}_\tau(s_0)$ as

$$\tilde{R}_\tau(s_0) \equiv \frac{\Gamma(\tau{\rightarrow}\nu_\tau + \text{hadrons}; s_{had} < s_0)}{\Gamma(\tau{\rightarrow}\nu_\tau e\bar{\nu}_e)} = \int_0^{s_0} ds \frac{d\tilde{R}_\tau(s)}{ds} \,, \qquad (6.90)$$

where $\frac{d\tilde{R}_\tau}{ds}$ is the inclusive hadronic spectrum. $\tilde{R}_\tau(s_0)$ can be extracted from the experimental data for $\frac{d\tilde{R}_\tau}{ds}$ using the procedure outlined in [62], i.e., multiplying the normalised distribution by the world average for $\tilde{R}_\tau$ and integrating (summing) bins.

In terms of the various theoretical contributions, we have

$$\tilde{R}_\tau(s_0) = N(|V_{ud}|^2)S_{EW}[(2x - 2x^3 + x^4) + \frac{3}{4}C_F R_\tau(s_0) + \delta_{PC}] \,, \qquad (6.91)$$
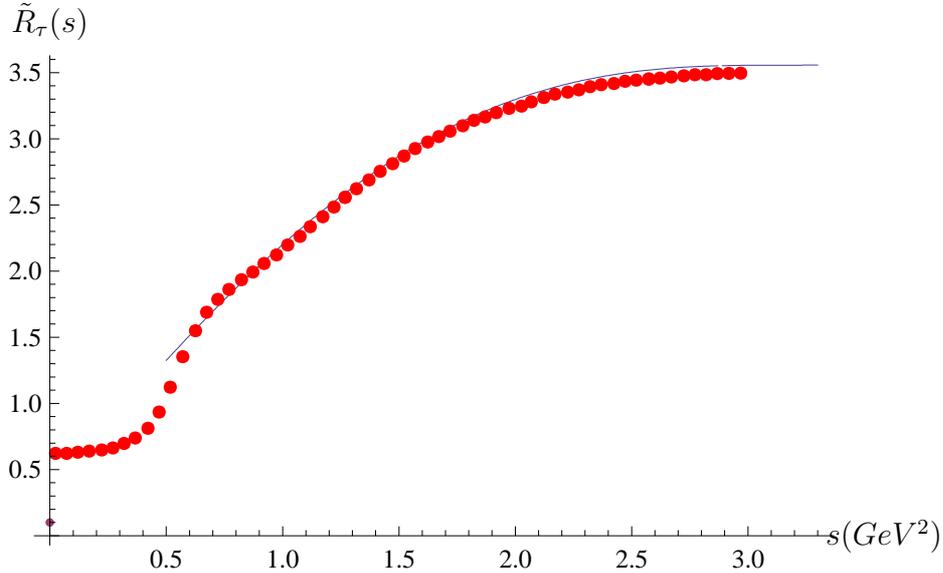
Figure 6.7 :  $\tilde{R}_\tau(s)$ *as a function of energy s (GeV$^2$) versus ALEPH data*
*extracted from [53] using the procedure of [62].*

with $x \equiv s_0/m_\tau^2$. It is then possible to compute $R_\tau(s_0)$ from Eq. (6.64) with
the appropriate weight function,

$$W(\theta) = 2x(1 + e^{i\theta}) - 2x^3(1 + e^{3i\theta}) + x^4(1 - e^{4i\theta}) \ . \qquad (6.92)$$

Fig. (6.7) shows the close fit of the all-orders leading-$b$ CORGI resummation
(solid line) in comparison to the ALEPH data for $\tilde{R}_\tau(s)$ (red dots) extracted
from [53] using the procedure of [62] with data fitted at $s = m_\tau^2$ and where
we have $R_\tau(m_\tau^2) = \tilde{R}_\tau$. Referring to Eq. (6.71), the CORGI coupling has
a Landau pole at $\sqrt{s} = \Lambda_D$ and by fitting to the experimental value of $R_\tau$,
we determine the value of $\Lambda_D = 0.725$GeV. This implies that the prediction
is valid only for $s > 0.525$ GeV$^2$. This shows an excellent agreement with
the data. On the scale chosen for the plot the fixed-order CORGI or FOPT
result would be indistinguishable from the all-orders CORGI result and so
we have not displayed them separately.

## 6.6  SUMMARY

We began this chapter with the definition of the dimensionless $R_{e^+e^-}$ ratio
for some value of the center of mass energy $\sqrt{s}$ where $R(s)$ denotes the QCD
perturbative corrections to the parton model result. This could be related to
the Adler $D$-function $D(-s)$ by performing an analytical continuation from

Euclidean to Minkowskian regions represented by a contour integral in the complex $s$-plane. This enabled us to introduce contour improved perturbation theory (CIPT) which resum to all-orders known and large analytical continuation terms involving powers of $\pi^2 b^2$. We could also write a similar contour integral for the inclusive tau-decay ratio $R_\tau$. Using the recently computed $N^3LO$ corrections $d_3$ of [40], a good description of $R(M_Z)$ and $R_\tau$ were also obtained. Various different versions of perturbation theory involving CIPT , and also using the CORGI approach described in Chapter 3, were employed to extract $\alpha_s(m_\tau^2)$. We also used leading-$b$ renormalon techniques discussed in Chapter 5 to construct all-orders CORGI and CIPT resummations which could be compared with fixed-order $N^3LO$ results. We also evolved through flavour thresholds to obtain corresponding $\alpha_s(M_Z^2)$ values and estimated an uncertainty $\delta\alpha_s(M_Z^2) \approx 0.003$. These $\alpha_s$ values below and above threshold are tabulated in Tables 6.1 and 6.2. We saw that the $N^3LO$ CORGI result for $\alpha_s(m_\tau^2)$ was consistent with other determinations using CIPT and FOPT. Fits to the $\tau$ spectral function $R_\tau(s)$ were also performed.

# Chapter 7

# FULLY ANALYTIC IR FREEZING

## 7.1 INTRODUCTION

In Chapter 5, it has been shown that in the leading-$b$ approximation, perturbative corrections to the GLS and unpolarized[1] Bjorken Sum Rules (denoted by $K_{PT}^{(L)}$ and $U_{PT}^{(L)}$ respectively) are simply linear combinations of the following functions,

$$F_+^{(n)}(Q^2) \equiv \left(\frac{\Lambda^2}{Q^2}\right)^n \text{Ei}\left(n \ln \frac{Q^2}{\Lambda^2}\right), \tag{7.1}$$

and

$$F_-^{(n)}(Q^2) \equiv \left(\frac{Q^2}{\Lambda^2}\right)^n \text{Ei}\left(-n \ln \frac{Q^2}{\Lambda^2}\right). \tag{7.2}$$

Where $\text{Ei}(x)$ is the Exponential Integral function, defined for $x < 0$ by

$$\text{Ei}(x) = -\int_{-x}^{\infty} dt \frac{e^{-t}}{t}. \tag{7.3}$$

Here we assume that the principal value (PV) of $\text{Ei}(x)$ is taken for $x > 0$. The $F_+^{(n)}(Q^2)$ terms correspond to contributions from the IR renormalon singularities , located at $z_n = 2n/b$ on the positive real semi-axis of the Borel plane. Equivalently, the $F_-^{(n)}(Q^2)$ terms are the contributions from UV renormalon singularities, located at $z_n = -2n/b$ on the negative real semi-axis of the Borel plane. The leading-$b$ form of Adler D function, $D_{PT}^{(L)}$, can also

---

[1]Perturbative corrections to the *polarized* Bjorken Sum Rules are identical to those of the GLS Sum Rule, up to a series of 'light-by-light' corrections which we do not consider here.

be written as a combination of $F_{\pm}^{(n)}$ terms, but with additional $(1/a(Q^2))F_{\pm}^{(n)}$ $^2$ contributions.

These leading-$b$ results are finite overall when all contributions are combined, furthermore, they are also continuous at $Q^2 = \Lambda^2$, due to cancellations between potentially divergent IR and UV renormalon contributions as demonstrated in Chapter 5. Additionally, one finds smooth infrared freezing behaviour, with the corrections to the parton model result vanishing as $Q^2 \longrightarrow 0$.

The first logarithmic derivative in $Q^2$ is also continuous at $Q^2 = \Lambda^2$, however higher derivatives are neither finite or continuous, and hence there is only piecewise continuity and finiteness. The true result, of course, should be an analytic function in the $Q^2$-plane, with all derivatives finite and continuous at $Q^2 = \Lambda^2$.

With the PV definition one has

$$\mathrm{Ei}(x) = \ln|x| + \gamma_E + \mathcal{O}(x). \tag{7.4}$$

It is then straightforward to show that one can rewrite the $\mathrm{Ei}(x)$ functions in $F_{\pm}(Q^2)$ as,

$$
\begin{aligned}
\mathrm{Ei}\left(n\ln\frac{Q^2}{\Lambda^2}\right) &= \mathrm{Ei}\left(-n\ln\frac{\Lambda^2}{Q^2}\right) \\
&= \ln\left[n\left(1-\frac{\Lambda^2}{Q^2}\right)\right] + \gamma_E + f_n\left(1-\frac{\Lambda^2}{Q^2}\right) \tag{7.5} \\
&= \ln\left[n\left(1-\frac{Q^2}{\Lambda^2}\right)\right] + \gamma_E + \tilde{f}_n\left(1-\frac{Q^2}{\Lambda^2}\right) \tag{7.6} \\
&= \ln\left[n\left(1-\frac{Q^2}{\Lambda^2}\right)\right] + \gamma_E + f_n\left(1-\frac{\Lambda^2}{Q^2}\right) + \ln\frac{\Lambda^2}{Q^2}, \tag{7.7}
\end{aligned}
$$

---

$^2(1/a(Q^2))F_{\pm}^{(n)}$ is required to be treated separately to avoid singularity at $Q = 0$, more detailed discussion on $(1/a(Q^2))F_{\pm}^{(n)}$ will be made in explaining the relevance of adding a non-perturbative term to this equation.

and

$$
\begin{aligned}
\mathrm{Ei}\left(-n\ln\frac{Q^2}{\Lambda^2}\right) &= \mathrm{Ei}\left(n\ln\frac{\Lambda^2}{Q^2}\right) \\
&= \ln\left[n\left(1-\frac{\Lambda^2}{Q^2}\right)\right] + \gamma_E + \tilde{f}_n\left(1-\frac{\Lambda^2}{Q^2}\right) \qquad (7.8) \\
&= \ln\left[n\left(1-\frac{\Lambda^2}{Q^2}\right)\right] + \gamma_E + f_n\left(1-\frac{Q^2}{\Lambda^2}\right) + \ln\frac{Q^2}{\Lambda^2} \\
&\qquad\qquad\qquad\qquad\qquad\qquad\qquad\qquad\qquad\qquad (7.9) \\
&= \ln\left[n\left(1-\frac{Q^2}{\Lambda^2}\right)\right] + \gamma_E + f_n\left(1-\frac{Q^2}{\Lambda^2}\right). \qquad (7.10)
\end{aligned}
$$

Here, $f_n(1-\Lambda^2/Q^2)$ and $\tilde{f}_n(1-Q^2/\Lambda^2)$ are power series in $(1-\Lambda^2/Q^2)$ and $(1-Q^2/\Lambda^2)$, respectively. As such, they are fully differentiable at $Q^2 = \Lambda^2$ with all derivatives finite. In contrast, the $\ln[n(1-\Lambda^2/Q^2)]$ and $\ln[n(1-Q^2/\Lambda^2)]$ terms diverge at $Q^2 = \Lambda^2$. As was discussed in [40], relations between IR and UV renormalon residues ensure that these ln terms cancel for the combined $F_\pm^{(n)}$ terms, and also for their first logarithmic $Q^2$ derivative. However, similar cancellations do not take place for higher derivatives, which are therefore not finite at the Landau pole.

As is well known these renormalon resummations of perturbation theory will also have to be combined with the non-perturbative contributions of the OPE which are required in order to remove IR renormalon ambiguities due to poles on the positive axis in the Borel $z$-plane. These ambiguities are easily seen to be $\sim \left(\frac{\Lambda^2}{Q^2}\right)^n$ effects for an IR renormalon. For $Q^2 > \Lambda^2$ one therefore expects a standard OPE of the form

$$
D_{NP} = \sum_{n=1}^{\infty} \mathcal{C}_n \left(\frac{\Lambda^2}{Q^2}\right)^n .
$$

In reality the coefficients are actually coefficient functions of the coupling. For $Q^2 < \Lambda^2$ one needs to switch to a modified Borel representation where the contour of integration is along the negative $z$-axis (see Eq. (5.29)) [37]. There will then be Borel ambiguities associated with UV renormalons. It is easily seen that these ambiguities will be of the form $\sim \left(\frac{Q^2}{\Lambda^2}\right)^n$. One then anticipates a modified OPE for $Q^2 < \Lambda^2$ of the form

$$
D_{NP} = \sum_{n=0}^{\infty} \tilde{\mathcal{C}}_n \left(\frac{Q^2}{\Lambda^2}\right)^n .
$$

Notice that a constant $n = 0$ first term is allowed in this expansion, but of course is absent in the regular OPE which must vanish as $Q^2 \to \infty$ due to asymptotic freedom.

Our crucial observation is that for $Q^2 > \Lambda^2$, the $\ln[n(1 - \Lambda^2/Q^2)]$ term in Eqs. (7.5, 7.8, 7.9) has a valid expansion in powers of $\Lambda^2/Q^2$, of the same form as the standard operator product expansion (OPE) above. Thus, by adding a suitable non-perturbative contribution to the perturbative component, the ln term can be cancelled, and a function $F^*(Q^2)$ is obtained all of whose derivatives are finite at $Q^2 = \Lambda^2$. Similarly for $Q^2 < \Lambda^2$, the $\ln[n(1 - Q^2/\Lambda^2]$ term in Eqs. (7.6, 7.7, 7.10) has a valid expansion in powers of $Q^2/\Lambda^2$, which is of the same form as the modified non-perturbative OPE expansion above. Again, by adding a suitable non-perturbative term to the perturbative component, one can arrange that the ln term is cancelled. Hence by adding suitable compensating non-perturbative terms in the two regions $Q^2 > \Lambda^2$ and $Q^2 < \Lambda^2$, one can arrange that a single analytic function $F_{\pm}^{*(n)}(Q^2)$ is obtained which is holomorphic in $Q^2$, and all of whose derivatives are finite and continuous at $Q^2 = \Lambda^2$.

## 7.2  THE $n = 1$ AND $n = 2$ CASES

We shall first show how this works for the $n = 1$ and $n = 2$ cases, relevant for the DIS sum rules $K_{pBJ}$ and $U_{uBJ}$. For $Q^2 > \Lambda^2$ we can use Eq. (7.5) to rearrange the expression for $F_+^{(1)}(Q^2)$ as follows

$$
\begin{aligned}
F_+^{(1)}(Q^2) \ = \ & \left\{ \frac{\Lambda^2}{Q^2} \ln \left( 1 - \frac{\Lambda^2}{Q^2} \right) - \frac{\Lambda^2}{Q^2} \ln \frac{\Lambda^2}{Q^2} \right\} + \gamma_{\mathrm{E}} \frac{\Lambda^2}{Q^2} \\
& + \ \frac{\Lambda^2}{Q^2} f_1 \left( 1 - \frac{\Lambda^2}{Q^2} \right) + \left[ \frac{\Lambda^2}{Q^2} \ln \frac{\Lambda^2}{Q^2} \right].
\end{aligned}
\tag{7.11}
$$

Similarly, for $Q^2 < \Lambda^2$, it can be rearranged using Eq. (7.7) as

$$
\begin{aligned}
F_+^{(1)}(Q^2) \ = \ & \left\{ \frac{\Lambda^2}{Q^2} \ln \left( 1 - \frac{Q^2}{\Lambda^2} \right) \right\} + \gamma_{\mathrm{E}} \frac{\Lambda^2}{Q^2} + \frac{\Lambda^2}{Q^2} f_1 \left( 1 - \frac{\Lambda^2}{Q^2} \right) \\
& + \ \frac{\Lambda^2}{Q^2} \ln \frac{\Lambda^2}{Q^2}.
\end{aligned}
\tag{7.12}
$$

The terms in curly brackets are non-perturbative OPE-like terms in the $Q^2 > \Lambda^2$ region, and of the form of a modified non-perturbative term in the $Q^2 < \Lambda^2$ region. Explicitly the OPE has the form of an expansion in powers of $(\Lambda^2/Q^2)$, with a leading term $\mathcal{O}(\Lambda^2/Q^2)$, whereas the modified expansion

proposed in Chapter 5 is an expansion in powers of $Q^2/\Lambda^2$ with the leading term potentially a constant. No such constant is allowed in the OPE because non-perturbative terms have to vanish as $Q^2 \longrightarrow \infty$, in order to satisfy asymptotic freedom.

Note that such a constant is present in the curly bracket of the $Q^2 < \Lambda^2$ expression in Eq. (7.12). As $Q^2 \longrightarrow 0$ this tends to the limit $-1$. The terms involving $\Lambda^2/Q^2$ in the remaining part of the expression are singular as $Q^2 \longrightarrow 0$, but this will be cancelled by a singularity in the $f_1$ term. The remaining part of the expression freezes to the limit 1, ensuring that overall $F_+^{(1)}(Q^2) \sim \mathcal{O}(a(Q^2))$ freezes to $F_+^{(1)}(0) = 0$.

The idea is that compensating OPE or modified expansion terms should be added in the two $Q^2$ regions to ensure that the *same* function of $Q^2$ is obtained in the two regions. In the present case the compensating term is that in the square bracket in Eq. (7.11). It is a non-perturbative OPE term in the $Q^2 > \Lambda^2$ region, and so can be simply added and subtracted again inside the curly bracket. The non-perturbative contribution to be added to $F_\pm^{(n)}(Q^2)$, which we denote by $\bar{F}_\pm^{(n)}(Q^2)$, is then chosen to be minus the term in the curly bracket

$$\bar{F}_+^{(1)}(Q^2) \;=\; -\frac{\Lambda^2}{Q^2}\ln\left(1 - \frac{\Lambda^2}{Q^2}\right) + \frac{\Lambda^2}{Q^2}\ln\frac{\Lambda^2}{Q^2} \;\;(Q^2 > \Lambda^2), \quad (7.13)$$

$$\bar{F}_+^{(1)}(Q^2) \;=\; -\frac{\Lambda^2}{Q^2}\ln\left(1 - \frac{Q^2}{\Lambda^2}\right) \qquad (Q^2 < \Lambda^2). \quad (7.14)$$

Note that up to an $\pm i\pi$ term (reflecting the Landau cut), the same function is obtained in both $Q^2$ regions. Combining this non-perturbative component with the perturbative component, leads to a single function at all $Q^2$, $F_\pm^{*(n)}(Q^2) \equiv F_\pm^{(n)}(Q^2) + \bar{F}_\pm^{(n)}(Q^2)$, which is a holomorphic function, with all derivatives finite and continuous in the whole $Q^2$ plane. Discarding the curly brackets in Eqs. (7.11,7.12) we find

$$F_+^{*(1)}(Q^2) = \gamma_{\rm E}\frac{\Lambda^2}{Q^2} + \frac{\Lambda^2}{Q^2}f_1\left(1 - \frac{\Lambda^2}{Q^2}\right) + \frac{\Lambda^2}{Q^2}\ln\frac{\Lambda^2}{Q^2}. \quad (7.15)$$

In effect, the non-analyticity of the perturbative component is cancelled exactly by the non-analyticity of the non-perturbative component. This results in a perturbative + non-perturbative expression which exhibits the necessary analytic properties which the observables must have, and which were the basis for the criticism of the work in [31] found in [63].

Using similar rearrangements we can now obtain the remaining expressions for $n = 1, 2$. For $Q^2 > \Lambda^2$ we have

$$F_+^{(2)}(Q^2) = \left\{ \left(\frac{\Lambda^2}{Q^2}\right)^2 \ln\left(2\left(1 - \frac{\Lambda^2}{Q^2}\right)\right) + \frac{\Lambda^2}{Q^2} - \left(\frac{\Lambda^2}{Q^2}\right)^2 \ln\frac{\Lambda^2}{Q^2} - \ln 2\left(\frac{\Lambda^2}{Q^2}\right)^2 \right\}$$
$$+ \gamma_{\text{E}}\left(\frac{\Lambda^2}{Q^2}\right)^2 + \left(\frac{\Lambda^2}{Q^2}\right)^2 f_2\left(1 - \frac{\Lambda^2}{Q^2}\right)$$
$$+ \left[ -\frac{\Lambda^2}{Q^2} + \left(\frac{\Lambda^2}{Q^2}\right)^2 \ln\frac{\Lambda^2}{Q^2} + \left(\frac{\Lambda^2}{Q^2}\right)^2 \ln 2 \right], \tag{7.16}$$

and for the region $Q^2 < \Lambda^2$

$$F_+^{(2)}(Q^2) = \left\{ \left(\frac{\Lambda^2}{Q^2}\right)^2 \ln\left(2\left(1 - \frac{Q^2}{\Lambda^2}\right)\right) + \frac{\Lambda^2}{Q^2} - \ln 2\left(\frac{\Lambda^2}{Q^2}\right)^2 \right\}$$
$$+ \gamma_{\text{E}}\left(\frac{\Lambda^2}{Q^2}\right)^2 + \left(\frac{\Lambda^2}{Q^2}\right)^2 f_2\left(1 - \frac{\Lambda^2}{Q^2}\right)$$
$$- \frac{\Lambda^2}{Q^2} + \left(\frac{\Lambda^2}{Q^2}\right)^2 \ln\frac{\Lambda^2}{Q^2} + \left(\frac{\Lambda^2}{Q^2}\right)^2 \ln 2, \tag{7.17}$$

The non-perturbative terms that need to be added to $F_+^{(2)}(Q^2)$ are

$$\bar{F}_+^{(2)}(Q^2) = -\left(\frac{\Lambda^2}{Q^2}\right)^2 \ln\left(2\left(1 - \frac{\Lambda^2}{Q^2}\right)\right) - \frac{\Lambda^2}{Q^2}$$
$$+ \left(\frac{\Lambda^2}{Q^2}\right)^2 \ln\frac{\Lambda^2}{Q^2} + \left(\frac{\Lambda^2}{Q^2}\right)^2 \ln 2, \quad (Q^2 > \Lambda^2), \tag{7.18}$$
$$\bar{F}_+^{(2)}(Q^2) = -\left(\frac{\Lambda^2}{Q^2}\right)^2 \ln\left(2\left(1 - \frac{Q^2}{\Lambda^2}\right)\right) - \frac{\Lambda^2}{Q^2} + \left(\frac{\Lambda^2}{Q^2}\right)^2 \ln 2, \quad (Q^2 < \Lambda^2). \tag{7.19}$$

One then finds the holomorphic function

$$F_+^{*(2)}(Q^2) = (\gamma_{\text{E}} + \ln 2)\left(\frac{\Lambda^2}{Q^2}\right)^2 + \left(\frac{\Lambda^2}{Q^2}\right)^2 f_2\left(1 - \frac{\Lambda^2}{Q^2}\right) - \frac{\Lambda^2}{Q^2} + \left(\frac{\Lambda^2}{Q^2}\right)^2 \ln\frac{\Lambda^2}{Q^2}. \tag{7.20}$$

Finally we consider the expressions for $F_-^{(1),(2)}$. For $Q^2 > \Lambda^2$ we find

$$F_-^{(1)}(Q^2) = \left\{ \frac{Q^2}{\Lambda^2} \ln\left(1 - \frac{\Lambda^2}{Q^2}\right) + 1 \right\} + \gamma_{\text{E}}\frac{Q^2}{\Lambda^2} + \frac{Q^2}{\Lambda^2} f_1\left(1 - \frac{Q^2}{\Lambda^2}\right) + \frac{Q^2}{\Lambda^2} \ln\frac{Q^2}{\Lambda^2} - 1. \tag{7.21}$$

and for the region $Q^2 < \Lambda^2$

$$
\begin{aligned}
F_-^{(1)}(Q^2) & = \left\{ \frac{Q^2}{\Lambda^2} \ln\left(1 - \frac{Q^2}{\Lambda^2}\right) + 1 - \frac{Q^2}{\Lambda^2} \ln\frac{Q^2}{\Lambda^2} \right\} + \gamma_{\text{E}} \frac{Q^2}{\Lambda^2} \\
& + \frac{Q^2}{\Lambda^2} f_1\left(1 - \frac{Q^2}{\Lambda^2}\right) + \left[\frac{Q^2}{\Lambda^2} \ln\frac{Q^2}{\Lambda^2} - 1\right].
\end{aligned} \tag{7.22}
$$

The non-perturbative terms that need to be added to $F_-^{(1)}(Q^2)$ are

$$
\bar{F}_-^{(1)}(Q^2) = -\frac{Q^2}{\Lambda^2} \ln\left(1 - \frac{\Lambda^2}{Q^2}\right) - 1 \quad (Q^2 > \Lambda^2), \tag{7.23}
$$

$$
\bar{F}_-^{(1)}(Q^2) = -\frac{Q^2}{\Lambda^2} \ln\left(1 - \frac{Q^2}{\Lambda^2}\right) - 1 + \frac{Q^2}{\Lambda^2} \ln\frac{Q^2}{\Lambda^2} \quad (Q^2 < \Lambda^2). \tag{7.24}
$$

One then finds the holomorphic function

$$
F_-^{*(1)}(Q^2) = \gamma_{\text{E}} \frac{Q^2}{\Lambda^2} + \frac{Q^2}{\Lambda^2} f_1\left(1 - \frac{Q^2}{\Lambda^2}\right) + \frac{Q^2}{\Lambda^2} \ln\frac{Q^2}{\Lambda^2} - 1. \tag{7.25}
$$

For $F_-^{(2)}(Q^2)$ in the region $Q^2 > \Lambda^2$ one has

$$
\begin{aligned}
F_-^{(2)}(Q^2) & = \left\{ \left(\frac{Q^2}{\Lambda^2}\right)^2 \ln\left(2\left(1 - \frac{\Lambda^2}{Q^2}\right)\right) + \frac{Q^2}{\Lambda^2} + \frac{1}{2} - \left(\frac{Q^2}{\Lambda^2}\right)^2 \ln 2 \right\} \\
& - \frac{Q^2}{\Lambda^2} + \left(\frac{Q^2}{\Lambda^2}\right)^2 \ln 2 - \frac{1}{2} + \gamma_{\text{E}} \left(\frac{Q^2}{\Lambda^2}\right)^2 \\
& + \left(\frac{Q^2}{\Lambda^2}\right)^2 f_2\left(1 - \frac{Q^2}{\Lambda^2}\right) + \left(\frac{Q^2}{\Lambda^2}\right)^2 \ln\frac{Q^2}{\Lambda^2},
\end{aligned} \tag{7.26}
$$

and for the region $Q^2 < \Lambda^2$

$$
F_-^{(2)}(Q^2) = \left\{ \left(\frac{Q^2}{\Lambda^2}\right)^2 \ln\left(2\left(1 - \frac{Q^2}{\Lambda^2}\right)\right) + \frac{1}{2} - \left(\frac{Q^2}{\Lambda^2}\right)^2 \ln\frac{Q^2}{\Lambda^2} + \frac{Q^2}{\Lambda^2} - \left(\frac{Q^2}{\Lambda^2}\right)^2 \ln 2 \right\}
$$

$$
+ \left[-\frac{Q^2}{\Lambda^2} + \left(\frac{Q^2}{\Lambda^2}\right)^2 \ln 2 - \frac{1}{2} + \left(\frac{Q^2}{\Lambda^2}\right)^2 \ln\frac{Q^2}{\Lambda^2}\right] + \gamma_{\text{E}} \left(\frac{Q^2}{\Lambda^2}\right)^2 + \left(\frac{Q^2}{\Lambda^2}\right)^2 f_2\left(1 - \frac{Q^2}{\Lambda^2}\right).
$$

$$
\tag{7.27}
$$

The non-perturbative terms that need to be added to $F_-^{(2)}(Q^2)$ are

$$
\bar{F}_-^{(2)}(Q^2) \;=\; -\left(\frac{Q^2}{\Lambda^2}\right)^2 \ln\left(2\left(1 - \frac{\Lambda^2}{Q^2}\right)\right) - \frac{Q^2}{\Lambda^2} + \left(\frac{Q^2}{\Lambda^2}\right)^2 \ln 2 - \frac{1}{2}, \;\; (Q^2 > \Lambda^2),
$$
(7.28)

$$
\begin{aligned}
\bar{F}_-^{(2)}(Q^2) \;=\;& -\left(\frac{Q^2}{\Lambda^2}\right)^2 \ln\left(2\left(1 - \frac{Q^2}{\Lambda^2}\right)\right) - \frac{Q^2}{\Lambda^2} + \left(\frac{Q^2}{\Lambda^2}\right)^2 \ln 2 \\
& + \left(\frac{Q^2}{\Lambda^2}\right)^2 \ln \frac{Q^2}{\Lambda^2} - \frac{1}{2}, \;\; (Q^2 < \Lambda^2).
\end{aligned}
$$
(7.29)

The resulting holomorphic function is

$$
F_-^{*(2)}(Q^2) = -\frac{1}{2} + (\gamma_{\mathrm{E}} + \ln 2)\left(\frac{Q^2}{\Lambda^2}\right)^2 + \left(\frac{Q^2}{\Lambda^2}\right)^2 f_2\left(1 - \frac{Q^2}{\Lambda^2}\right) - \frac{Q^2}{\Lambda^2} + \left(\frac{Q^2}{\Lambda^2}\right)^2 \ln \frac{Q^2}{\Lambda^2}.
$$
(7.30)

This completes the evaluation of the $n = 1, 2$ functions required for the sum rules $K_{pBJ}$ and $U_{uBJ}$.

In terms of the $F_\pm^{(1),(2)}(Q^2)$ we have

$$
K_{PT}^{(L)}(Q^2) \;=\; \frac{1}{9b}[16 F_+^{(1)}(Q^2) - 10 F_+^{(2)}(Q^2) - 8 F_-^{(1)}(Q^2) + 2 F_-^{(2)}(Q^2)],
$$
(7.31)

$$
U_{PT}^{(L)}(Q^2) \;=\; \frac{1}{3b}[8 F_+^{(1)}(Q^2) - 6 F_+^{(2)}(Q^2) - 2 F_-^{(2)}(Q^2)].
$$
(7.32)

The non-perturbative (NP) components to be added to obtain full analyticity are

$$
\bar{K}_{NP}^{(L)}(Q^2) \;=\; \frac{1}{9b}[16 \bar{F}_+^{(1)}(Q^2) - 10 \bar{F}_+^{(2)}(Q^2) - 8 \bar{F}_-^{(1)}(Q^2) + 2 \bar{F}_-^{(2)}(Q^2)],
$$
(7.33)

$$
\bar{U}_{NP}^{(L)}(Q^2) \;=\; \frac{1}{3b}[8 \bar{F}_+^{(1)}(Q^2) - 6 \bar{F}_+^{(2)}(Q^2) - 2 \bar{F}_-^{(2)}(Q^2)].
$$
(7.34)

Adding the perturbative and non-perturbative components together gives the fully analytic functions $K^{*(L)}(Q^2)$ and $U^{*(L)}(Q^2)$. These functions are simply the original leading-$b$ perturbative form of the observables, plus a non-perturbative term, the exact form of which is determined by the analyticity constraint. In effect, we use this constraint to determine the form of the non-perturbative terms.

## 7.3  FREEZING AND LANDAU POLE BEHAVIOUR OF THE FULLY ANALYTIC FORM OF $\mathcal{K}$ AND $\mathcal{U}$

From Eqs. (7.14,7.19,7.24,7.29), one can read off the infrared freezing limits of the non-perturbative component. One finds

$$\bar{F}_+^{(1)}(0) \;=\; 1, \;\; \bar{F}_+^{(2)}(0) = \frac{1}{2}, \tag{7.35}$$

$$\bar{F}_-^{(1)}(0) \;=\; -1, \;\; \bar{F}_-^{(2)}(0) = -\frac{1}{2}. \tag{7.36}$$

Since the perturbative component freezes to zero as $Q^2 \longrightarrow 0$, the freezing limits of the analytic functions are found to be

$$K^{*(L)}(0) \;=\; \frac{1}{9b}\left[16 - 5 + 8 - 1\right] = \frac{2}{b}, \tag{7.37}$$

$$U^{*(L)}(0) \;=\; \frac{1}{3b}\left[8 - 3 + 1\right] = \frac{2}{b}. \tag{7.38}$$

Remarkably, one finds the *same* freezing limit for $K(Q^2)$ and $U(Q^2)$, even though different UV and IR renormalon residues are involved. This suggests the existence of yet another relation between UV and IR residues. The sum is required to vanish to screen the Landau pole, and the weighted sum is 2 in each case. It is interesting that $\frac{2}{b}$ is also the freezing limit found in the Analytic Perturbation Theory (APT) approach of Shirkov and collaborators [64]. This connection will be discussed further later in the Chapter.

We can also find the values of the analytic functions at $Q^2 = \Lambda^2$. From Eqs. (7.15,7.20,7.25,7.30) one finds

$$F_+^{*(1)}(\Lambda^2) \;=\; \gamma_{\mathrm{E}}, \tag{7.39}$$

$$F_+^{*(2)}(\Lambda^2) \;=\; \gamma_{\mathrm{E}} + \ln 2 - 1, \tag{7.40}$$

$$F_-^{*(1)}(\Lambda^2) \;=\; \gamma_{\mathrm{E}} - 1, \tag{7.41}$$

$$F_-^{*(2)}(\Lambda^2) \;=\; \gamma_{\mathrm{E}} + \ln 2 - \frac{3}{2}. \tag{7.42}$$

Assembling these results gives

$$K^{*(L)}(\Lambda^2) \;=\; \frac{(-8\ln 2 + 15)}{9b}, \tag{7.43}$$

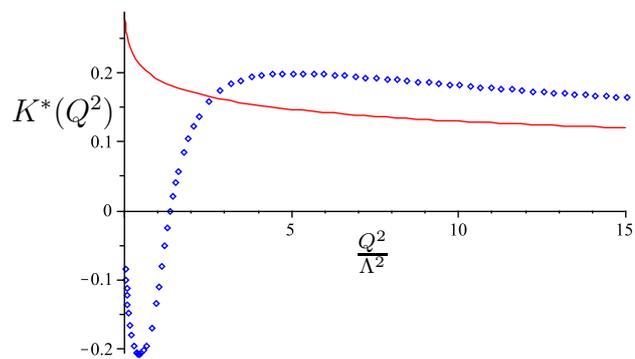$$U^{*(L)}(\Lambda^2) \;=\; \frac{(-8\ln 2 + 9)}{3b}. \tag{7.44}$$

Figure 7.1: Combination of Perturbative and Non-Perturbative Part of Polarised Bjorken Sum Rule $K^*(Q^2)$ versus $\frac{Q^2}{\Lambda^2}$
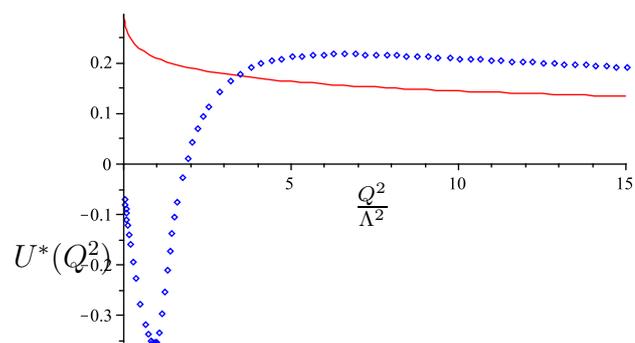


Figure 7.2: Combination of Perturbative and Non-Perturbative Part of Un-Polarised Bjorken Sum Rule $U^*(Q^2)$ versus $\frac{Q^2}{\Lambda^2}$

The $\ln 2$ pieces correspond to the results found in Chapter 5, and are shifted by the extra terms added to achieve full analyticity.

We plot in Fig(7.1) and Fig(7.2) the analytic functions $K^{*(L)}(Q^2)$ and $U^{*(L)}(Q^2)$ (solid line), and for comparison the piecewise analytic functions $K_{PT}^{(L)}(Q^2)$ and $U_{PT}^{(L)}(Q^2)$ (dashed line), as in Chapter 5, we assume $N_f = 0$ active quark flavours. As it has been discussed that this is the minimal model, this is the reason why Fig(7.1) and Fig(7.2) disagree at high $Q^2$ despite we change numerous parameters significantly, the disagreement will still be significant. A solution to this problem is to introduce another non-perturbative terms but some questions that remain will be what and why?

## 7.4 THE ADLER D FUNCTION

For the Adler D function, one has an infinite sum (of renormalon singularities) over $n$, and so to consider its freezing behaviour one needs a general result for $F_{\pm}^{(n)}(Q^2)$. We find the holomorphic functions

$$
\begin{aligned}
F_+^{*(n)}(Q^2) &= -\sum_{k=1}^{n-1} \frac{1}{k}\left(\frac{\Lambda^2}{Q^2}\right)^{n-k} + \ln n \left(\frac{\Lambda^2}{Q^2}\right)^n + \gamma_{\mathrm{E}}\left(\frac{\Lambda^2}{Q^2}\right)^n \\
&+ \left(\frac{\Lambda^2}{Q^2}\right)^n f_n\left(1 - \frac{\Lambda^2}{Q^2}\right) + \left(\frac{\Lambda^2}{Q^2}\right)^n \ln \frac{\Lambda^2}{Q^2}, \quad (7.45)
\end{aligned}
$$

$$
\begin{aligned}
F_-^{*(n)}(Q^2) &= -\sum_{k=1}^{n} \frac{1}{k}\left(\frac{Q^2}{\Lambda^2}\right)^{n-k} + \ln n \left(\frac{Q^2}{\Lambda^2}\right)^n + \gamma_{\mathrm{E}}\left(\frac{Q^2}{\Lambda^2}\right)^n \\
&+ \left(\frac{Q^2}{\Lambda^2}\right)^n f_n\left(1 - \frac{Q^2}{\Lambda^2}\right) + \left(\frac{Q^2}{\Lambda^2}\right)^n \ln \frac{Q^2}{\Lambda^2}. \quad (7.46)
\end{aligned}
$$

The non-perturbative terms that need to be added to $F_+^{(n)}(Q^2)$ are for $Q^2 > \Lambda^2$

$$
\begin{aligned}
\bar{F}_+^{(n)}(Q^2) &= -\left(\frac{\Lambda^2}{Q^2}\right)^n \ln\left(n\left(1 - \frac{\Lambda^2}{Q^2}\right)\right) - \sum_{k=1}^{n-1} \frac{1}{k}\left(\frac{\Lambda^2}{Q^2}\right)^{n-k} + \left(\frac{\Lambda^2}{Q^2}\right)^n \ln \frac{\Lambda^2}{Q^2} \\
&+ \ln n \left(\frac{\Lambda^2}{Q^2}\right)^n, \quad (7.47)
\end{aligned}
$$

and for $Q^2 < \Lambda^2$,

$$
\bar{F}_+^{(n)}(Q^2) = -\left(\frac{\Lambda^2}{Q^2}\right)^n \ln\left(n\left(1 - \frac{Q^2}{\Lambda^2}\right)\right) - \sum_{k=1}^{n-1} \frac{1}{k}\left(\frac{\Lambda^2}{Q^2}\right)^{n-k} + \ln n \left(\frac{\Lambda^2}{Q^2}\right)^n. \quad (7.48)
$$

For $F_-^{(n)}(Q^2)$ in the region $Q^2 > \Lambda^2$ the NP terms to be added are

$$\bar{F}_-^{(n)}(Q^2) = -\left(\frac{Q^2}{\Lambda^2}\right)^n \ln\left(n\left(1 - \frac{\Lambda^2}{Q^2}\right)\right) - \sum_{k=1}^{n} \frac{1}{k}\left(\frac{Q^2}{\Lambda^2}\right)^{n-k} + \ln n\left(\frac{Q^2}{\Lambda^2}\right)^n,$$

$$(7.49)$$

and for $Q^2 < \Lambda^2$

$$\begin{aligned}
\bar{F}_-^{(n)}(Q^2 &= -\left(\frac{Q^2}{\Lambda^2}\right)^n \ln\left(n\left(1 - \frac{Q^2}{\Lambda^2}\right)\right) - \sum_{k=1}^{n} \frac{1}{k}\left(\frac{Q^2}{\Lambda^2}\right)^{n-k} + \ln n\left(\frac{Q^2}{\Lambda^2}\right)^n \\
&\quad + \left(\frac{Q^2}{\Lambda^2}\right)^n \ln\frac{Q^2}{\Lambda^2}.
\end{aligned}$$

$$(7.50)$$

$D_{\mathrm{PT}}^{(L)}(Q^2)$ in terms of the $F_\pm^{(n)}(Q^2)$ is given by

$$\begin{aligned}
D_{\mathrm{PT}}^{(L)}(Q^2) &= \sum_{n=1}^{\infty} z_n \left\{ F_-^{(n)}(Q^2)\left[\frac{z_n}{a(Q^2)}\left(A_0(n) - z_n A_1(n)\right) - z_n A_1(n)\right] \right. \\
&\qquad\qquad \left. + \left(A_0(n) - z_n A_1(n)\right) \right\} \\
&\quad + \sum_{n=1}^{\infty} z_n \left\{ F_+^{(n)}(Q^2)\left[\frac{z_n}{a(Q^2)}\left(B_0(n) + z_n B_1(n)\right) - z_n B_1(n)\right] \right. \\
&\qquad\qquad \left. - \left(B_0(n) + z_n B_1(n)\right) \right\}.
\end{aligned}$$

$$(7.51)$$

The non-perturbative component which needs to be added for analyticity is

$$\begin{aligned}
\bar{D}_{\mathrm{NP}}^{(L)}(Q^2) &= \sum_{n=1}^{\infty} z_n \left\{ \bar{F}_-^{(n)}(Q^2)\left[\frac{z_n}{a(Q^2)}\left(A_0(n) - z_n A_1(n)\right) - z_n A_1(n)\right] \right\} \\
&\quad + \sum_{n=1}^{\infty} z_n \left\{ \bar{F}_+^{(n)}(Q^2)\left[\frac{z_n}{a(Q^2)}\left(B_0(n) + z_n B_1(n)\right) - z_n B_1(n)\right] \right\}.
\end{aligned}$$

$$(7.52)$$

Nevertheless, adding such a non-perturbative term will definitely lead to an infinite freezing limit, this is due to the $1/a(Q^2)$ term which diverges to $\infty$ as $Q^2$ goes to 0. However, we shall show in Section 7.7 that one can define the non-perturbative $\bar{F}_\pm^{(n)}$ functions for a renormalon with a single pole Borel singularity as a differential operator involving $D \equiv \frac{d}{d\tau}$ acting on the coupling

$a(\tau) = \frac{1}{\tau}$. For the Adler $D$-function one has double poles in the Borel plane and hence needs to act with the square of this operator. In this way one finds a different $\bar{\bar{F}}_+^n(Q^2)$ non-perturbative term for $Q^2 > \Lambda^2$

$$
\begin{aligned}
\bar{\bar{F}}_+^{(n)}(Q^2) \;=\; & -n\left(\frac{\Lambda^2}{Q^2}\right)^n \\
& \times \left[L_2\left(1 - \frac{\Lambda^2}{Q^2}\right) - \frac{\pi^2}{3} - \sum_{k=1}^{n-1}\left(\frac{1}{k^2}\left(\frac{\Lambda^2}{Q^2}\right)^{n-k}\right) - \frac{1}{2}\left(\frac{\Lambda^2}{Q^2}\right)^n \ln\left(\frac{\Lambda^2}{Q^2}\right)^2\right],
\end{aligned}
$$
(7.53)

Here $L_2$ denotes a dilogarithm (see Eq. (5.40) for the definition), and for $Q^2 < \Lambda^2$

$$
\bar{\bar{F}}_+^{(n)}(Q^2) = n\left(\frac{\Lambda^2}{Q^2}\right)^n \left[L_2\left(1 - \frac{Q^2}{\Lambda^2}\right) - \sum_{k=1}^{n-1}\left(\frac{1}{k^2}\left(\frac{\Lambda^2}{Q^2}\right)^{n-k}\right)\right].
$$
(7.54)

The other two analogous $(-)$ equations, for $Q^2 > \Lambda^2$ are

$$
\bar{\bar{F}}_-^{(n)}(Q^2) = -n\left(\frac{Q^2}{\Lambda^2}\right)^n \left[L_2\left(1 - \frac{\Lambda^2}{Q^2}\right) + \sum_{k=1}^{n}\left(\frac{1}{k^2}\left(\frac{Q^2}{\Lambda^2}\right)^{n-k}\right)\right],
$$
(7.55)

and for $Q^2 < \Lambda^2$

$$
\begin{aligned}
\bar{\bar{F}}_-^{(n)}(Q^2) \;=\; & -n\left(\frac{Q^2}{\Lambda^2}\right)^n \\
& \times \left[L_2\left(1 - \frac{Q^2}{\Lambda^2}\right) - \frac{\pi^2}{3} + \sum_{k=1}^{n}\left(\frac{1}{k^2}\left(\frac{Q^2}{\Lambda^2}\right)^{n-k}\right) + \frac{1}{2}\left(\frac{Q^2}{\Lambda^2}\right)^n \ln\left(\frac{Q^2}{\Lambda^2}\right)^2\right].
\end{aligned}
$$
(7.56)

Using these new double pole non-perturbative terms, we modify the $\bar{D}_{\mathrm{NP}}^{(L)}(Q^2)$ such that

$$
\begin{aligned}
\bar{D}_{\mathrm{NP}}^{(L)}(Q^2) \;\; = \;\; & \sum_{n=1}^{k} \left[ \bar{\bar{F}}_{-}^{n}(Q^2) z_n \left( A_0 n - z_n A_1(n) \right) - \bar{F}_{-}^{n}(Q^2) z_n \left( z_n A_1(n) \right) \right] \\
& + \sum_{n=3}^{k+2} \left[ \bar{\bar{F}}_{+}^{n}(Q^2) z_n \left( B_0 n + z_n B_1(n) \right) - \bar{F}_{+}^{n}(Q^2) z_n \left( z_n B_1(n) \right) \right] \\
& - \;\; \bar{F}_{+}^{(2)}(Q^2) \left( \frac{4}{b} \right)^2 \left( -\frac{1}{4} \right).
\end{aligned}
\tag{7.57}
$$

To match our calculation in Chapter 6, we truncate Eq. (7.57) at $k = 15$.

Adding the above perturbative and non-perturbative components gives the analytic function $D^{*(L)}(Q^2)$. The infrared freezing limit of the non-perturbative component is given by

$$
\bar{F}_{+}^{(n)}(0) = \frac{1}{n}, \;\; \bar{F}_{-}^{(n)}(0) = -\frac{1}{n}, \bar{\bar{F}}_{+}^{(n)}(0) = \frac{1}{n^2}, \;\; \bar{\bar{F}}_{-}^{(n)}(0) = -\frac{1}{n^2}, \tag{7.58}
$$

which is consistent with Eqs. (7.35,7.36). One then finds the freezing limit for the analytic function $D^{*(L)}(Q^2)$

$$
\begin{aligned}
D^{*(L)}(0) &= \sum_{n=1}^{k} \left[ -\left(\frac{1}{n^2}\right) z_n \left(A_0 n - z_n A_1(n)\right) + \left(\frac{1}{n}\right) z_n \left(z_n A_1(n)\right) \right] \\
&+ \sum_{n=3}^{k+2} \left[ \left(\frac{1}{n^2}\right) z_n \left(B_0 n + z_n B_1(n)\right) - \left(\frac{1}{n}\right) z_n \left(z_n B_1(n)\right) \right] \\
&- \left(\frac{1}{2}\right) \left(\frac{4}{b}\right)^2 \left(-\frac{1}{4}\right) = \frac{2}{b}.
\end{aligned}
\tag{7.59}
$$

This freezing limit is absolutely amazing and it agrees with the APT version of analytic perturbation theory provided by Shirkov and collaborators [64] which we will touch on in Section 7.8. This matches the predictions with $K(Q^2)$ and $U(Q^2)$ which both also freeze to a $2/b$ limit. In fact we shall show that our $D$-operator construction of the $\bar{F}$ and $\bar{\bar{F}}$, is equivalent to an all-orders resummation of Shirkov's APT series.

We now plot the analytic function $D^{*(L)}(Q^2)$ in Fig. (7.3) and the non-perturbative part defined by $K_{NP}(Q^2)$, $U_{NP}(Q^2)$ and $D_{NP}(Q^2)$ in Fig. (7.4). We will assume $N_f = 0$ in our plots.

One can generalize the $Q^2 = \Lambda^2$ values of the components into Eqs. (7.39-7.42),

$$
F_+^{*(n)}(\Lambda^2) = \gamma_{\mathrm{E}} + \ln n - \sum_{k=1}^{n-1} \frac{1}{k},
\tag{7.60}
$$

$$
F_-^{*(n)}(\Lambda^2) = \gamma_{\mathrm{E}} + \ln n - \sum_{k=1}^{n} \frac{1}{k}.
\tag{7.61}
$$

Substituting these results in Eq. (7.51) and Eq. (7.57) one finds

$$
D^{*(L)}(\Lambda^2) \approx \frac{(0.679938 + 0.121342)}{b}.
\tag{7.62}
$$

The first term in the numerator is the result found in [31], this is shifted by the extra terms required for analyticity.

We have shown that it is possible to add non-perturbative terms to the piecewise analytic one-chain skeleton expansion result in the regions $Q^2 > \Lambda^2$ and $Q^2 < \Lambda^2$, such that when combined, an analytic function of $Q^2$ results. Although both perturbative and non-perturbative components are
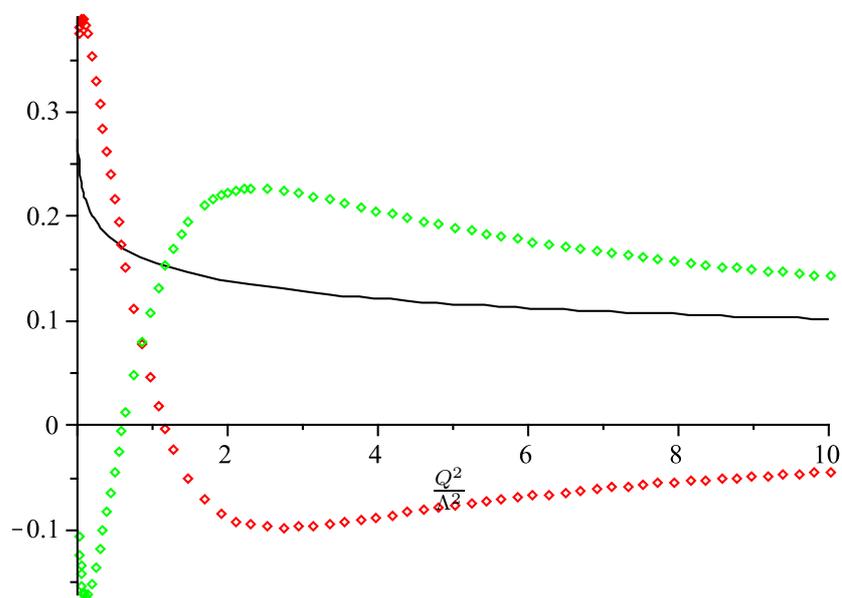
Figure 7.3: $D^{*(L)}(Q^2)$ (solid line), $D_{PT}(Q^2)$ (green dots) and $D_{NP}(Q^2)$ (red dots) against$\frac{Q^2}{\Lambda^2}$
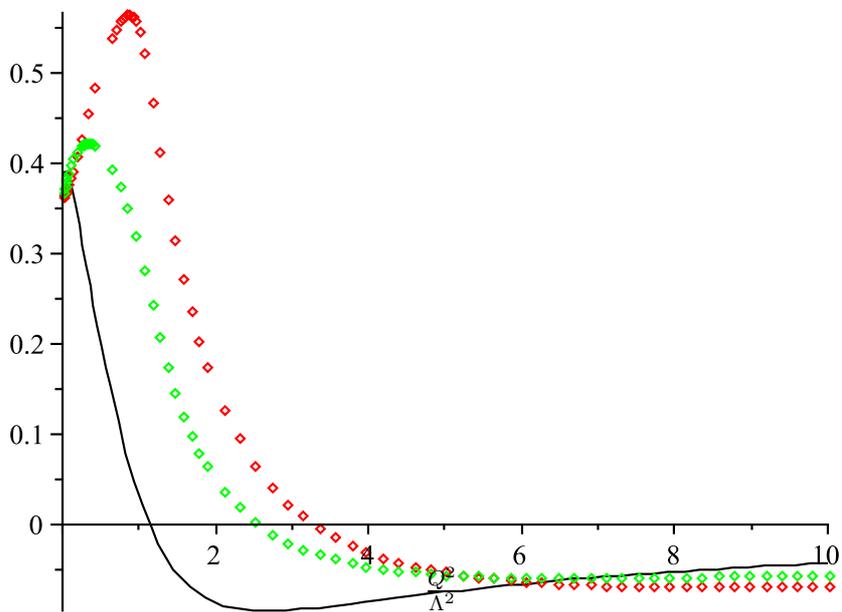


Figure 7.4: Non-perturbative terms - $K_{NP}(Q^2)$ (green dots), $U_{NP}(Q^2)$ (red dots) and $D_{NP}(Q^2)$ (solid line) against $\frac{Q^2}{\Lambda^2}$

only piecewise analytic functions, their sum is fully analytic. The non-perturbative terms to be added are constrained by requiring asymptotic freedom as $Q^2 \longrightarrow \infty$, and finite freezing behaviour as $Q^2 \longrightarrow 0$. Of course, one can always add additional analytic and asymptotically free non-perturbative contributions to the fully analytic function. Hence, the non-perturbative contribution we have derived here may be subject to further corrections. Crucially however, we have demonstrated that the remarkable freezing and Landau pole behaviour of the leading-$b$ expressions discovered in [31], is compatible with the necessary analyticity requirements of QFT, which were expounded by the authors of [63].

## 7.5 The GDH Sum Rule and freezing behaviour of $K_{pBj}(Q^2)$

In this section, we consider the exact low-energy Gerasimov-Drell-Hearn (GDH) Sum Rule which can be related to the $K_{pBj}(Q^2)$ polarized Bjorken DIS sum rule. We shall show that it is possible to add an extra holomorphic non-perturbative function to $K^{*(L)}(Q^2)$ in such a way that the GDH Sum Rule is satisfied. [65] Consider the $Q^2$-dependent integral

$$I_1(Q^2) = \frac{2M^2}{Q^2} \int_0^1 g_1(x, Q^2) \, dx. \qquad (7.63)$$

This is define for all $Q^2$ with $g_1(x, Q^2)$ being the generalization for all $Q^2$ of $g_1(x)$. Note that $g_1(x)$ is the standard scale-invariant structure function independent of $Q^2$. We ignore elastic contribution at $x = 1$ to the sum rule. We define $x = Q^2/2M\nu$ and making the relevant change of variable, one recovers the integral over all energies of spin-dependent photon-nucleon cross section $Q^2 = 0$, whose value is given in [66, 67]. Here $M$ is the nucleon mass and $\nu$ is the energy transfer. The low energy GDH sum rule is

$$I_1(0) = \frac{-\mu_A^2}{4}, \qquad (7.64)$$

where $\mu_A$ is the nucleon anomalous magnetic moment in units of nuclear magnetons [68]. [69] For the polarized Bjorken Sum Rule [70], we have

$$\begin{aligned} K_{pBj}(Q^2) &\equiv \int_0^1 g_1^{ep-en}(x, Q^2) dx \\ &= \frac{1}{6} \left| \frac{g_A}{g_V} \right| \left( 1 - \frac{3}{4} C_F K(Q^2) \right), \end{aligned} \qquad (7.65)$$

with the spin-dependent proton and neutron structure functions $g_1^{ep}$, $g_1^{en}$. $g_A = 1.267 \pm 0.004$ is the nucleon axial charge obtained from the neutron $\beta$-decay. We would then expect that as $Q^2 \longrightarrow 0$

$$\frac{2M^2}{Q^2} K_{pBj}(Q^2) \longrightarrow \frac{(\mu_{A,n}^2 - \mu_{A,p}^2)}{4}. \tag{7.66}$$

Here $\mu_{A,n}$ and $\mu_{A,p}$ are, respectively, the anomalous magnetic moments of the neutron and proton in units of nuclear magnetons. It is immediately obvious that the freezing behaviour of $K^{*(L)}(Q^2)$ plotted in Fig 7.1 violates the GDH low energy sum rule expectation in Eq. (7.66). Approximating $K(Q^2)$ by $K^{*(L)}(Q^2)$ we have as $Q^2 \longrightarrow 0$

$$\frac{2M^2}{Q^2} K_{pBj}(Q^2) \approx \frac{2M^2}{Q^2} \frac{1}{6} \left| \frac{g_A}{g_V} \right| \left( 1 - \frac{2}{b} + \mathcal{O}(a(Q^2)) + \mathcal{O}(\frac{Q^2}{\Lambda^2}) \right). \tag{7.67}$$

This diverges like $Q^{-2}$ as $Q^2 \longrightarrow 0$ and a finite GDH infrared limit is not found. To satisfy the GDH Sum Rule we need to add an additional non-perturbative analytic term which cancels the constant and $\mathcal{O}(a(Q^2))$ terms in Eq. (7.63). This fixes the form of $K(Q^2)$ to be

$$K(Q^2) = K^{*(L)}(Q^2) + (1 - K^{*(L)}(Q^2))\mathcal{F}(Q^2). \tag{7.68}$$

Here $\mathcal{F}(Q^2)$ is an analytic function of $Q^2$ which for $Q^2 < \Lambda^2$ has a modified NP expansion of the form

$$\mathcal{F}(Q^2) = 1 + \lambda \frac{Q^2}{\Lambda^2} + \mathcal{O}\left( \left( \frac{Q^2}{\Lambda^2} \right)^2 \right). \tag{7.69}$$

Whilst for $Q^2 > \Lambda^2$ it admits an OPE expansion in powers of $\Lambda^2/Q^2$. One then finds the $Q^2 \longrightarrow 0$ behaviour

$$K_{pBj}(Q^2) \approx -\frac{1}{6} \left| \frac{g_A}{g_V} \right| \left( 1 - \frac{2}{b} \right) \lambda \frac{Q^2}{\Lambda^2} + \mathcal{O}\left( \left( \frac{Q^2}{\Lambda^2} \right)^2 \right). \tag{7.70}$$

Fixing the value of the coefficient $\lambda$ to be

$$\lambda = -\frac{\Lambda^2}{2M^2} 6 \left| \frac{g_V}{g_A} \right| \left( 1 - \frac{2}{b} \right)^{-1} \frac{(\mu_{A,n}^2 - \mu_{A,p}^2)}{4}, \tag{7.71}$$

the GDH Sum Rule of Eq. (7.66) will be satisfied.

## 7.6 CONFORMAL NON-PERTURBATIVE EXPANSIONS

We will need to construct analytic functions $\mathcal{F}(Q^2)$ which admit expansions in powers of $(\frac{\Lambda^2}{Q^2})$ valid for $Q^2 > \Lambda^2$ of the same form as the OPE,

$$\mathcal{F}(Q^2) = \sum_{n=1}^{\infty} \mathcal{C}_n \left(\frac{\Lambda^2}{Q^2}\right)^n. \tag{7.72}$$

For $Q^2 < \Lambda^2$ they must admit the modified expansion in powers of $(\frac{Q^2}{\Lambda^2})$,

$$\mathcal{F}(Q^2) = \sum_{n=1}^{\infty} \tilde{\mathcal{C}}_n \left(\frac{Q^2}{\Lambda^2}\right)^{n-1}, \tag{7.73}$$

where in satisfying the GDH Sum Rule we require $\tilde{\mathcal{C}}_1 = 1$. Crucially these expansions must correspond to a *single* analytic function of $Q^2$ at *all values* of $Q^2$. This can be ensured by formulating the following modified "conformal" expansions,

$$\mathcal{F}(Q^2) = \sum_{n=1}^{\infty} \hat{\mathcal{C}}_n \frac{\left(\frac{\Lambda^2}{Q^2}\right)^n}{\left(1 + \frac{\Lambda^2}{Q^2}\right)^{2n-1}} \tag{7.74}$$

$$= \sum_{n=1}^{\infty} \hat{\mathcal{C}}_n \frac{\left(\frac{Q^2}{\Lambda^2}\right)^{n-1}}{\left(1 + \frac{Q^2}{\Lambda^2}\right)^{2n-1}}. \tag{7.75}$$

Term-by-term these series are identical functions of $Q^2$ at all values of $Q^2$, and for $Q^2 < \Lambda^2$ Eq. (7.74) admits an expansion in powers of $(\frac{\Lambda^2}{Q^2})$ which must be equivalent to Eq. (7.72), whilst for $Q^2 < \Lambda^2$ Eqn(7.75) admits an expansion in powers of $(\frac{Q^2}{\Lambda^2})$ which must be equivalent to Eqn(7.73). Using the Binomial theorem and equating coefficients one finds

$$\begin{aligned}
\hat{\mathcal{C}}_1 &= \mathcal{C}_1 = \tilde{\mathcal{C}}_1 \\
\hat{\mathcal{C}}_2 &= \mathcal{C}_2 + \mathcal{C}_1 = \tilde{\mathcal{C}}_2 + \tilde{\mathcal{C}}_1. \\
&\vdots
\end{aligned} \tag{7.76}$$

From which we conclude that the coefficients in the OPE of Eqn(7.72) and the modified expansion of Eqn(7.73) are *identical*, $\mathcal{C}_n = \tilde{\mathcal{C}}_n$. The conformal expansions are essentially an Euler transformation of the original non-perturbative expansions.

We can now fix the $\hat{\mathcal{C}}_n$ coefficients in such a way that the GDH Sum Rule holds. We write

$$(1 - K(Q^2)) = 1 - K^{*(L)}(Q^2) - (1 - K^{*(L)}(Q^2))\mathcal{F}(Q^2), \qquad (7.77)$$

where the analytic function $\mathcal{F}(Q^2)$ has the conformal expansion

$$\mathcal{F}(Q^2) = \frac{1}{\left(1 + \frac{Q^2}{\Lambda^2}\right)} + \frac{\left[1 - \frac{\tilde{\mathcal{C}}_2^K}{(1 - K^{*(L)}(Q^2))}\right]\frac{Q^2}{\Lambda^2}}{\left(1 + \frac{Q^2}{\Lambda^2}\right)^3} + \frac{\left[2 - \frac{(3\tilde{\mathcal{C}}_2^K - \tilde{\mathcal{C}}_3^K)}{(1 - K^{*(L)}(Q^2))}\right]\left(\frac{Q^2}{\Lambda^2}\right)^2}{\left(1 + \frac{Q^2}{\Lambda^2}\right)^5} + \dots$$

$$(7.78)$$

We then find for $(1 - K(Q^2))$ the "conformal expansion"

$$
\begin{aligned}
(1 - K(Q^2)) &= 1 - K^{*(L)}(Q^2) - \frac{(1 - K^{*(L)}(Q^2))}{\left(1 + \frac{Q^2}{\Lambda^2}\right)} - \frac{\left[(1 - K^{*(L)}(Q^2)) - \tilde{\mathcal{C}}_2^K\right]\frac{Q^2}{\Lambda^2}}{\left(1 + \frac{Q^2}{\Lambda^2}\right)^3} \\
&+ \frac{\left[3\tilde{\mathcal{C}}_2^K + \tilde{\mathcal{C}}_3^K - 2(1 - K^{*(L)}(Q^2))\right]\left(\frac{Q^2}{\Lambda^2}\right)^2}{\left(1 + \frac{Q^2}{\Lambda^2}\right)^5} + \dots
\end{aligned}
\qquad (7.79)
$$

This expansion should be valid at all values of $Q^2$. In the infrared region $Q^2 < \Lambda^2$ as $Q^2 \longrightarrow 0$ this has the modified non-perturbative expansion

$$(1 - K(Q^2)) = \tilde{\mathcal{C}}_2^K\left(\frac{Q^2}{\Lambda^2}\right) + \tilde{\mathcal{C}}_3^K\left(\frac{Q^2}{\Lambda^2}\right)^2 + \dots, \qquad (7.80)$$

where, by construction, the coefficients are independent of $K^{*(L)}(Q^2)$. To ensure the GDH Sum Rule one needs to fix

$$\tilde{\mathcal{C}}_2^K|_{\text{GDH}} = \frac{(\mu_{A,n}^2 - \mu_{A,p}^2)}{4}\left(\frac{\Lambda^2}{2M^2}\right)6\left|\frac{g_V}{g_A}\right|. \qquad (7.81)$$

Using PDG booklet values for these quantities one finds $\tilde{\mathcal{C}}_2^K|_{\text{GDH}} \approx 0.308\frac{\Lambda^2}{\text{GeV}^2}$. For $Q^2 > \Lambda^2$, $Q^2 \longrightarrow \infty$, the result has the form of the analytized perturbative result $(1 - K^{*(L)}(Q^2))$ plus a non-perturbative OPE expansion

$$
\begin{aligned}
(1 - K(Q^2)) &= (1 - K^{*(L)}(Q^2)) - (1 - K^{*(L)}(Q^2))\left(\frac{\Lambda^2}{Q^2}\right) + \tilde{\mathcal{C}}_2^K\left(\frac{\Lambda^2}{Q^2}\right)^2 \\
&+ \tilde{\mathcal{C}}_3^K\left(\frac{\Lambda^2}{Q^2}\right)^3 + \dots
\end{aligned}
$$

$$(7.82)$$

One might be tempted to conclude that the higher OPE terms have the same coefficients as the terms in the modified non-perturbative expansion which applies in the infrared, but this would be claiming too much. The function $K^{*(L)}(Q^2)$ is the *minimal* way of combining piecewise analytic perturbative and non-perturbative components to achieve an analytic behaviour overall. As we noted earlier we can always add any additional analytic non-perturbative term $\mathcal{H}(Q^2)$, replacing $K^{*(L)}(Q^2)$ everywhere by $K^{*(L)}(Q^2) + \mathcal{H}(Q^2)$. If we assume that $\mathcal{H}(Q^2)$ admits the OPE expansion

$$\mathcal{H}(Q^2) = \sum_{n=1}^{\infty} \mathcal{H}_n \left(\frac{\Lambda^2}{Q^2}\right)^n, \tag{7.83}$$

then Eq. (7.80) still applies as $Q^2 \longrightarrow 0$, but the OPE expansion in Eq. (7.82) will be modified to

$$
\begin{aligned}
(1 - K(Q^2)) &= (1 - K^{*(L)}(Q^2)) - (1 - K^{*(L)}(Q^2) + \mathcal{H}_1)\left(\frac{\Lambda^2}{Q^2}\right) \\
&+ (\tilde{\mathcal{C}}_2^K - \mathcal{H}_2 - \mathcal{H}_1)\left(\frac{\Lambda^2}{Q^2}\right)^2 + (\tilde{\mathcal{C}}_3^K - \mathcal{H}_3 + \mathcal{H}_2)\left(\frac{\Lambda^2}{Q^2}\right)^3 + \ldots
\end{aligned}
\tag{7.84}
$$

## 7.7 THE INVERSE D OPERATOR

Consider a QCD observable $R$ having the Borel representation

$$R = \int_0^\infty dz e^{-z/a} B[R](z). \tag{7.85}$$

Here we assume as usual that $R$ has the perturbative expansion

$$R = a + r_1 a^2 + r_2 a^3 + \ldots + r_n a^{n+1} + \ldots. \tag{7.86}$$

The main result we will need is that if $B[R](z) = 1/(z - z_i)^n$ i.e. a pole in the $z$-plane, then introducing the differential operator $D \equiv \frac{d}{d\tau}$ where we assume a one loop coupling $a(\tau) = \frac{1}{\tau}$, we have the operator relation

$$R = \frac{(-1)^n}{(D \mp z_i)^n} a(\tau) . \tag{7.87}$$

So elegantly one has an inverse $D$-operator acting on the coupling. To prove this one simply writes $a(\tau) = \int_0^\infty dz e^{-z/a(\tau)}$. Noting that $e^{-z/a} = e^{-z\tau}$ we see that acting with $D^n$ pulls down a factor $(-1)^n z^n$ inside the integrand which

on integration over $z$ will reproduce the series expansion for $R$. We shall show that the functions $F_\pm^{(n)}$ involving the contributions of renormalon single poles are reproduced by the $D$-operator expression. Note that this result does not work only for poles. We have the general result $R = B[R](-D)a(\tau)$ for any Borel summable series with a one loop coupling.

The further interest is in reproducing the non-perturbative contributions $\bar{F}_\pm^{(n)}$ which need to be added to obtain an analytic result. It turns out that these can be constructed from the function $\mathcal{A}_1(Q^2)$ in Shirkov's APT formalism which will be discussed in the next section. One has the APT expansion

$$R = \mathcal{A}_1(Q^2) + r_1\mathcal{A}_2(Q^2) + \ldots + r_n\mathcal{A}_{n+1}(Q^2) + \ldots . \qquad (7.88)$$

Defining $L \equiv \ln(\frac{Q^2}{\Lambda^2})$ one has at the one loop level

$$\mathcal{A}_1(Q^2) = \frac{2}{b}\left[\frac{1}{L} + \frac{1}{(1-e^L)}\right] . \qquad (7.89)$$

The second OPE-like term regulates the Landau pole at $Q^2 = \Lambda^2$ in the first term which is simply the coupling $a(\tau)$. The $\mathcal{A}_i$ terms satisfy the beta-function like equation

$$\mathcal{A}_{k+1}(Q^2) = -\frac{1}{kb}\frac{d\mathcal{A}_k(Q^2)}{dL} . \qquad (7.90)$$

This is enough to ensure that for a simple pole contribution $B[R](z) = \frac{1}{(z\pm z_i)}$ one has

$$R = \frac{1}{z_i \pm D}\mathcal{A}_1(Q^2) . \qquad (7.91)$$

Again we note that this does not just work for poles but more generally we have the result $R = B[R](-D)\mathcal{A}_1(Q^2)$, where $\mathcal{A}_1(Q^2)$ is the one loop APT function. The $D^{-1}$ operator acting on the NP $\frac{1}{(1-e^L)}$ piece of $\mathcal{A}_1(Q^2)$ can be used to generate the non-perturbative $\bar{F}_\pm^{(n)}$ terms which need to be added to the PT $F_\pm^{(n)}$ terms arising from the $D^{-1}$ operator acting on the first term $a(\tau)$. The implication is that one can formally construct an all-orders resummation of the APT series for $R$ using this technique. Before we discuss all of this further we need to provide an introduction to the $D$-operator method for solving constant coefficient linear ODE's.

We consider linear differential equations where a general linear differential equation of order $n$ can be written in the form of

$$a_0(x)\frac{d^n y}{dx^n} + a_1(x)\frac{d^{n-1}y}{dx^{n-1}} + ... + a_{n-1}(x)\frac{dy}{dx} + a_n(x)y = R(x). \qquad (7.92)$$

If $R(x) = 0$, the resulting equation is a *homogeneous* equation and if $R(x) \neq 0$, the resulting equation is a *non-homogeneous* equation. Generally, we adopt the notation $Dy$, $D^2 y$,....,$D^n y$ to denote $\frac{dy}{dx}$, $\frac{d^2 y}{dx^2}$,....,$\frac{d^n y}{dx^n}$. These notations $Dy$, $D^2 y$,....,$D^n y$ are called *differential operators* and have properties of algebraic quantities. With this notations, it is permitted for us to write

$$[a_0(x)D^n + a_1(x)D^{n-1} + ... + a_{n-1}(x)D + a_n(x)]y = R(x), \qquad (7.93)$$

or simply

$$\phi(D)y = R(x), \qquad (7.94)$$

where $\phi = [a_0(x)D^n + a_1(x)D^{n-1} + ... + a_{n-1}(x)D + a_n(x)]$ is the *operator polynomial in $D$*. In order to obtain the general solution of Eq. (7.86) for $R(x) \neq 0$, let $y_c(x)$ be the Complementary homogeneous equation

$$\phi(D)y = 0, \qquad (7.95)$$

$y_c(x)$ is referred as the complementary homogeneous solution. The superposition theorem

**Theorem $-$ 1** - The general solution of Eq. (7.87) is obtained by adding the complementary solution $y_c(x)$ to a particular solution $y_p(x)$ such that

$$c(x) + y_p(x). \qquad (7.96)$$

A simple example is the complementary solution $y_c(x) = c_1 e^x + c_2 e^{2x}$ for $(D^2 - 3D + 2)y = 0$ and the particular solution $y_p(x) = 2x^2 + 6x + 7$ for $(D^2 - 3D + 2)y = 4x^2$, the general solution for $(D^2 - 3D + 2)y = 4x^2$ will then be $y = c_1 e^x + c_2 e^{2x} + 2x^2 + 6x + 7$. We will not touch the other theorems from [71] but proceed directly to method of inverse operators.

Let us define a particular solution $y_p$ for $\frac{1}{\phi(D)}R(x)$ such that $\phi(D)y_p = R(x)$. We will refer $\frac{1}{\phi(D)}$ as the *inverse operator*. Without going into the mathematical depth of why $\frac{1}{\phi(D)}$ is simply a linear operator as well as the rigorous proof of finding the particular solutions for the inverse operators, we simply present the following two important relations which will be essential in our thesis

$$\frac{1}{D-m}R(x) = e^{mx}\int^x e^{-mx}R(x)dx, \tag{7.97}$$

and in case of multiple inverse operators acting on $R(x)$ where we will have

$$\frac{1}{(D-m_1)(D-m_2)....(D-m_n)}R(x) = e^{m_1 x}\int e^{m_1 x}e^{m_2 x}$$
$$.... \int e^{m_{n-1}x}e^{m_n x}\int e^{-m_n x}R(x)dx. \tag{7.98}$$

We note an important property of the $D^{-1}$ operator, we have only specified the upper limit of integration in Eq. (7.97). Specifying a constant lower limit of integration corresponds to adding a complementary function proportional to $e^{mx}$.

The first simplest example to consider is

$$\begin{aligned}
\frac{1}{D-\lambda}\frac{1}{\tau} &= e^{\lambda\tau}\int^\tau \frac{e^{-\lambda t}}{t}dt \\
&= e^{\lambda\tau}\int_\infty^{\lambda\tau} \frac{e^{-u}}{u} \\
&= e^{\lambda\tau}Ei(-\lambda\tau).
\end{aligned} \tag{7.99}$$

Here we have introduced the substitution $u = \lambda\tau$ from line 1 to line 2. This result is what we need to derive the $F_\pm^{(n)}(Q^2)$ functions needed for the $K_{PT}^{(L)}$ and $U_{PT}^{(L)}$ Sum Rules.

$$\begin{aligned}
\frac{1}{1+\frac{z}{z_1}} \to \frac{z_1}{z+z_1} \to \frac{-z_1}{D-z_1}\frac{1}{\tau} \\
&= -z_1 e^{z_1\tau}Ei(-z_1\tau) \\
&= -z_1 F_-^{(1)}(Q^2), \tag{7.100}
\end{aligned}$$

and similarly

$$\begin{aligned}
\frac{1}{1-\frac{z}{z_1}} \to \frac{-z_1}{z-z_1} \to \frac{z_1}{D+z_1}\frac{1}{\tau} \\
&= z_1 e^{-z_1\tau}Ei(z_1\tau) \\
&= z_1 F_+^{(1)}(Q^2). \tag{7.101}
\end{aligned}$$

The $n$th order operators can be generalized as follows

$$\frac{1}{1 + \frac{z}{z_n}} \quad \rightarrow \quad -z_n F_-^{(n)}(Q^2), \tag{7.102}$$

$$\frac{1}{1 - \frac{z}{z_n}} \quad \rightarrow \quad z_n F_+^{(n)}(Q^2). \tag{7.103}$$

The last job will be showing how the transformation of the non-perturbative part in the Shirkov's APT Euclidean functions [72] in the 1-loop case is equivalent to the non-perturbative part required to be added to $F_+^{(n)}$ and $F_-^{(n)}$ for both the regions of $Q^2 > \Lambda^2$ and $Q^2 < \Lambda^2$ which we denote as $\bar{F}_+^{(n)}$ and $\bar{F}_-^{(n)}$ in Eqs. (7.47, 7.48, 7.49, 7.50). The non-perturbative contribution of Shirkov's APT Euclidean functions [72] in the one loop case is simply given by

$$\left(\frac{\Lambda^2}{\Lambda^2 - Q^2}\right) \quad = \quad \left(\frac{1}{1 - \frac{Q^2}{\Lambda^2}}\right),$$
$$= \quad \left(\frac{1}{1 - e^L}\right),$$

we first consider applying the operator corresponding to the simple pole $1/(1 - \frac{z}{z_n})$ to $\frac{\Lambda^2}{\Lambda^2 - Q^2}$. We shall redefine $D \equiv \frac{d}{dL}$ (rather than using $\tau$)

$$\frac{n}{D + n} \left(\frac{1}{1 - e^L}\right) \quad = \quad n e^{-nL} \int^L e^{nt} \frac{1}{(1 - e^t)} dt$$
$$= \quad n \left(\frac{\Lambda^2}{Q^2}\right)^n \int^{\Lambda^2/Q^2} \frac{x^{-n}}{(1 - x^{-1})} \frac{-dx}{x}$$
$$= \quad n \left(\frac{\Lambda^2}{Q^2}\right)^n \int^{\Lambda^2/Q^2} \frac{x^{-n}}{(x - 1)} dx. \tag{7.104}$$

Here we have used the substitution $x = e^{-t}$ when going from line 1 to line 2. The integral in Eq. (7.104) has the form

$$\int^{\Lambda^2/Q^2} \frac{x^{-n}}{(x - 1)} dx = \left[ -\ln(x - 1) - \sum_{k=1}^{n-1} \frac{1}{k} \left(\frac{1}{x}\right)^k + \ln(x) \right]_0^{\frac{\Lambda^2}{Q^2}}. \tag{7.105}$$

After some manipulation, we finally arrive at

$$\int^{\Lambda^2/Q^2} \frac{x^{-n}}{(x-1)} dx = -\ln\left(n\left(1-\frac{\Lambda^2}{Q^2}\right)\right) - \sum_{k=1}^{n-1} \frac{1}{k}\left(\frac{\Lambda^2}{Q^2}\right)^{-k} + \ln\frac{\Lambda^2}{Q^2} + \ln(n).$$

This reproduces all of the terms in Eq. (7.47) for $\bar{F}_n^{(+)}$ in the region $Q^2 > \Lambda^2$. Changing the upper limit to $Q^2/\Lambda^2$ for the region $Q^2 < \Lambda^2$, it is possible to obtain Eq. (7.48) for $\bar{F}_n^{(+)}$. Repeating a similar procedure but with the operator corresponding to $1/(1+\frac{z}{z_n})$ acting on $\frac{\Lambda^2}{\Lambda^2-Q^2}$, Eqs. (7.49, 7.50) for $\bar{F}_n^{(-)}$ in the two energy regions are reproduced.

We now need to consider the double pole contributions which appear in the Borel transform for $D_{PT}^{(L)}$. We need the square of the appropriate operator. We apply the operator corresponding to $(\frac{1}{1-\frac{z}{z_n}})$ again to Eq. (7.105), this gives

$$\int^{\frac{\Lambda^2}{Q^2}} \left[ -\ln(x-1) - \sum_{k=1}^{n-1} \frac{1}{k}\left(\frac{1}{x}\right)^k + \ln(x) \right] x^{-n} \frac{dx}{x}. \qquad (7.106)$$

Solving this particular integral, it has the form

$$\left[ L_2\left(1-\frac{\Lambda^2}{Q^2}\right) - \sum_{k=1}^{n-1}\left(\frac{1}{k^2}\left(\frac{\Lambda^2}{Q^2}\right)^{n-k}\right) - \frac{1}{2}\left(\frac{\Lambda^2}{Q^2}\right)^n \ln\left(\frac{\Lambda^2}{Q^2}\right)^2 \right], \quad (7.107)$$

for any positive real integer $n$. This reproduces part of the structure of Eq. (7.53) for $\bar{\bar{F}}_+^{(n)}$ in the region $Q^2 > \Lambda^2$. Crucially we see that there is an additional $-\pi^2/3$ contribution in Eq. (7.53). This additional term is required to achieve continuity at $Q^2 > \Lambda^2$ when changing over to the $Q^2 < \Lambda^2$ region and Eq. (7.54). We are allowed to add this additional contribution of $n(\Lambda^2/Q^2)^n \pi^2/3$ since this power correction term is part of the complementary function, and corresponds to specifying a lower limit of integration when applying the $D^{-1}$ operator. We have previously not needed to add such contributions in discussing the single pole contributions. The $\pi^2/3$ arises via the dilogarithm relation

$$L_2(x) + L_2(1-x) = -\ln(x)\ln(1-x) + \frac{\pi^2}{6}. \qquad (7.108)$$

We can similarly obtain Eqs. (7.55, 7.56) using the squared operator corresponding to the $1/(1+\frac{z}{z_n})^2$ double pole. Similar $\pi^2/3$ terms are also needed to ensure continuity between the two regions $Q^2 > \Lambda^2$ and $Q^2 < \Lambda^2$ of Eq. (7.55) and Eq. (7.56). We now move on to a brief discussion of Analytic Perturbation Theory.

## 7.8 ANALYTIC PERTURBATION THEORY

The whole idea of Analytic Perturbation Theory arose from considering the problem of unphysical or ghost singularities of invariant charges in QCD. Such a difficulty first appeared in QED in the mid 1950s. It played a crucial role in the advancement and development of Quantum Field Theory.

In the 1950s, Shirkov and collaborators suggested the resolution to this problem by merging the renormalization group method with a Kallen-Lehman representation. This simply implies analyticity in the complex $Q^2$-variable. The considerations underlying APT are reviewed at length in Ref. [64].

The APT expansion has the form of Eq. (7.88) where at the one loop level we will denote the appropriate $\mathcal{A}_i(Q^2)$ functions as [72]

$$\mathcal{A}^{(1)}_{shir-1}(Q^2) \;\;=\;\; \frac{2}{b}\left[\frac{1}{L}+\frac{1}{1-e^L}\right], \tag{7.109}$$

$$\mathcal{A}^{(1)}_{shir-2}(Q^2) \;\;=\;\; \frac{2}{b^2}\left[\frac{1}{L^2}-\frac{e^L}{(e^L-1)^2}\right], \tag{7.110}$$

$$\mathcal{A}^{(1)}_{shir-k+1}(Q^2) \;\;=\;\; -\frac{1}{kb}\frac{d\mathcal{A}^{(1)}_k}{dL}, \tag{7.111}$$

where the superscript implies we are considering the 1-loop case and the subscript simply means Shirkov. These functions all vanish as $Q^2 \to \infty$. The $\mathcal{A}_1(Q^2)$ function has the freezing limit of $2/b$ as $Q^2 \to 0$ while the higher $\mathcal{A}_i$ functions vanish as $Q^2 \to 0$. We can now obtain LO, NLO and $N^2LO$ truncations of the APT series for $K^{(L)}_{PT}$, $U^{(L)}_{PT}$ and $D^{(L)}_{PT}$ which we denote by $K^1_{shir-LO}$, $K^1_{shir-NLO}$, $K^1_{shir-N^2LO}$, $U^1_{shir-LO}$, $U^1_{shir-NLO}$, $U_{shir-N^2LO}$, and $D^1_{shir-LO}$, $D^1_{shir-NLO}$ and $D^1_{shir-N^2LO}$, respectively. These are calculated using the $K^{(L)}_i$, $U^{(L)}_i$ and $d^{(L)}_i$ leading-$b$ $V$-scheme coefficients. In Figs(7.5, 7.6, 7.7) these truncated APT results are plotted versus $Q^2/\Lambda^2$ and compared with the analytized $U^{*(L)}(Q^2)$, $K^{*(L)}(Q^2)$ and $D^{*(L)}(Q^2)$ results. We have claimed that the analytized results combining the PT+NP, $F+\bar{F}$, contributions should be a formal all-orders resummation of the APT series. This is confirmed nicely by the plots of Fig(7.5) and (7.6) for the Sum Rules where we see that the $N^2LO$ results lie on the solid line representing the analytized (supposedly all-orders) APT result. For the $D^{*(L)}(Q^2)$ case in Fig(7.7), however, we see that the $N^2LO$ result and analytized result (solid line) are discrepant. This discrepancy is plotted in Fig(7.8). It behaves like $\Lambda^2/Q^2$ as $Q^2 \to \infty$ and vanishes as $Q^2 \to 0$, so the behavior is like that of an $\mathcal{A}_i(Q^2)$

function. We suspect that this discrepancy is connected with the need to restore continuity at $Q^2 = \Lambda^2$ by adding a complementary function contribution when applying the $D^{-1}$ method to the double pole contributions (see discussion below Eq. (7.108)), but it needs further investigation.

In the next section we shall need higher-loop APT functions. One possibility is to approximate the 2 and 3 loop Euclidean and Minkowskian APT cases using the so-called *effective log approach.* In this context, it is possible to use the simple model one loop expressions of Eqs. (7.110, 7.111, 7.112) with some *effective two loop log $L^*$* accumulating the two loop "log-of-log",

$$\mathcal{A}^{(3)}_{shir-1,2,3}((L)) \quad \longrightarrow \quad \mathcal{A}^{mod}_{shir-1,2,3} = \mathcal{A}^{(a)}_{shir-1,2,3}(L^*), \qquad (7.112)$$

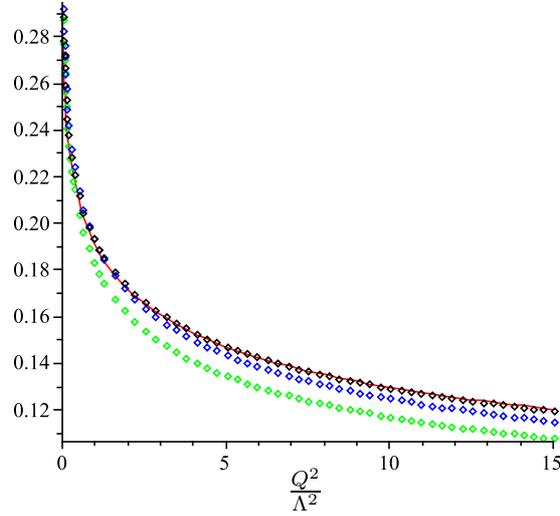$$L^* \quad = \quad L + \frac{c}{b^2} \ln(\sqrt{L^2 + 2\pi^2}). \qquad (7.113)$$

Figure 7.5: Polarised Bjorken Sum Rule $K^*(Q^2)$ (in red line) and the corresponding $K^1_{shir-LO,NLO,N^2LO}$ (in dots) versus $\frac{Q^2}{\Lambda^2}$ - observe that $K^*(Q^2)$ and $K^1_{shir-N^2LO}$( in black dots) lay on top one another at each particular point
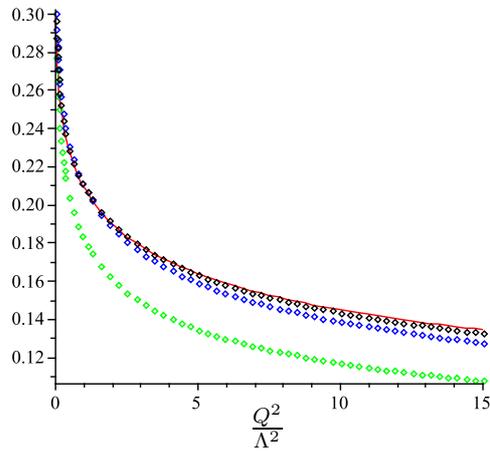


Figure 7.6: Unpolarised Bjorken Sum Rule $U^*(Q^2)$ (in red line) and the corresponding $U^1_{shir-LO,NLO,N^2LO}$ (in dots) versus $\frac{Q^2}{\Lambda^2}$ - observe that $U^*(Q^2)$ and $U^1_{shir-N^2LO}$( in black dots) lay on top of one another at each particular point
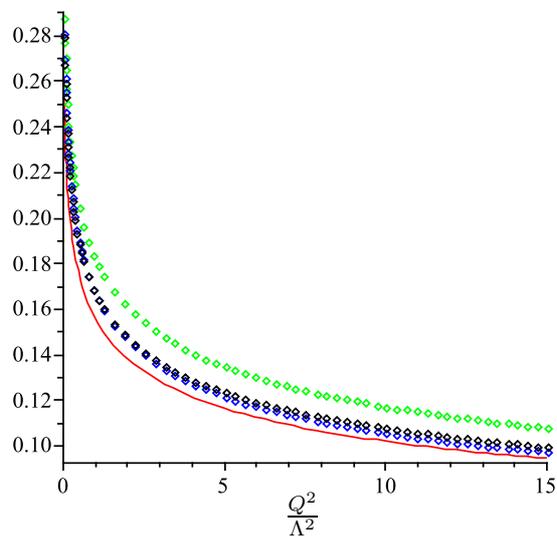
Figure 7.7: $D^*(Q^2)$ (in red line) and the corresponding $D^1_{shir-LO,NLO,N^2LO}$ (in dots) versus $\frac{Q^2}{\Lambda^2}$ - observe that $D^*(Q^2)$ and $D^1_{shir-N^2LO}$( in black dots) show slight discrepancy
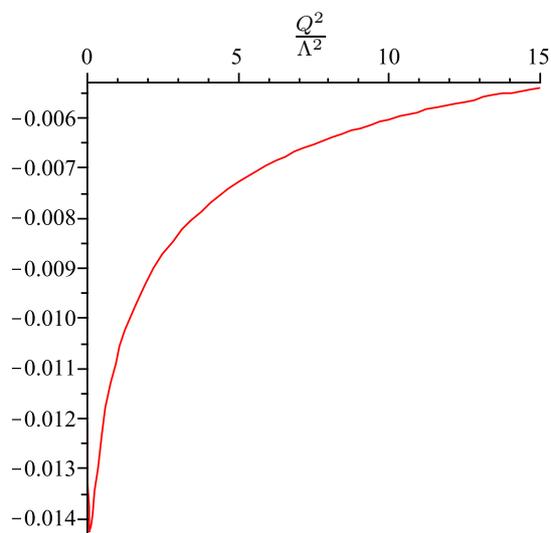


Figure 7.8: Discrepancy between$D^*(Q^2)$ and $D^1_{shir-N^2LO}$( in black dots)

## 7.9 FITS TO LOW ENERGY JLAB DATA

In this section we shall perform fits to the recent Jefferson Lab (JLab) and some existing data for $K_{pBj}(Q^2)$ (Eq. (7.65)) at low $Q^2$ values $0.1 < Q^2 < 3 \text{ GeV}^2$. We shall use the "conformal expansion" of Eq. (7.79) which provides a toy model to describe the $Q^2$ behavior at all values of $Q^2$ down to $Q^2 = 0$. We shall replace $K^{*(L)}$ in Eq. (7.79) by various truncated APT series analytic results. We assume a minimal model in which we fix $\tilde{C}_2^K$ to the value in Eq. (7.81) required to reproduce the low-energy GDH Sum Rule, and set higher coefficients in Eq. (7.80) to zero. We also set $\mathcal{H}(Q^2)$ in Eq. (7.83) to zero so we do not add any additional analytic contribution.

To construct two loop APT analytization we shall use the results of Magradze in [73] who shows that one can write the two loop APT functions as

$$\mathcal{A}_n^{(2)}(s) = \alpha_s^{(2)n}(s) = \frac{1}{\pi} \int_0^\infty \frac{\rho_n^{(2)}(\sigma)}{\sigma + s} d\sigma = \frac{1}{\pi} \int_{-\infty}^\infty \frac{e^t}{e^t + s/\Lambda^2} \tilde{\rho}_n^{(2)}(t) dt, \quad (7.114)$$

where

$$\tilde{\rho}_n^{(2)}(t) = \left(\frac{b}{c}\right)^n Im\left[-\frac{1}{1 + W_1(\frac{b^2}{ce} exp(-b^2 t/c + i(b^2/c - 1)\pi))}\right]. \quad (7.115)$$

We construct a two loop LO analytization and a NLO analytization using these functions.

$$K_{1-Magradze}^2 = \mathcal{A}_1^{(2)}(s), \qquad (7.116)$$

$$K_{2-Magradze}^2 = \mathcal{A}_1^{(2)}(s) + k_1 \mathcal{A}_2^{(2)}(s), \qquad (7.117)$$

where the superscript denotes that the equations are in two loop approximation. $K_1$ is simply the first exact calculated NLO perturbative coefficient of the polarized Bjorken Sum Rule given by $-0.333 N_f + 1.48 N + 0.438/N$. Substituting these results for $K^{*(L)}$ in Eq. (7.79) one obtains the red and blue lines plotted in Fig 7.9. We can also consider LO and NLO APT results using the one loop Shirkov functions in Section 7.8. These are the green and black curves in Fig(7.9). Finally we can consider a NLO truncation using the Shirkov two loop effective log result of Eqs. (7.113, 7.114). These are the diamond points in Fig(7.9). We have used $\Lambda_{\overline{MS}}^{(3)} = 380$ MeV, this is the value of $\Lambda_{\overline{MS}}$ used by Shirkov and collaborators for their theoretical model, thus

it is a good check if the theoretical toy plots we obtained will be similar to the experimental results.

Fig. (7.9) shows the comparison of these theoretical predictions with existing and recent experimental data. All points with error bars correspond to experimental data [74, 75, 76] with the color blue denoting JLab Hall B CLAS EG1b (calculation of the virtual photon asymmetry $A_1$ and the longitudinal spin structure function $g$ as well as the moments of $g$ and then extracting the neutron spin structure function $g_1^{en}$ from the combined proton $g_1^{ep}$ and deuteron $g_1^{ed}$ data using ammonia $NH^3$ and $ND^3$), green denoting JLab Hall B CLAS EG1a (a previous calculation with lesser kinematic range and less advanced statistics), red denoting JLab Halls A,B E94010/EG1a [2002] (measurement of the neutron spin structure function $g_1^{en}$ at low $Q^2$ using ($He^3$) Helium for E94010) and black denoting SLAC E143. For further details of the experimental analyses, see [77] for example. CLAS is the acronym of CEBAF (Continuous Electron Beam Accelerator Facility) Large Acceptance Spectrometer and SLAC is the acronym of Stanford Linear Accelerator. We see that given that we have used a minimal model with no adjustable parameters, as described above, all the APT analytizations are in good qualitative agreement with the data. This could of course be improved by adjusting the higher $\mathcal{C}_n^K$ coefficients and introducing an extra analytic function $\mathcal{H}(Q^2)$.

## 7.10 SUMMARY

We have considered in this Chapter how to make the sum of PT+NP effects for the Sum Rules and Adler D function in leading-$b$ approximation an analytic function of $Q^2$, as the true physical result must be. The PT component contributed by an UV or IR renormalon can be represented by functions $F_+^{(n)}(Q^2)$ and $F_-^{(n)}(Q^2)$. These functions involve the $Ei$ function and they contain a logarithmic branch point at $Q^2 = \Lambda^2$. This means that the freezing results investigated in Chapter 5 were only piecewise analytic. We showed that we could remove the branch cut in a minimal way by adding non-perturbative contributions $\bar{F}_+^{(n)}(Q^2)$ and $\bar{F}_-^{(n)}(Q^2)$. The separate PT and NP functions are piecewise analytic with separate definitions for the regions $Q^2 > \Lambda^2$ and $Q^2 < \Lambda^2$, but the sum of the two components yields a single analytic function $F_\pm^{*(n)}(Q^2)$ for each renormalon. We found that these analytized renormalon contributions resulted in a freezing limit of $2/b$ for the Sum Rules, the same as that found in the APT formalism of Shirkov and collaborators. We showed that we could reproduce our non-perturbative $\bar{F}_\pm^{(n)}$ functions by acting with a $D^{-1}$ operator on the non-perturbatve part
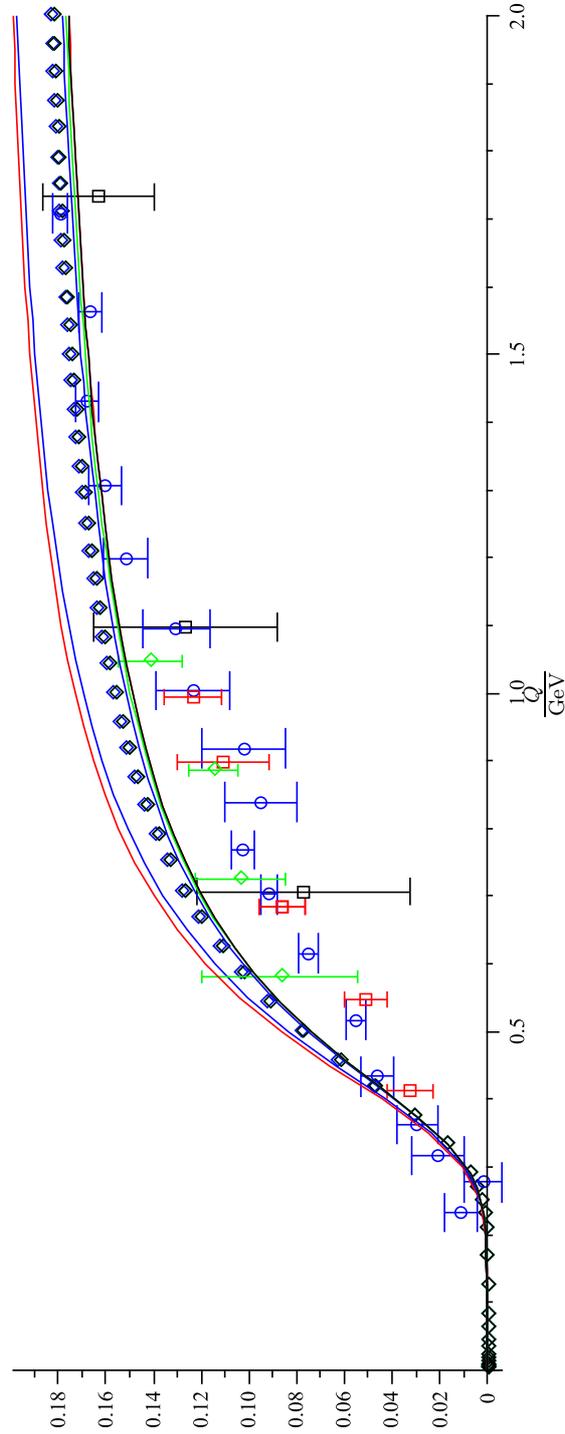
Figure 7.9: $K_{pBj}(Q^2)$ plotted versus $Q/\text{GeV}$. All points with error bars correspond to existing and recent experimental data. The four lines of red, blue, green and black arise, respectively, from inserting the two loop LO and NLO, and one loop analytizations at LO and NLO in Eq (7.79). The diamond shape points correspond to the NLO two loop "effective log" Shirkov analytization. We chose $\Lambda = 380\text{MeV}$.

of the leading APT function $\mathcal{A}_1(Q^2)$. In this way our analytized renormalon contributions could be considered as an all-orders resummation of the APT series. There are complications for the Adler-$D$ function which has double poles in its Borel transform. We showed that for the polarized Bjorken Sum Rule the exact low-energy Gerasimov-Drell-Hearn (GDH) Sum Rule gave important constraints on the form of infrared freezing, and we could derive the "conformal expansion" of Eq. (7.79) which should be valid at both small and large values of $Q^2$. We considered a minimal toy model based on this result and were able to find good qualitative agreement with the recent JLab data for $K_{pBj}(Q^2)$ on the range $0.1 < Q^2 < 3$ GeV$^2$ using various truncated one and two loop APT predictions.

# Chapter 8

# CONCLUSIONS

The fundamental ingredient underpinning the research in this thesis is vacuum polarization. The calculation of QED one loop vacuum polarization was undertaken in Chapter 2. The renormalized result for vacuum polarization $\Pi(k^2)$ in the so-called V-scheme is proportional to $b \ln(\frac{-k^2}{\mu^2})$, where $k$ is the momentum flowing through the bubble. In QED $b = -\frac{2N_f}{3}$ is the first beta-function coefficient.

As discussed in Chapter 4 this simple result has amazing consequences when one considers calculating a complete photon propagator with the insertion of chains of bubbles inside the vacuum polarization loop. One finds that the class of so-called "renormalon" diagrams containing a single chain of $n$ bubbles has a $b^n n!$ growth in $n$th order perturbation theory. The $b^n n!$ growth arises because of the powers of $b \ln(\frac{-k^2}{\mu^2})$ arising from each bubble, integrated over $k$. Using a Borel representation one finds evenly spaced singularities in the Borel $z$-plane on both positive and negative semi-axes at intervals of $2/b$, arising from small and large $k$ regions, respectively, in the loop integration over $k$.

In QCD one has $b = (33 - 2N_f)/6$ and so one can recast QCD perturbative coefficients at $n$th order as an expansion in powers of the QCD $b$. The "leading-$b$", $b^n$ term can then be used as an approximation for the perturbative coefficient and all-orders resummations of this piece of the coefficient performed. One thinks of this QCD leading-$b$ term as built from chains of effective bubbles which involve gauge invariant combinations of gluon and ghost loops resulting in the same $b \ln(\frac{-k^2}{\mu^2})$, and it is a more sophisticated construct than the simple QED chain of fermion bubbles.

In the case of QCD the singularities on the positive real Borel $z$ semi-axis

are infrared (IR) renormalons , and they imply that the resummed pertur-
bation theory (PT) result must be supplemented by extra non-perturbative
(NP) terms in the form of the operator product expansion (OPE) in pow-
ers of $\Lambda^2/Q^2$. The IR renormalon ambiguity can then be cancelled and a
well-defined result obtained for the sum of the PT and NP components. The
singularities on the negative real $z$ semi-axis are ultraviolet (UV) renormalons
and do not impede the Borel summation (at least for large enough energies
where the renormalized one loop coupling is positive). Leading-$b$ resumma-
tions with a one loop coupling therefore provide a toy model test laboratory
to investigate the interplay of PT and NP physics.

In Chapter 5 the results of [31] for all-orders leading-$b$ resummations for
the Adler $D$-function associated with vacuum polarization and some Deep
Inelastic scattering (DIS) sum rules were reproduced. One obtains a freezing
behavior for the resummed PT result as $Q^2 \to 0$ which remains finite at
the Landau pole $Q^2 = \Lambda^2$ where the one loop coupling $a(\Lambda^2)$ diverges. The
observables then change sign and freeze smoothly to vanish in the infrared
at $Q^2 = 0$. For $Q^2 < \Lambda^2$ one needs to introduce a different Borel repre-
sentation with the integral along the negative real $z$ semi-axis and with UV
renormalon ambiguities. This freezing behavior is unphysical, however, as
higher $Q^2$ derivatives are not finite and the freezing in $Q^2$ is only piecewise
analytic. In reality the sum of the PT and NP components must be analytic
in $Q^2$.

In Chapter 6 a new perturbative QCD calculation of the $N^3LO$ $(\mathrm{O}(\alpha_s^4))$
coefficient $d_3$ in Ref. [40] was used to perform fits to data on the inclusive
$R_{e^+e^-}$ ratio at $s = M_Z$, and on the related $R_\tau$ inclusive decay ratio. Both
of these quantities can be related to the Adler $D$-function of vacuum po-
larization via a contour integration in the complex energy-squared $s$-plane,
which serves to analytically continue the Euclidean $D$ to the Minkowskian
$R_{e^+e^-}$ and $R_\tau$. Contour improved PT (CIPT) was applied in which the $D$-
function is expanded perturbatively inside the integral which is then evalu-
ated term-by term, serving to resum to all-orders potentially large analytical
continuation terms involving $\pi^2 b^2$ and other beta-function coefficients. In
Chapter 3 the problem of the renormalization scheme (RS) dependence of
fixed-order perturbative predictions was reviewed. The so-called CORGI ap-
proach was introduced in order to avoid renormalization scale $\mu$-dependence
by a resumming to all-orders the RG-predictable scale logarithms. Fits to
ALEPH data on $R_\tau$ were made using various perturbative approaches involv-
ing CIPT and CORGI at $N^3LO$, $NNLO$ and $NLO$, and making contact with
the leading-$b$ renormalon discussions of earlier chapters all-orders resumma-

tions of the Adler D-function inside the contour integral were made to obtain an all-orders CORGI result matched to the exactly known perturbative coefficients. The differences between the fits for $\alpha_s(m_\tau^2)$ obtained using these different approaches were discussed. One sees reassuringly that the successive $NLO$, $NNLO$, and $N^3LO$ CORGI results get progressively closer to the all-orders result. By evolving up to $\alpha_s(M_Z^2)$ using the three-loop matching conditions to cross quark flavour thresholds one obtains the values tabulated in Table 6.2. An estimate of the uncertainty in $\alpha_s(M_Z^2)$ of $\delta\alpha(M_Z^2) = 0.003$ was made. Data on the spectral function $R_\tau(s)$ was also successfully fitted using the $N^3LO$ CORGI results.

Finally in Chapter 7 we returned to the problem of how the sum of PT + NP components can be rendered analytic, given that the PT component by itself is only piecewise analytic. We showed that the leading-$b$ PT theory component for an IR or UV renormalon, $F_{\pm}^{(n)}(Q^2)$, involves exponential integral functions $Ei$ and has a logarithmic "Landau" branch cut extending from $Q^2 = 0$ to $Q^2 = \Lambda^2$ in the complex $Q^2$ plane, this could be removed in a minimal way by adding non-perturbative OPE terms (expansion in powers of $\Lambda^2/Q^2$) for $Q^2 > \Lambda^2$ and modified non-perturbative terms (expansion in powers of $Q^2/\Lambda^2$) in the region $Q^2 < \Lambda^2$, denoting these non-perturbative pieces as $\bar{F}_{\pm}^{(n)}(Q^2)$ The PT+NP split is $F_{\pm}^{(n)}(Q^2)+ \bar{F}_{\pm}^{(n)}(Q^2)$. Each term separately is piecewise analytic having a different form in the two regions, but the sum of the two denoted $F^{*(n)}(Q^2)$ is a single analytic function of $Q^2$ for both regions. We showed that the freezing limit as $Q^2 \to 0$ of the fully analytic leading-$b$ results was $2/b$ for the DIS sum rules, but formally infinite for the Adler $D$-function. This was interesting since $2/b$ is also the freezing limit of observables in the Analytic Perturbation Theory (APT) approach of Shirkov and collaborators. We showed that our analytized renormalons are equivalent to an all-orders resummation of the APT series, by developing a formalism in which observables are represented as a differential operator acting on the coupling. This approach also produced a finite freezing limit of $2/b$ for the Adler D-function. We showed how for the polarized Bjorken Sum Rule the exact IR Gerasimov-Drell-Hearn (GDH) Sum Rule as $Q^2 \to 0$ imposes strong constraints on how observables behave at low $Q^2$ values, and we constructed a "conformal expansion" Eq. (7.78) which is simultaneously an expansion in $Q^2/\Lambda^2$ and $\Lambda^2/Q^2$. This provides a model that can be tested against data in the large $Q^2$ perturbative region right down to $Q^2 = 0$. We analyzed particularly low energy JLab data for the Bjorken sum rule down to very low $Q^2 \sim 1\text{GeV}^2$ values, and obtained surprisingly successful fits Fig(7.9). This analytic leading-$b$ resummation looks very promising for fur-

ther interesting studies of the interplay between large $Q^2$ perturbative QCD physics and the more intractable strong-coupling low-$Q^2$ physics.

# Bibliography

[1] L.H. Ryder, Quantum Field Theory, 2nd edn, Cambridge University Press, 1996

[2] M.E. Peskin and D.V. Schroeder, An Introduction to Quantum Field Theory, Westview, 1995

[3] A.G. Grozin, Lectures on QED and QCD: Practical Calculation and Renormalization of one and multi-loop Feynman diagrams, World Scientific, 2007

[4] R.K. Ellis, W.J. Stirling and B.R. Webber, QCD and Collider Physics, Cambridge University Press, 2003

[5] W.A. Bardeen, A.J. Buras, D.W. Duke and T. Muta. Phys. Rev.**18** (1978) 3998.

[6] A. Smilga, Lectures on Quantum Chromodynamics, World Scientific Publishing, 2001

[7] S.A. Larin and J.A.M. Vermaseren, Phys. Lett.**B303** (1993) 334.

[8] D.R.T. Jones, Nucl. Phys.**B75** (1994) 537.

[9] O.V. Tarisov, A.A. Vladimirov and A.Y. Zharkov, Phys. Lett, B93 (1980) 429.

[10] S.A. Larin and J.A.M. Vermaseren, Phys. Lett. B303 (1993) 334 [hep-ph/9302208]

[11] T. van Ritbergen, J.A.M. Vermaseren and S.A. Larin, Phys. Lett. B400 (1997) 379 [hep-ph/9701390]

[12] A.J. Buras, E.G. Floratos, D.A. Ross and C.T.Sachrajda, Phys. Rev. B131 (1977) 308.

[13] R. Corless *et al*, Advances in Computational Mathematics 5 (1996) 329.

[14] E. Gardi and G. Grunberg, and M. Karliner, JHEP 07 (1998) 007 [hep-ph/9806462]

[15] W.A. Bardeen, A.J. Buras, D.W. Duke and T. Muta. Phys. Rev.**18** (1978) 3998.

[16] W. Celmaster and R.J. Gonsalves, Phys. Rev.**D121** (1980) 3112.

[17] C.J. Maxwell, [arXiv:hep-ph/9908463v1].

[18] P.M. Stevenson, Phys. Rev.**D23** (1981) 2916.

[19] G. Grunberg, Phys. Rev. D29 (1984) 2315.

[20] C.J. Maxwell and D.G. Tonge, Nucl. Phys. B481 (1996) 681 [hep-ph/9606392].

[21] F.J. Dyson, Phys. Rev. 85 (1952) 631

[22] G. Parisi, Nucl. Phys. B150 (1979) 163.

[23] M. Neubert, Phys. Rev. D51 (1995) 5924.

[24] D.J. Broadhurst, Z. Phys. C58 (1993) 339.

[25] M.Beneke, Nucl. Phys. B 405 (1993) 424.

[26] M. Beneke, Renormalons, Phys. Rept. 317 (1999) 1 [hep-ph/9807443].

[27] D. Drechsel, Prog. Part. Nucl. Phys. 34 (1995) 181 [nucl-th/9411034].

[28] K.G. Chetyrkin, A.L. Kataev and F.V. Tkachov, Phys. Lett. B85 (1979) 277.

[29] S.G. Gorishny and S.A.Larin, Phys. Lett. B172 (1986) 109.

[30] S.I. Alekhin, A.L. Kataev, J. Phys. G29 (2003) 1993 [hep-ph/0209165].

[31] P.M. Brooks and C. J. Maxwell, Phys. Rev. D **74** (2006) 065012 [arXiv:hep-ph/0604267].

[32] P.M. Brooks, Infrared Behaviour And Renormalization Scheme Invariance of QCD Observables, Durham University Thesis, 2006, http://etheses.dur.ac.uk/2590/

[33] C.N. Lovett-Turner and C.J. Maxwell, Nucl. Phys. B452 (1995) 18.

[34] D.J. Broadhurst, A.L. Kataev, Phys. Lett. B 315 (1993) 179.

[35] M. Abramowitz and I.A. Stegun, Handbook of Mathematical Functions, 9th edn., Dover, 1964, p. 556.

[36] M. Baker and K. Johnson, Phys. Rev. 183 (1969) 1292.

[37] D.M. Howe and C.J. Maxwell, Phys. Rev. D70 (2004) 014002.

[38] D.M. Howe, Infrared Behavior of QCD Observables, Durham University Thesis, 2004, `http://etheses.dur.ac.uk/3071/`

[39] P.M. Stevenson, Phys. Rev. D23 (1981) 2916.

[40] P.A. Baikov, K.G, Chetyrkin and J.H. Kuhn, Phys. Rev. Lett. B131 (2008) 012002.

[41] J. Alcaraz et al. (LEP Collaboration and ALEPH Collaboration and DELPHI Collaboration and L3 Collaboration and OPAL Collaboration and LEP Electroweak Working Group) (2007), arXiv:0712.0929 [hep-ex].

[42] http://www.lns.cornell.edu/public/CLEO/CLEO3/cleo3/proposal/subsection3_3_3.html

[43] A. Pich, Adv. Ser. Direct. High Energy Phys. 15 (1998) 453 [hep-ph/9704453].

[44] J. Beringer *et al.* [Particle Data Group Collaboration], Phys. Rev. D **86** (2012) 010001.

[45] M. Davier, A. Hoecker and Z. Zhang, Rev. Mod. Phys. 78 (2006) 1043 [hep-ph/0507078].

[46] A. Pich, Nucl. Phys. Proc. Suppl. **186** (2009) 187 [arXiv:0811.1347 [hep-ph]].

[47] C.J. Maxwell and D.G. Tonge, Nucl. Phys. B535 (1998) 19.

[48] C.J. Maxwell and A. Mirjalili, Nucl. Phys. B577 (2000) 209.

[49] C.N. Lovett-Turner and C.J. Maxwell, Nucl. Phys. B452 (1995) 188.

[50] G. Grunberg, Phys. Lett. B95 (1980) 70.

[51] C.J. Maxwell and A. Mirjalili, Nucl Phys. B611 (2001) 423. arxiv:hep-ph/0103164.

[52] G. Grunberg, Phys. Lett. B325 (1994) 441.

[53] ALEPH collaboration, Eur. Phys. J. C4 (1998) 409.

[54] M. Davier et al., Eur. Phys. J. C56 (2008) 305.

[55] C. Amsler et al., The Review of Particle Physics, Phys. Lett. B667 (2008) 1.

[56] R. Rodrigo, A. Pich and A. Santamaria, Phys. Lett. B424 (1998) 367.

[57] S. Menke, arXiv:0904.1796 [hep-ph].

[58] A. Pich, Acta Phys. Polon. Supp. 3 (2010) 165 [arXiv:1001.0389 [hep-ph]].

[59] M. Beneke and M. Jamin, JHEP 0809 (2008) 044.

[60] K. Maltman and T. Yavin, Phys. Rev. D78 (2008) 094020.

[61] I. Caprini and J. Fischer Eur. Phys. J. C64 (2009) 35.

[62] M. Girone and M. Neubert, Phys. Rev. Lett. 76 (1996) 3061.

[63] I. Caprini and J. Fischer, arXiv:hep-ph/0612274.

[64] N.N. Bogoliubov, A.A. Logunov and D.V. Shirkov, [Zh. Eksp. Teor. Fiz. 1959, 37 3(9), 805].

[65] J. Soffer and O. Teryaev Phys. Rev. D70 (2004) 116004 [hep-ph/0410228].

[66] S. B. Gerasimov, Yad. Fiz. 2, 598 (1965) [Sov. J. Nucl Phys. 2, 430(1966)].

[67] S.D. Drell and A.C. Hearn, Phys. Rev. Lett. 16 (1966) 908.

[68] A.L. Kataev, G. Parante and A.V. Sidorov, Nucl. Phys. B573 (2000) 405 [hep-ph/9905310].

[69] R.S. Pasechnik, D.V. Shirkov, O.V. Teryaev, Phys. Rev. D78 (2008) 071902 arXiv:0808.0066v2 [hep-ph].

[70] J.D. Bjorken, Phys. Rev. 148 (1966) 1467; Phys. Rev. D1 (1970) 1376.

[71] M.R. Spiegel, Advanced Mathematics for Engineers and Scientists, Schaum, 1983.

[72] R.S. Pasechnik, D.V. Shirkov and O.V. Teryaev, Phys. Rev. D78 (2008) 071902(R) [arXiv:0808.0066v2 [hep-ph]].

[73] B.A. Magradze, JINR Rapid Comm. 222 (2000) 19. [arXiv:hep-ph/0010070].

[74] E143 Collaboration, K. Abe et al., Phys. Rev. Lett. 78 (1997) 815.

[75] E94010 Collaboration, M. Amarian et al.,, Phys. Rev. Lett. 89, 242301 (2002).

[76] CLAS Collaboration, J. Yun et al., Phys. Rev. C67 (2003) 055204 and R. Fatemi et al., Phys. Rev. Lett. 91 (2003) 222002.

[77] E. Leader, Spin in Particle Physics, Cambridge Monographs On Particle Physics, Nuclear Physics and Cosmology 15